The original approaches to the problems of the dynamics of the vibrating transport and technological machine with electromagnetic excitation of vibrations are considered. A generalized mathematical model of the spatial motion of the system "vibratory exciter - working member - operational load in the form of bulk material" was constructed and comprehensive modeling was carried out.
The results of modeling on the dynamic stability of the electromagnetic vibrating machines are presented and cases concerning the use of numerical methods are shown, taking into account non-linearity in the electromagnetic vibratory exciters.
The mechanism for generating subharmonic vibrations, as well as the method of taking account for the hysteresis phenomenon of the electromagnet in the mathematical model are described. A new scheme of the exciter with frequency division of operating vibrations has been developed and investigated. Some new designs of the electromagnetic vibratory feeders are presented.
The book may be used by engineers and scientists working in the area of vibration engineering and technology, as well as using a systems approach in the field of dynamics of complex mechanical systems.

Victor Zviadauri S.: Prof. of Georgian Technical University; Chief of the Department of Machine Dynamics of the Institute of Machine Mechanics. (www.imm.ge)
Merab Chelidze A.: Candidate of Technical Sciences; Senior Researcher of the Institute of Machine Mechanics
Merab Tedoshvili M.: Candidate of Technical Sciences; Senior Researcher of the IMM.

9 786203 581096

MONOGRAPH

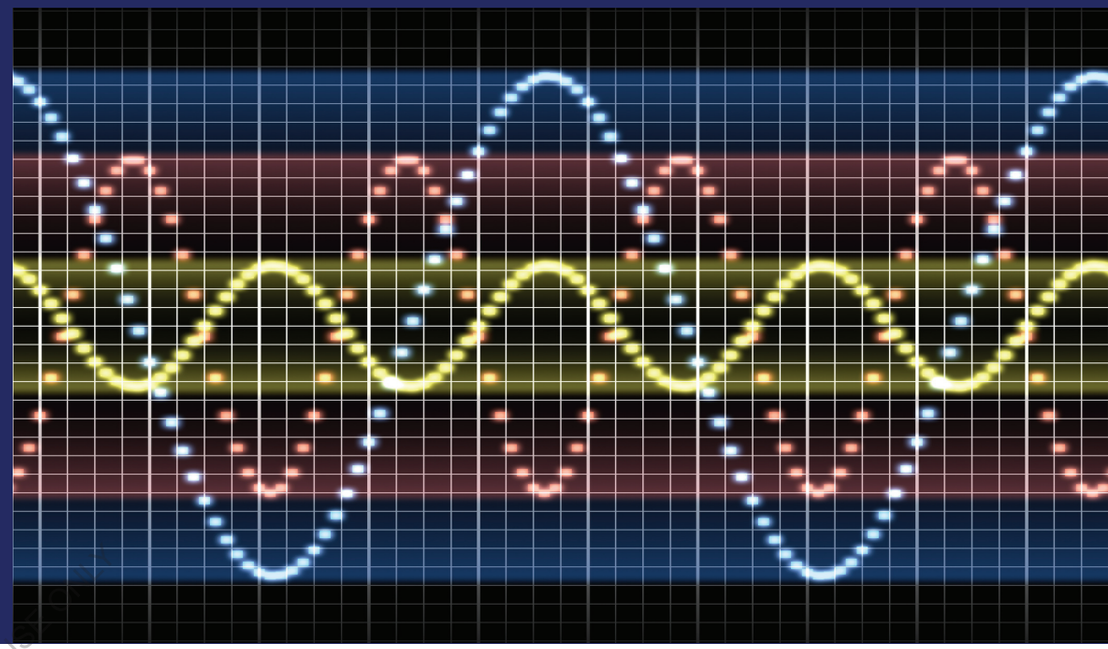

Victor Zviadauri
Merab Chelidze
Merab Tedoshvili

Dynamics of vibratory technological machines and processes

Movement of the Friable Materials on the Spatially Vibrating Plane

LAP LAMBERT Academic Publishing

Zviadauri, Chelidze, Tedoshvili

Victor Zviadauri
Merab Chelidze
Merab Tedoshvili

Dynamics of vibratory technological machines and processes

Victor Zviadauri
Merab Chelidze
Merab Tedoshvili

Dynamics of vibratory technological machines and processes

Movement of the Friable Materials on the Spatially Vibrating Plane

LAP LAMBERT Academic Publishing

Imprint

Cover image: www.ingimage.com

Publisher:
LAP LAMBERT Academic Publishing
is a trademark of
International Book Market Service Ltd., member of OmniScriptum Publishing Group
17 Meldrum Street, Beau Bassin 71504, Mauritius
Printed at: see last page
ISBN: 978-620-3-58109-6

Victor Zviadauri, Merab Chelidze, Merab Tedoshvili

Dynamics of vibratory technological machines and processes

Movement of the Friable Materials on the Spatially Vibrating Plane

The original approaches to the problems of the dynamics of the vibrating transport and technological machine with electromagnetic excitation of vibrations are considered. A generalized mathematical model of the spatial motion of the system "vibratory exciter - working member - operational load in the form of bulk material" was constructed and comprehensive modeling was carried out.

The results of modeling on the dynamic stability of the electromagnetic vibrating machines are presented and cases concerning the use of numerical methods are shown, taking into account non-linearity in the electromagnetic vibratory exciters.

The mechanism for generating subharmonic vibrations, as well as the method of taking account for the hysteresis phenomenon of the electromagnet in the mathematical model are described. A new scheme of the exciter with frequency division of operating vibrations has been developed and investigated. Some new designs of the electromagnetic vibratory feeders are presented.

The book may be used by engineers and scientists working in the area of vibration engineering and technology, as well as using a systems approach in the field of dynamics of complex mechanical systems.

Contents

Preface

The vibrating machines and processes are widely used in many areas of production, due to their advantage over similar transport and technological equipment. The most common ones are the vibrating machines and devices designed for movingvarious materials (feeding, transporting, dissemination, screening, etc.) to perform a range of operations in the metallurgical, mining, chemical, engineering, construction and other industries.

Despite the simplicity of their design and servicing, the fairly complicated high-intensity dynamic processes of various nature and forms (the interaction of the masses of the vibrating machine, operating member and technological load, particles and layers of materials, the dynamic processes in the vibratory drives, etc.) are developing in the vibrating machines during their operation, and this predetermines the main directions in vibration technology.

In the extensive literature on the study of the vibration processes of movement, the emphasis is mostly placed on the individual pointsin the process (the displacement of masses, oscillations ofthe vibrating machine elements, dynamic processes in the vibratory drives, etc.), and only in some cases - taking into account their interlinkages, brought to theoretical assessments.

The first partis mainly devoted to the consideration of a single dynamic model of the generalized vibrating transport and technological machine, which unites its components, such as an energy source, elastic system, operating member, and technological load. It takes into account the principal geometric parameters (common for these machines) and the real characteristics of each part.

Based on a systems approach, a mathematical model of the movements of units of machine describes the interrelated dynamic processes in space and can bring it to specific cases arising out of a practical requirement.

The book covers numerous computational experiments and their results along with a comparison with experimental data.

As an integral component of modern research, based on the analysis of the existing methods, a methodology has been developed to optimize the spatial dynamic model of thevibrating machine of general type and specific real machines. New designs of the progressive vibrating machines for transport and technological purposes are presented.

The second part examines the issues of the design of the elastic elements of the vibrating machines, taking into account the opening of the elastic-frictional fixturing (shaft-bushingjoint), which, depending on the magnitude of torsional moment, causes

both a nonlinear change in the rigidity of the elastic element and the generation of a damping coefficient. As an elastic element, a spatial torsional elastic system is taken, the design of which includes the identification of power factors caused by the joint action of the torsional and bending moments. It should be noted that the design of the torsional spatial system includes the bending analysis that would allow for calculating the rigidity of a double-sided clamped spring system, and thereby determining the structural damping coefficient for bending deformation. It should be especially noted that in this work some issues of mathematical modeling are considered when constructing a nonlinear amplitude-frequency diagram and obtaining stable operating modes of the electromagnetic vibratory exciters, the electrical line of which includes a semiconductor diode.

The electromagnetic exciters of vibrations are widely used in the vibrating technological machines of resonant action, on which the requirements ofcontrolling the amplitude, frequency, damping of vibrations, and so on are imposed.

The third part dwells on the solutions to these issues by creating the low-frequency nonlinear electromagnetic exciters of resonant vibrations.The mechanism for generating subharmonic vibrations, as well as the method of taking account for the hysteresis phenomenon of the electromagnet in the mathematical model are described. A new scheme of the exciter with frequency division of operating vibrations has been developed and investigated. The issues of controlling the amplitude, natural frequency and damping of the system at low-frequency vibrations are described.

Studies of the nonlinear electromagnetic exciter of vibrations have been conducted through the theoretical calculations and mathematical modeling of the main electric and mechanical characteristics, as well as by conducting the field tests of a real physical model.

The results obtained in this work allowto reduce significantly the weight and dimensions of the vibratory exciter, reduce the level of radiated noise and the transfer of dynamic loads to the supporting structures.

The results obtained in this work can significantly reduce the weight and dimensions of the vibration exciter, lower the level of radiated noise and the transfer of dynamic loads to the support structures.

PART I
THE MOVEMENT OF FRIABLE MATERIALS ALONG THE SPATIALLY VIBRATING PLANE AND FEATURES OF ITS SIMULATION

Introduction

The essence of vibration engineering for processing applications is based on interaction of the vibrating operating member with a procesable object. Initial research in the field of vibration engineering and technology involves the study of the patterns of vibratory displacement of the rigid single bodies in the form of material particle, single-piece parts of various shapes, as well as some of the simplest models of bulk material [1, 7, 10, 11, 15, 17, 20].

Vibration technological processes are indispensable component parts of production across numerous industry sectors, such as mechanical engineering, chemical and metallurgical industries, construction industry, mining, agriculture, etc.; they may be associated with the oriented displacement of single-piece parts, sorting and transportation of bulk materials, with forming the articles of the construction industry, using vibration in conjunction with hydraulic and pneumatic processes, and so on.

The nature of the process of the vibrational movement of materials is formed by different factors, such as parameters of the operating member, vibration exciter, properties of the process material, the cross impact of the medium being treated and the vibration machine; among these, operational load, which can be represented in the form of a material point, rigid body or bulk material, appears to occupy an important place.

The first of these is more open to analytical investigation; the second one - a generalized type of material (a rigid body) - is separated into several typical shapes: cylindrical, spherical, polyhedral, flat and so on.

A more complex type material is bulk material thatcombines the diversity of bulk cargo. The vibrational movement of bulk cargo is associated with complex physical processes occurring between the lower layers of the cargo and the load-carrying surface; the patterns of displacement are also significantly influenced by the medium in which cargo moves. So, for example, when mass cargo moves in the tossing mode, there takes placerarefaction or compression of air, depending on whether the load falls or comes away. The effect of air-gap clearances formed between the load and the working

member's surface is the stronger, the finer the particles of load, and the pressure drops in some cases exceed the gravity of the material by a multiple [10, 18].

The wide application of the vibration processes is due to the simplicity of their servicing and the relatively easy binding of the vibrating machines, especially with the electromagnetic exciters of operating vibrations, to technological processes with various physical parameters.

Owing toa variety of tasks associated with the use of vibration engineering, the problems of studying the relationship of individual structural parts and units of machine both in a static and dynamic states, taking the dynamic coupling of the operating members and the medium being treated into account simultaneously, assumea primary importance. Thus, the study of work processes should be carried out in an integrated manner, given the linkbetween the main component parts ofmachine that form the end result of technological process.

The first part of a monograph considers issues of the emergence of three-dimensional (non-working) vibrations of the operating member of the vibrating machine.

One of the critical units in the vibrating machines is an elastic system that transmits vibrations from avibratory exciter to the operating members; the features of the elastic elements create the preconditions for the emergence of three-dimensional vibrations (in addition to working ones) of the working member of a vibration machine, which in turn affects the performance of a given (calculated) work process by machine.

Unavoidable (even within tolerances) errors in the manufacture and installation of individual units and machine in general, play an important role in the emergence of three-dimensional (parasitic) oscillations in the vibrating machines; they are themselves a causeof deviation of the pointing direction of transmission of the exciting force and the mutual position of the masses (1- vibratory exciter, 2 - the working member) and the elastic system (Fig. 1.1): *a*) inaccuracy in the processing of the supporting surface of springs, *b*) inaccuracy in the processing of the surface of the working member connecting it with an elastic element, *c*) inaccuracy in the location of the axis of an elastic element, *d*) transverse deformation of spring, *e*) torsional deformation of spring.

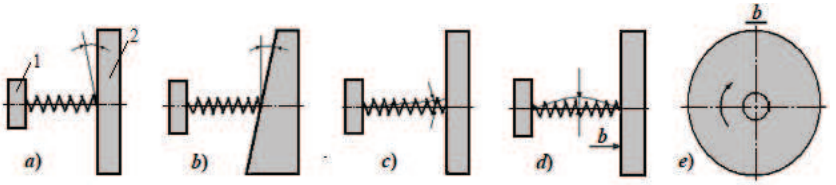

Fig.I.1. Deviations (inaccuracies) of the mutual position of the elastic system and the design elements of the vibrating machine

In the dynamic model of the vibrating machine, deviations caused by above mentioned inaccuracies can be divided into two types: deviations of the coordinate axes of masses and deviations of the direction of the exciting forces.

To illustrate this point, Figure 1.2 shows the system of two bodies M_1 (stationary-vibratory exciter) and M_2 (movable-working member), interconnected by spring K and moving through space $Oxyz$; deviations of the working member caused by various possible inaccuracies are shown as follows: I - the initial (design) position of the working member, II - the position of the working member, taking into account initial inaccuracies, among which e_x, e_y, $e_z$are the eccentricities of the movement of the center of gravity from point O_1 to point $O_1^{'}$; $\theta_0, \psi_0, \varphi_0$ rotation of the axes of a coordinate system causedby installation inaccuracies of the vibrating machine and their transition from the positions $O_1x_1y_1z_1$ to $O_1^{'}x_1^{'}y_1^{'}z_1^{'}$(Fig. 1a, b); III - $O_1^{''}x_1^{''}y_1^{''}z_1^{''}$- the spatial dynamic (working) position of the working member; the coordinate system$O_vx_vy_vz_v$is connected with avibratory exciter, 1 - the main (working) elastic system of thevibrating machine, 2 - the suspensions of the vibrating machine, the mass M_2, for the reasons stated, might be found in the positions $O_1^{'}x_1^{'}y_1^{'}z_1^{'}$ and $O_1^{''}x_1^{''}y_1^{''}z_1^{''}$ (dotted lines). Owing to displacement of the point of force application from the initial position, Q_x will decomposeinto components$Q_{x_1}^{'}$, $Q_{x_2}^{'}$, which creates conditions for the appearance ofthe moment of forces about the center of the mass and, therefore, bending and rotational vibrations.

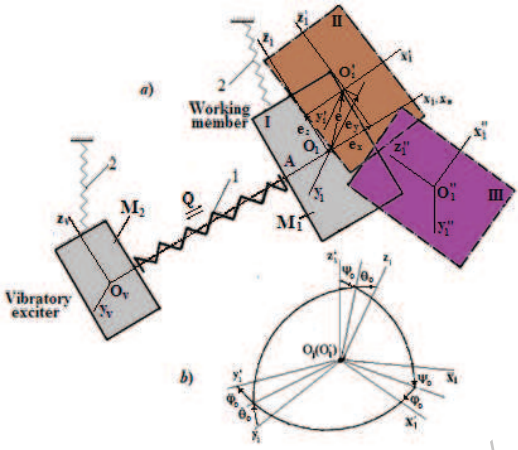

Fig.I.2. The possible location masses caused by errors in the connection of the elastic system with masses: I - ideal, II - design, III – dynamic

Chapter 1.
The movement of friable materials along the spatially vibrating plane

1.1. A spatial dynamic model of the loaded vibrating transport machine

1.1.1. A spatial dynamic model of the friable technological load (TL)

To include a technological load of friable type in the overall three-dimensional system and to make it generic, we formally represent it as a rigid body with an elastic system, which constitutes a tentative model of elastic characteristics of bulk material.

At a fixed moment in time, the elastic system of load decomposes into six components that describe the elastic damping characteristics of material in space.

Peculiarity of the mentioned elastic model of material consists in its unilateralconstraint with the working member (WM) of the vibrating machine. The conditional elastic elements describe the nature of interaction of the layers of material with each other and with a base of the working member. Unlike other models, it can provide a degree of freedom in any direction and, accordingly, its inclusion in a spatial model of the overall dynamic system; at the same time, it can be brought to a simpler form: flat, linear, etc.

The representation of operational load (TL) in the form of a rigid body (when composing the kinetic energy expression) is due to the need forobtaining more generalized equations of motion of TL - not only linear(in this case, a material point could be taken as a model of load), but also rotational movements.

As will be shown later, during modeling, the elastic and damping coefficients will vary depending on theoperating mode of thevibratory exciter –the movement with or without lifting the WM off the surface.

In Figure I.3, deformations of the layers of bulk material are described by the elastic elements with elastic coefficients $k_{x_3}, k_{y_3}, k_{z_3}, k_{\theta_3}, k_{\psi_3}, k_{\varphi_3}$; during deformation of the layers, the energy absorption is described by damping coefficients $c_{x_3}, c_{y_3}, c_{z_3}, c_{\theta_3}, c_{\psi_3}, c_{\varphi_3}$.

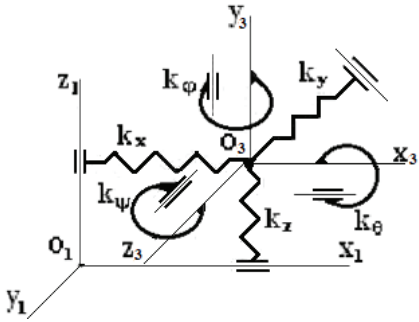

Fig.I.3. A generalized spatial dynamic model of bulk OL connected with the working member's surface ($O_1x_1y_1z_1$) ofthevibratingmachine

1.1.2. A spatial dynamic model of the working member of the vibrating machine with technological load.

The movement of operational load of the working member of the vibrating machine can be considered on the basis of complex motion of the rigid bodies [5, 8, 9].

The spatial motion of operational load (of a system $O_3x_3y_3z_3$) is considered to be a relative to the working member - and complex - relative to the stationary system (Fig. I.4).

Figure I.4 illustrates changes in the Euler rotation angles θ_1, ψ_1, φ_1 and θ_2, ψ_2, φ_2 of each mass and the corresponding positions of the coordinate axes $O_1'x_1'y_1'z_1'$and$O_2'x_2'y_2'z_2'$.

1.1.3. A generalized dynamic model of the system "vibratory exciter – WM of the vibrating machine - TL"

As mentioned in the introduction, there are many arguments justifying the advisability of representing and considering the vibrating technological machine in space.

Let us represent a loaded vibrating machine in space (Fig.I.5).

On the basis of classical methods of mechanics, we will consider the relative, translatory and absolute motion of a rigid body and material particle in space; to this end, we will connect fixedly the three-axis coordinate system $O_1x_1y_1z_1$, $O_2x_2y_2z_2$, $O_3x_3y_3z_3$,

respectively, to each component of the system "the vibrating machine's working member - vibratory exciter - operational load".

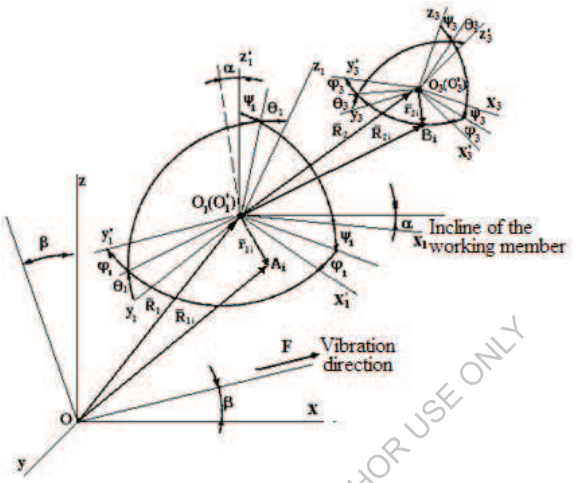

Fig.I.4.A spatial dynamic model of WM ($O_1 x_1 y_1 z_1$)
of the vibrating machinewith TL ($O_3 x_3 y_3 z_3$)

Let us consider the absolute spatial motion relative to the stationary (inertial) system *Oxyz* (Fig. I.5a); *V* – is the speed of material movement in the longitudinal direction of the working member; 2 - suspension; 3- the conditional elastic elements associated with bulk material; 1 - the main elastic system, through which vibrations from the vibration exciter are transmitted to the working member; *Q(t)* –the periodic exciting force.

Based on the above, thevibrating technological machine can be treated as a three-mass vibratory system, consisting of the following elements: active mass (working member) - M_1,reaction mass (vibratory exciter) - M_2,operational load (process or transport mass) - M_3 (Fig. I .6).

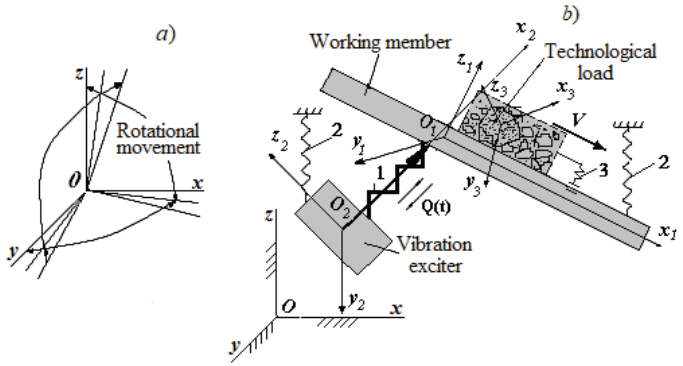

Fig. I.5. The movement of the loaded vibrating machine in space

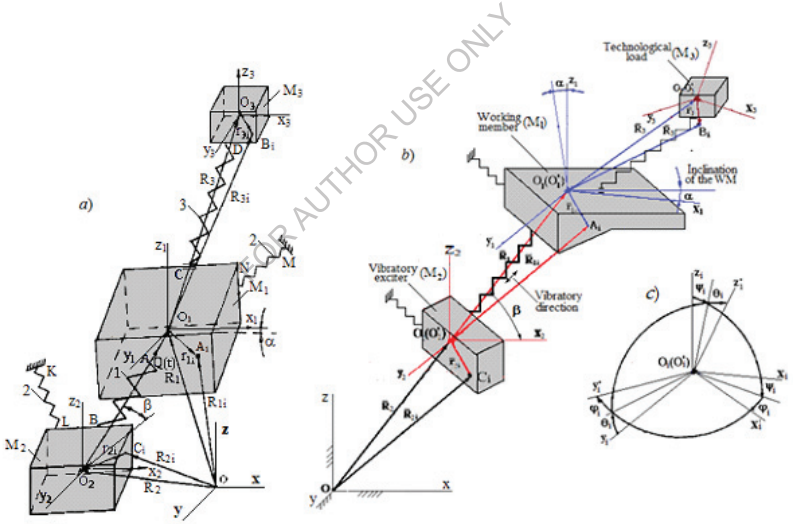

Fig.I.6. The tree-mass oscillatory system – an analogue of the vibrating technological machine: a) classical form, b) in the form of the vibrating machine

The main difference between the system under considerationand the classical *n*-mass system is associated with the following aspects: 1) the specificity of technological massperformingthe relative motion in relation to the operating member, while the masses M_1 and M_2 are coming into the independent movement from the external sources of energy; 2) the certain initial positions of masses M_1, M_2, M_3 relative to each other (such a condition turns the generally accepted sequence of mathematical model buildingintothe asymmetric one); 3) the singularities of interaction betweenM_1 and M_2, as masses attached to each other by conditional elastic joints; 4) taking into account deviation of the elastic joints from the unreformed state at large (for example, resonant) displacements.

1.2. Kinetic and potential energies of the system "vibratory exciter – elastic elements - WM of the vibrating machine - TL"

1.2.1. Determination of coordinates of points of the location of masses and the attachments of the elastic connections in a three-mass model of the vibrator

Consider the absolute motion of a system shown in Figure I.6, both in aggregate and for specific masses, both in relation to one other and to the inertial system.

Figure I.6 illustrates the points *A*, *B*, *C*, *D* of fixing the elastic elements of the vibration exciter; *K*, *L*, *M*, *N* – the suspension fixing points; A_i, B_i, C_i – the free points of corresponding masses; the masses are considered in three positions: I – an ideal position - motionless (according to design drawing), II –a post-installation position - motionless, III – a dynamic position - movable. The location of the coordinate systems associated with masses in the mentioned three positions is determined usingangular coefficients (directional cosines) in accordance with Table 1, where i = 1, 2, 3; m = I, II, III.

TableI.1

	x_i	y_i	z_i
x_i^m	$(\alpha_i^m)_{11}$	$(\alpha_i^m)_{12}$	$(\alpha_i^m)_{13}$
y_i^m	$(\alpha_i^m)_{21}$	$(\alpha_i^m)_{22}$	$(\alpha_i^m)_{23}$
z_i^m	$(\alpha_i^m)_{31}$	$(\alpha_i^m)_{32}$	$(\alpha_i^m)_{33}$

We represent the directional cosines (Table I.1) in the form of the Euler-Krylov angles θ_i, ψ_i, φ_1 [1]; in this case, due to the smallness of the rotational movements, the products of no higher than the second order will be taken into consideration. Taking into

account only the dynamic displacement, the directional cosines will be in the form shown in Table I.2.

If we take into account deviations of the coordinate systems caused by imperfection of the machine and some geometricspecifications, such as angles of vibration and slope α and β of the working member, we obtain an extended form of Table I.2 (Table I.3); with this aim in view, we use the expression

$$\left|\lambda_{ij}\right| = \left|\alpha_{ij}\right| \cdot \left|\alpha'_{ij}\right|, \qquad \text{(I.1)}$$

Table I.2

	x_1^{II}	y_1^{II}	z_1^{II}
x_1^{I}	$1-\psi_1^2/2$ $-\phi_1^2/2$	$-\varphi_1+\psi_1\theta_1$	ψ_1
y_1^{I}	ϕ_1	$1-\theta_1^2/2-$ $\phi_1^2/2$	$-\theta_1$
z_1^{I}	$-\psi_1-\phi_1\theta_1$	$-\phi_1\psi_1+\theta_1$	c

whereα_{ij} -resulting from initial imperfection, and α'_{ij} - caused by dynamic displacement – directional cosines. The right side disclosure (I.1) is made by multiplyingthe rows of the first factor by the columns of the second one, for example,

$$\begin{aligned}\lambda_{11} &= \alpha_{11}\alpha'_{11}+\alpha_{12}\alpha'_{21}+\alpha_{13}\alpha'_{31}\\ \lambda_{12} &= \alpha_{11}\alpha'_{12}+\alpha_{12}\alpha'_{22}+\alpha_{13}\alpha'_{32}\\ &\ldots\ldots\ldots\ldots\ldots\ldots\end{aligned} \qquad \text{(I.2)}$$

In this case, the location of the coordinate system $O^{\mathrm{I}}_1\, x^{\mathrm{I}}_1\, y^{\mathrm{I}}_1\, z^{\mathrm{I}}_1$ in relation to the *Oxyz* system is described in accordance with Table I.3

Table I.3

	$x_1^{''}$	$y_1^{''}$	$z_1^{''}$
x_1	$(1-\psi_1^2/2-\varphi_1^2/2-\varphi_{O1}^2/2-\psi_{O1}^2/2-$ $-\varphi_1\varphi_{O1}-\psi_1\psi_{O1})\cos\alpha+(\varphi_{O1}\theta_{O1}-\psi_{O1}+$ $+\varphi_1\theta_{O1}-\psi_1-\varphi_1\theta_1)\sin\alpha$	$(\psi_1\theta_1-\varphi_1-\varphi_{O1}+\psi_{O1}\theta_{O1}+$ $+\theta_1\psi_{O1})\cos\alpha+(\varphi_1\psi_{O1}+\varphi_{O1}\times$ $\times\psi_{O1}+\theta_{O1}-\varphi_1\psi_1+\theta_1)\sin\alpha$	$(\psi_{O1}-\theta_1\varphi_{O1}+\psi_{O1})\cos\alpha+$ $+(1-\psi_1\psi_{O1}-\theta_1\theta_{O1}-\psi_1^2/2-$ $-\theta_1^2/2-\psi_{O1}^2/2-\theta_{O1}^2/2)\sin\alpha$
y_1	$(\varphi_{O1}-\varphi_1-\psi_{11}\theta_{O1}$	$-1-\varphi_1\varphi_{O1}-\varphi_1^2/2-\theta_1^2/2-$ $-\varphi_{O1}^2/2-\theta_{O1}^2/2-\theta_1\theta_{O1}$	$\psi_1\varphi_{O1}-\theta_1-\theta_{O1}$

z_1	$-(1-\psi_1^2/2-\varphi_1^2/2-\varphi_{O1}^2/2-\psi_{O1}^2/2-$ $-\varphi_1\varphi_{O1}-\psi_1\psi_{O1})\times\sin\alpha+(\varphi_{O1}\theta_{O1}-$ $-\psi_{O1}+\varphi_1\theta_{O1}-\psi_1-\varphi_1\theta_1)\cos\alpha$	$-(\psi_1\theta_1-\varphi_1-\varphi_{O1}+\psi_{O1}\theta_{O1}+$ $+\theta_1\psi_{O1})\sin\alpha+\psi_{O1}(\varphi_1+$ $+\varphi_{O1})+\theta_{O1}-\varphi_1\psi_1+\theta_1)\cos\alpha$	$-(\psi_{O1}-\theta_1\varphi_{O1}+\psi_{O1})\times\sin\alpha+$ $+(1-\psi_1\psi_{O1}-\theta_1\theta_{O1}-\psi_1^2/2-$ $-\theta_1^2/2-\psi_{O1}^2/2-\theta_{O1}^2/2)\cos\alpha$

In Table I.3, the index *"i"* marks the angles that are obtained by rotating the axes as a result of dynamic displacement, and the index *"o_i"* marks the angles obtained by initial deviations from an ideal (design) position, due to errors in the manufacture of components and machine installation.

The locations of other coordinate systems are determined in the same way.

To determine the position of masses of the multi-mass interlocking oscillatory system in space, it is necessary to determine the coordinates of the centers of gravity, the fixing points of the elastic elements and suspensions to masses, as well as to bring them to a single, particular coordinate system; this operation is carried out using the above directional cosines. For example, let us turn the coordinates of the fixing point A of the main elastic element into the coordinate system $Oxyz$, after dynamic displacement of masses

$$\begin{aligned} x_A &= x_{O_1} + x_{1A}\alpha_{11} + y_{1A}\alpha_{12} + z_{1A}\alpha_{13} \\ y_A &= y_{O_1} + x_{1A}\alpha_{21} + y_{1A}\alpha_{22} + z_{1A}\alpha_{23} \\ z_A &= z_{O_1} + x_{1A}\alpha_{31} + y_{1A}\alpha_{32} + z_{1A}\alpha_{33}, \end{aligned} \qquad \text{(I.3)}$$

were $x_{O_1}, y_{O_1}, z_{O_1}$ - are the coordinates of a point O_1 in a coordinate system Oxyz; x_{1A}, y_{1A}, z_{1A} - the coordinates of a point A in a coordinate system $O_1x_1y_1z_1$; α_{11},.....,α_{33} - directional cosines in accordance with Table I.3.

1.2.2. The vector expression for the kinetic energy of the three-mass spatial vibration system –theanalogue of a loaded vibration machine

When determining the kinetic energy of the three-mass kinetic energy, the initial deviations (due to malfunction) of the coordinate systems will be taken into account. The movements of masses M_1 and M_2 will be treated as independent, while the mass movement is considered to be a relative to the mass M_1.

To obtain the general vector kinetic energy expressions, we determine the absolute velocities of the free points A_i, B_i, C_i of each mass. These points are connected to the origins of the coordinate systems, both their own and the fixed coordinate system; in addition, M_3 is connected to the center of gravity of the mass (to the origin of the coordinate system); this connection can be unilateral, depending on the type of cargo and the type of motion mode. The vector expressions for the velocities of points A_i, B_i, C_i willtake the form as follows:

$$\begin{aligned} V_{A_i} &= V_{O_1} + \omega_{O_1} \times r_{1i}, \\ V_{C_i} &= V_{O_2} + \omega_{O_2} \times r_{2i}, \\ V_{B_i} &= V_{O_1} + \omega_{O_1} \times R_{3i} + V_{O_3} + \omega_{O_3} \times r_{3i}, \quad (R_3 = R + r_{3i}), \end{aligned} \tag{I.4}$$

where $R_{3i} = R_{3i} + r_{3i}$; $V_{O_1}, V_{O_2}, V_{O_3}$ - the linear velocities of points O_1, O_2, and O_3; r_{1i}, r_{2i}, r_{3i} - the radius-vectors of particles A_i, B_i, and C_i; $\omega_{O_1}, \omega_{O_2}, \omega_{O_3}$ - the velocities of the rotational movement of masses.

Accordingly, the kinetic energy expressions will take the form as follows:

$$T_1 = \frac{1}{2}\sum_{i=1}^{n_1} M_{1i}[V_{A_i}]^2; \qquad T_2 = \frac{1}{2}\sum_{i=1}^{n_2} M_{2i}[V_{B_i}]^2; \qquad T_3 = \frac{1}{2}\sum_{i=1}^{n_3} M_{3i}[V_{C_i}]^2. \tag{I.5}$$

By applying (I.4) to (I.5), we obtain

$$T_1 = \frac{1}{2}\sum_{i=1}^{n_1} M_{1i}[V_{01}^2 + (\omega_{01} \times r_{1i})^2 + V_{01}(\omega_{01} \times r_{1i})];$$

$$T_2 = \frac{1}{2}\sum_{i=1}^{n_2} M_{2i}[V_{02}^2 + (\omega_{02} \times r_{2i})^2 + V_{02}(\omega_{02} \times r_{2i})];$$

$$\begin{aligned} T_3 = \frac{1}{2}\sum_{i=1}^{n_3} M_{3i}[V_{01}^2 + (\omega_{01} \times R)^2 + (\omega_{01} \times r_{3i})^2 + V_{03} + (\omega_{03} \times r_{3i})^2 + 2V_{01}(\omega_{01} \times R) + 2V_{01}(\omega_{01} \times r_{3i}) + \\ + 2(\omega_{01} \times R)(\omega_{03} \times r_{3i}) + 2V_{03}(\omega_{01} \times r_{3i}) + 2(\omega_{01} \times r_{3i})(\omega_{03} \times r_{3i}) + 2V_{03}(\omega_{03} \times r_{3i}) \end{aligned}$$

where M_{1i}, M_{2i}, M_{3i} – the masses of particles A_i, B_i, and C_i.

1.2.3. An expansion of kinetic energy along the coordinate axes

If we decompose the components of the above obtained kinetic energy expressions with respect to the axes of the coordinate system $O_1''x_1''y_1''z_1''$ (for which we will use tables I.1 and I.3 and the expressions (I.1)), we obtain:

$$T_1 = \frac{1}{2}M_1(\dot{x}_1^2 + \dot{y}_1^2 + \dot{z}_1^2) + \frac{1}{2}(J_{x1}\dot{\theta}_1^2 + J_{z1}\dot{\phi}_1^2 + J_{y1}\dot{\psi}_1^2) + (J_{x1} - J_{y1})\dot{\theta}_1\dot{\psi}_1\dot{\phi}_1 - J_{z1}\dot{\phi}_1\dot{\psi}_1\theta_1; \quad \text{(I.6)}$$

$$T_2 = \frac{1}{2}M_2(\dot{x}_2^2 + \dot{y}_2^2 + \dot{z}_2^2) + \frac{1}{2}[(J_{x2}\cos^2\alpha_1 + J_{z2}\sin^2\alpha_1)\dot{\theta}_2^2 + (J_{x2}\sin^2\alpha_1 + J_{z2}\cos^2\alpha_1)\dot{\phi}_2^2 +$$
$$+ J_{y2}\dot{\psi}_2^2 + (J_{x2} - J_{z2})\sin\alpha_1\cos\alpha_1\dot{\theta}_2\dot{\varphi}_2 + (J_{x2}\cos^2\alpha_1 + J_{z2}\sin^2\alpha_1 - J_{y2})\dot{\theta}_2\dot{\psi}_2\varphi_2 + \quad \text{(I.7)}$$
$$+ (J_{z2} - J_{x2})\cos\alpha_1\dot{\theta}_2\dot{\psi}_2\theta_2 + (J_{x2} - J_{z2})\sin\alpha_1\dot{\varphi}_2\dot{\psi}_2\varphi_2 - (J_{x2}\sin^2\alpha_1 + J_{z2}\cos^2\alpha_1)\dot{\varphi}_2\dot{\psi}_2\theta_2;$$

$$T_3 = \frac{1}{2}M_3(\dot{x}_1^2 + \dot{y}_1^2 + \dot{z}_1^2 + \dot{x}_3^2 + \dot{y}_3^2 + \dot{z}_3^2) + \frac{1}{2}[J_{x1}(\dot{\theta}_1^2 + 2\dot{\theta}_1\dot{\psi}_1\varphi_1) + J_{z1}(\dot{\varphi}_1^2 - 2\dot{\varphi}_1\dot{\psi}_1\theta_1) +$$
$$+ J_{y1}(\dot{\psi}_1^2 + 2\dot{\psi}_1\dot{\theta}_1\varphi_1) + J_{x3}\dot{\theta}_1^2 + J_{y3}\dot{\psi}_1^2 + J_{z3}\dot{\varphi}_1^2 + J_{x3}\dot{\theta}_3^2 + J_{y3}\dot{\psi}_3^2 + J_{z3}\dot{\varphi}_3^2] + (J_{x3} - J_{y3})\dot{\theta}_1\dot{\psi}_1\varphi_1 -$$
$$- J_{z3}\dot{\varphi}_1\dot{\psi}_1\theta_1 + (J_{x3} - J_{y3})\dot{\theta}_3\dot{\psi}_3\varphi_{01} + (J_{x3} - J_{z3})\dot{\psi}_3\dot{\theta}_3\varphi_1 + (J_{x3} + J_{z3})(\dot{\varphi}_3\dot{\theta}_3\psi_3 - \dot{\theta}_3\dot{\varphi}_3\psi_{01} -$$
$$- \dot{\theta}_3\dot{\varphi}_3\psi_1) + (J_{y3} - J_{z3})(\dot{\varphi}_3\dot{\psi}_3\theta_{01} + \dot{\varphi}_3\dot{\psi}_3\theta_1) - J_{y3}\dot{\varphi}_3\dot{\psi}_3\theta_3 + M_3[\dot{\theta}_1\dot{z}_1y_3 + x_1\dot{\psi}_1\dot{z}_3 -$$
$$- \dot{\psi}_1\dot{z}_1x_3 - \dot{\varphi}_1\dot{x}_1y_3)\cos\alpha_1 + \dot{\theta}_1\dot{x}_1y_3 - z_1\dot{\psi}_1\dot{z}_3 - \dot{\psi}_1\dot{x}_1x_3 + \dot{\varphi}_1\dot{z}_1y_3)\sin\alpha_1 -$$
$$- \dot{\theta}_1\dot{\varphi}_1z_3 + \dot{\varphi}_1\dot{y}_1x_3] + (J_{y3} + J_{z3})\dot{\theta}_3\dot{\psi}_1\varphi_1 + (J_{x3} - J_{y3})\dot{\theta}_1\dot{\psi}_3\varphi_1 + (J_{y3} - J_{z3})\dot{\psi}_1\dot{\varphi}_3\theta_1 +$$
$$+ J_{y3}(\dot{\psi}_1\dot{\psi}_3 - \dot{\psi}_1\dot{\theta}_3\varphi_{01} - \dot{\psi}_1\dot{\varphi}_3\theta_3 + \dot{\psi}_1\dot{\varphi}_3\theta_{01}) + J_{z3}(\dot{\varphi}_1\dot{\theta}_3\psi_1 - \dot{\varphi}_1\dot{\theta}_3\psi_{01} - \dot{\varphi}_1\dot{\theta}_3\psi_3 - \dot{\varphi}_1\dot{\psi}_3\theta_1 -$$
$$- \dot{\varphi}_1\dot{\psi}_3\theta_{01} + \dot{\varphi}_1\dot{\varphi}_3) + J_{x3}(\dot{\theta}_1\dot{\theta}_3 + \dot{\theta}_1\dot{\psi}_3\varphi_{01} + \dot{\theta}_1\dot{\varphi}_3\psi_3 - \dot{\theta}_1\dot{\varphi}_3\psi_{01} - \dot{\theta}_1\dot{\varphi}_3\psi_1) +$$
$$+ M_3[x_1\dot{x}_3 - x_1\dot{z}_3\psi_{01} - z_1\dot{z}_3)\cos\alpha_1 + x_1\dot{y}_3\theta_1 + x_1\dot{y}_3\theta_{01} + x_1\dot{x}_3\psi_{01} - z_3\dot{x}_1\psi_1 - x_3\dot{z}_1 + z_1\dot{y}_3\varphi_1 +$$
$$+ z_1\dot{y}_3\varphi_1 - z_1\dot{y}_3\varphi_{01} + z_3\dot{x}_1 - z_3\dot{z}_1\psi_1 - z_1\dot{z}_3\psi_{01})\sin\alpha_1 + y_1\dot{x}_3\varphi_{01} + y_1\dot{x}_3\varphi_1 - y_3\dot{y}_1 - \quad \text{(I.8)}$$
$$- y_1\dot{z}_3\theta_1 - y_1\dot{z}_3\theta_{01}] + M_3(\theta_1\dot{z}_3y_3 - \dot{\theta}_1\dot{y}_3z_3 - \dot{\psi}_1\dot{z}_3x_3 + \dot{y}_3\dot{\varphi}_1x_3 + \dot{\varphi}_1\dot{x}_3y_3 - \dot{\psi}_1\dot{x}_3z_3],$$

where $x_1, y_1, z_1, x_2, y_2, z_2; \theta_1, \psi_1, \varphi_1, \theta_2, \psi_2, \varphi_2, x_3, y_3, z_3, \theta_3, \psi_3, \phi_3$ – the coordinates of the motion of centers O_1, O_2 andO_3 of the massesM_1, M_2, and M_3;

J_{x1}, J_{y1}, J_{z1}- the moments of inertiaof the mass M_1 relative to the axes $O_1x_1y_1z_1$; J_{x2}, J_{y2}, J_{z2} - the moments of inertia of mass M_2relative to the axes $O_2x_2y_2z_2$; J_{x3}, J_{y3}, J_{z3} - the moments of inertia of the mass M_3 relative to the axes $O_3''x_3''y_3''z_3''$.

The total kinetic energywill be equal to:

$$\Sigma T = T_1 + T_2 + T_3. \quad \text{(I.9)}$$

1.2.4. Potential energy and deformation forces of the main elasticsystem of the vibrating machines

The deformation forces of the elastic system *1* can be determined depending on the expected magnitude of deformation and the mode (for example, resonant mode), as well as on the operating conditions.

With the large displacements of the oscillating masses, the classical expression of potential energy, which is the basis for the Lagrange's equation and yielding the differential equations, loses its validity. In this case, it is necessary to directly compose the expressions of the elastic forces and their moments and put them into the differential equations. In this case, the operation of differentiating kinetic energy by the generalized velocity remains in force and is performed according to the Lagrange's equation.

This approach was chosen becausewith the large displacements, the direction of the deformed elastic element cannot follow its initial direction; therefore, it is necessary to define the projections of the elastic forces and their moments on the coordinate axes independently, that is, according to the projections of the difference between the lengths of the initial and deformed elastic element. To include operational load (M_3) in the overall spatial system (Fig. 1.6), and to give it a generalized scope, we represent it formally as a rigid body, where the elastic system 3 represents a tentative model of the elastic characteristics of technological bulk material.

At a fixed point in time, the elastic system 3 decomposes into 6 components, which describe the elastically damped nature of the transported material in space. The peculiarity of the elastic system 3 (Fig. I.3, I.5, I.6) consists in unilateral constraint with the working memberwhile moving; with the aid of the conditional elastic elements, there is described the nature of the inner layers of bulk material, interactions between the inner layers and between them and the surfaces of the working body.

As against existing models [1, 14, 16, 17], they are able to account all degrees of freedom and could therefore be included in acommon spatial system (Fig.); at the same

time, depending on the specific problem, this system can be brought to a simpler form: flat, linear, and punctual.

The representation of bulk operational load in the form of a rigid body is due to the need to obtain the equations of motion of cargo of a more general form - not only linear (in this case, operational load could be taken as a material point), but also rotational motion.

Let us represent the elastic system connecting two parts (active and reactive) of a resonant electromagnetic vibration machine, by means of the elastic elements decomposed in space (Fig. I.7).

The representation of one elastic element by two spatial systems is due to the fact that the elastic element connecting two moving parts of the resonant machine during their oscillations is stationary at a point whose position is a function of the values of the oscillating masses (Fig. I.7).

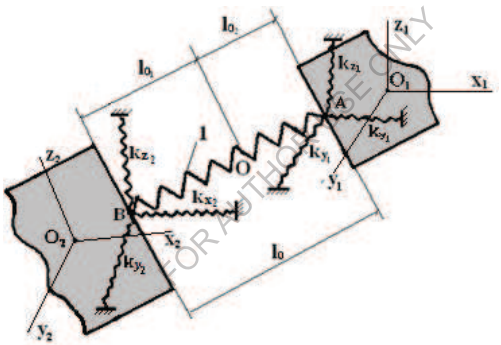

Fig. I.7. Decomposition in space of the main elastic system at the fixing points with the active and reactive masses of the resonant electro-vibrating machine

With a small displacement of the masses of the vibrating machine, the direction of movement is assumed to be identical with the axis of the elastic element, and the elastic force is proportional to its deformation; in this case, the elastic forces F_x, F_y, and F_z, are described in terms of linear expressions

$$F_{xA}=k_{xA}x_A\,;\ F_{yA}=k_{yA}y_A\,;\ F_{zA}=k_{zA}z_A. \qquad \text{(I.10)}$$

and the potential energy of the elastic system attached to point A is determined by the following expression

$$U_A = \frac{1}{2}\sum_{i=1}^{3}(k_{xA}x_{Ai}^2 + k_{yA}y_{Ai}^2 + k_{zA}z_{Ai}^2) \qquad \text{(I.11)}$$

The same expression is also obtained for point B.

1.2.5. The elastic and resistance forces at large (resonant) displacements of the vibrating masses

With the large displacements of the masses (resonance modes, etc.), the potential energy expression (I.11) cannot be valid, and in order to obtain the generalized elastic forces and moments, it is necessary to compose directly their expressions and put them into the differential equations; the kinetic energy differentiation operation remains valid. This approach is determined by the fact that at large displacements, the direction of the deformed elastic elements cannot be considered identical with its initial (undeformed) direction, and it is necessary to determine the elastic forces and their moments on each axis of the coordinate system independently [5].

Let us consider this approach briefly.

The deformation force of the elastic element has the form

$$F_1 = k_1 \Delta l_1 \quad , \qquad \text{(I.12)}$$

where Δl_1 is an elongation (truncation)

$$\Delta l_1 = l_1 - l_{01} \ ; \qquad \text{(I.13)}$$

k_1 - spring flexibility coefficient; l_{01} - the initial (undeformed) spring length;

The projections of the force F_1 on the coordinate axis $Oxyz$ will have the form as follows

$$F_{1x} = F_1 \cos(x, l_1); F_{1y} = F_1 \cos(y, l_1); F_{1z} = F_1 \cos(z, l_1), \qquad \text{(I.14)}$$

where $\cos(x,l_1) = \frac{x_{A'} - x_B}{l_1}$; $\cos(y,l_1) = \frac{y_{A'} - y_B}{l_1}$; $\cos(z,l_1) = \frac{z_{A'} - z_B}{l_1}$. (I.15)

If we put (I.15)into (I.14),and take account for (I.13), we shall obtain

$$F_{1x} = k_{1x}(1-\frac{l_{01}}{l_1})(x_A - x_B)\,; F_{1y} = k_{1y}(1-\frac{l_{01}}{l_1})(y_A - y_B)\,; F_{1z} = k_{1z}(1-\frac{l_{01}}{l_1})(z_A - z_B)\,. \quad \text{(I.16)}$$

Let us introduce the following notations

$$1-\frac{l_{01}}{l_1} = Q_1(q_1^{'}); \frac{l_{01}}{l_1} = f_1(q_1^{'})\,, \quad \text{(I.17)}$$

thenthe equation system (I.16) can be rewritten as follows

$$F_{1x} = k_{1x} f_1(q_1^{'})(x_A - x_B)\,; F_{1y} = k_{1y} f_1(q_1^{'})(y_A - y_B)\,; F_{1z} = k_{1z} f_1(q_1^{'})(z_A - z_B)\,. \quad \text{(I.18)}$$

The length of the elastic element after the dynamic displacements of the masses M_1 and M_2has the form:

$$l_1 = \sqrt{(x_A - x_B)^2 + (y_A - y_B)^2 + (z_A - z_B)^2}\,, \quad \text{(I.19)}$$

where x_A,…..,$x_B$are coordinates of the fixing points A and B (Fig. I. 2). The expression(I.19)can be represented as

$$l_1 = \sqrt{m^2 + q_1^{'}}\,, \quad \text{(I.20)}$$

where $q_1^{'}$is a function of linear and rotational motion of the masses M_1 and M_2; m – the square root of the sum of the constant valueson the right-hand side of the expression (I.19).

Let us expand the function

$$f_1(q_1^{'}) = l_{01}/l_1 = n(1+q_1)^{-1/2}$$

in a Maclaurin seriesand confine ourselves to the values of a second degree of the smallness

$$f_1(q_1^{'}) = n(1-\frac{1}{2}q_1 + \frac{3}{8}q_1^2\,, \quad \text{(I.21)}$$

where $q_1 = q_1^{'}/m^2$; $n = l_{01}/m$.

Let us rewrite the function $Q_1(q_1^{'})$ as follows

$$Q_1(q_1^{'}) = 1 - f_1(q_1) = 1 - n + \frac{1}{2} n q_1 - \frac{3}{8} n q_1^2 . \qquad \text{(I.22)}$$

Because of the smallness of q_1 in the expansionof (1.21), we'll keep the second-order terms

$$f_1(q_1) = \frac{l_{01}}{m_1} - \frac{l_{01}}{m_1^3} q_1^{'} . \qquad \text{(I.23)}$$

According to the expression (I.22), we'll have

$$Q(q_1) = 1 - \frac{l_{01}}{m_1} - \frac{l_{01}}{m_1^3} q_1^{'} \qquad \text{(I.24)}$$

1.2.6. Determination of potential energy and deformation forces of the elastic system of operational load

To include the transported material into the general spatial system "vibratory exciter –operating member - operational load - elastic system" and give it a generalized form, we represent it formally as a rigid body (Fig. I.8), where the elastic system 3 is a conditional model of the elastic characteristics of the transported bulk material.

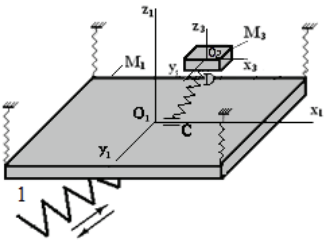

Fig. I.8.A spatial model of the system "vibratory exciter-elastic system-operating member-TL"

At a fixed point in time, the elastic system 3 decomposes into threeparts, which describe the elastic characteristics of material in three directions (k_{x3}, k_{y3}, k_{z3}).The originality of the elastic system 3 lays in the fragility of its link to TL and WM in both static and dynamic states.

By means of the elastic elements of ageneric spatial model (Fig. I.9), there are described: interlayer elastic-damping characteristics of bulk material; interaction between the layers of material and the surface of the working member. Unlike other models, it takes into account all degrees of freedom and can be included in a spatial model; at the same time, depending on the specific problem, it can be reduced to a simpler model (linear, plane, or punctual).

Representation of a TL in the form of a rigid body is due to the need to obtain a generalized equation of motion of TL - not only for linear (in this case, we could use a punctual model) but for rotational motion as well

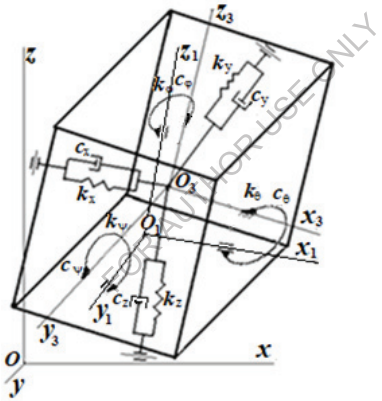

Fig. I.9. A generalized spatial model of TL

The modeling of deformations of the layers during motion is carried out by means of the elastic elements with elastic constants k_x, k_y, k_z, k_θ, k_ψ, and k_φ. The modeling of energy dissipation is provided by dampers with coefficients c_x, c_y, c_z, c_θ, c_ψ, $k_{\varphi;}$ direct contact of TL with the WMis changed by elastic-frictional bonds.

While determining the potential forces of a conditional elastic system 3, depending on the magnitude of displacement (bouncing), it is possible to use (as for the elastic system 1) two approaches, such as composing the expressions for potential energy at small displacements, and the direct determination of elastic forces at large displacements.

To determine the length of the conditional elastic system 3, it is necessary to determine the coordinates of its fixing points to the masses M_1 and M_2; in this case, points C and D are not fixed due to a change in the trajectory of load; but, if we assume that the machine is continuously filled with bulk material, its height and center of gravity can be considered constant. Now, if we connect the center of gravity of material with the center of gravity of the WM by means of the conditional elastic elements, the determination of their coordinates is easily implementable. Hereinafter, the determination of the elastic forces is carried out similarly to the elastic element 1 (Fig. I.5, I.8).

1.2.7. The force field of the vibrating system-the damping forces and their moments

Based on the expression (I.18), the projections of the elastic forces acting at point A of the body M_1 are determined

$$F_{X1} = Q_1(q_1)\ k_{X1}(x_{1A} - x_{1B}) = Q_1(q_1)\ k_{X1}(x_A\nu_{11} + y_A\nu_{12} + z_A\nu_{13} - x_B\nu_{11} - y_B\nu_{12} - z_B\nu_{13}) \tag{I.25}$$

where ν_{ij} - are the directyional cosine angles between the axes of the coordinate systems $Oxyz$ and $O_1''x_1''y_1''z_1''$.

A similar determination can be made for F_{Y1} and F_{Z1}

$$F_{Y1} = Q_1(q_1)\ k_{Y1}(y_{1A} - y_{1B});\ \ F_{Z1} = Q_1(q_1)\ k_{Z1}(z_{1A} - z_{1B}); \tag{I.26}$$

The moments of force F_1 applied to point A of the body M_1 relative to the ases of a coordinate system $O_1''x_1''y_1''z_1''$ are determined similarly to gliding vectors [6]

$$\begin{aligned} M_{X_1''} &= F_{Z_1}y_{1A} - F_{Y_1}z_{1A}; \\ M_{Y_1''} &= F_{X_1}z_{1A} - F_{Z_1}x_{1A}; \\ M_{Z_1''} &= F_{Y_1}x_{1A} - F_{X_1}y_{1A}. \end{aligned} \tag{I.27}$$

The same method is used to determine the moments of forces of other elastic materials.

To determine the forces and moments of resistance, the hypothesis [5] is used, according to which these forces are applied to the fixing points of the elastic elements to the masses (for the elastic system 1 - to points A and B), and they are proportional to the displacement velocities of

these points. In this case, the expressions of forces and moments in form shall be similar to the forces and moments of elasticity (I.26), (I.27), but the displacements will be replaced by the velocities and the elastic constants k_q - by the resistance coefficients c_q.

The projections of the resistance forces acting on point A will have the form as follows:

$$\begin{aligned}
\Phi_{X_1^*} &= c_{x_1} f_x(\dot{x}_1, \dot{y}_1, \dot{z}_1, \dot{x}_2, \dot{y}_2, \dot{z}_2, \dot{\varphi}_1, ..., \dot{\varphi}_2); \\
\Phi_{Y_1^*} &= c_{y_1} f_y(\dot{x}_1, \dot{y}_1, \dot{z}_1, \dot{x}_2, \dot{y}_2, \dot{z}_2, \dot{\varphi}_1, ..., \dot{\varphi}_2); \\
\Phi_{Z_1^*} &= c_{z_1} f_z(\dot{x}_1, \dot{y}_1, \dot{z}_1, \dot{x}_2, \dot{y}_2, \dot{z}_2, \dot{\varphi}_1, ..., \dot{\varphi}_2).
\end{aligned} \tag{1.28}$$

The moments of the resistance forces will be determining similarly by analogy with (I.27).

Due to the fact that the method for determining the forces and moments of elasticity and damping for the remaining elastic elements (2, 3, 4 - Fig. I.1) are similar to the elastic element 1, they are not given here.

1.3. A mathematical model of the spatial system "vibratory exciter - the rigid WM of the vibrating machine - TL"

1.3.1. The generalized differential equations

The main difference between the system under consideration and the classical n-mass system is associated with the following aspects: 1) the specificity of technological mass performing the relative motion in relation to the operating member, while the masses M_1 and M_2 are coming into the independent movement from the external sources of energy; 2) the certain initial positions of masses M_1, M_2, M_3 relative to each other (such a condition turns the generally accepted sequence of mathematical model building into the asymmetric one); 3) the singularities of interaction between M_1 and M_2, as masses attached to each other by conditional elastic joints; 4) taking into account

deviation of the elastic joints from the undeformed state at large (for example, resonant) displacements.

Using the method of Lagrange and taking into account the difference of the considered vibration system from the classical *n*-mass system (paragraph 2.3), on the basis of the above expressions for the kinetic energy and potential forces,it is possible obtain the corresponding system of differential equations.

The Lagrangianequation for the system under consideration will have the form as follows

$$\frac{d}{dt}\left(\frac{\partial T}{\partial \dot{q}} - \frac{\partial T}{\partial q}\right) = Q_q + Q_q',$$

where T – the system's kinetic energy; q – generalized coordinate, taking on the values $x_1, y_1, z_1, x_2, y_2, z_2; \theta_1, \psi_1, \varphi_1, \theta_2, \psi_2, \varphi_2$, $x_3, y_3, z_3, \theta_3, \psi_3, \varphi_3$; Q_q - potential forces associated with an elastic system of the machine; Q_q' - forces that are not associated with deformations of the elastic systems or inertia of masses of the system under consideration (external forces, gravitational forces, resistance forces of a type of external friction, etc.).

In view of the above assumption about the smallness of the displacement (vibration), the equations will take account for products no higher than the second degree of smallness.

For the mass M_1, the equations will have the form

$$(M_1 + M_3)\ddot{x}_1 + M_3[(\psi_1 z_3 + 2\dot{\psi}_1 z_3 + \ddot{\varphi}_1 y_3 - 2\dot{\varphi}_1 y_3 - \ddot{y}_3 \varphi_1 + \ddot{z}_3 \psi_1)\cos\alpha_1 +$$

$$(\cos\alpha + \psi_{01}\sin\alpha)\ddot{x}_3 - \varphi_{01}(\cos\alpha + \theta_{01}\sin\alpha)\ddot{y}_3 + \psi_{01}(\cos\alpha +$$

$$+\sin\alpha)\ddot{z}_3 + \ddot{\theta}_1 y_3 + \ddot{x}_3\psi_1 - 2\dot{\theta}_1\dot{y}_3 - 2\dot{x}_3\dot{\psi}_1 - \ddot{\psi}_1 x_3 + \ddot{y}_3\theta_1)\sin\alpha = Q_{x1} + Q_{x1}';$$

$$(M_1 + M_3)\ddot{y}_1 = M_3(\ddot{\varphi}_1 x_3 - \ddot{\theta}_1 z_3 - 2\dot{\theta}_1\dot{z}_3 - 2\dot{\varphi}_1\dot{x}_3 + \ddot{x}_3\varphi_{01} + \ddot{x}_3\varphi_1 +$$

$$+\ddot{y}_3 - \ddot{z}_3\theta_{01} - \ddot{z}_3\theta_1) = Q_{y1} + Q_{y1}'$$

$$(M_1 + M_3)\ddot{z}_1 + M_3[(\ddot{\theta}_1 y_3 + 2\dot{\theta}_1\dot{y}_3 - \ddot{\psi}_1 x_3 - 2\dot{\psi}_1\dot{x}_3 - \ddot{x}_3\psi_1 + \ddot{y}_3\theta_1)\cos\alpha_1 -$$

$$-(\sin\alpha_1 + \psi_{01}\cos\alpha_1)\ddot{x}_3 + +(\theta_{01}\cos\alpha_1 + \varphi_{01}\sin\alpha_1)\ddot{y}_3 + (\cos\alpha_1 -$$

$$-\psi_{01}\sin\alpha_1)\ddot{z}_3+\ddot{\varphi}_1\,y_3-\ddot{\psi}_1\,z_3-2\dot{\psi}_1\dot{z}_3+2\dot{y}_3\dot{\varphi}_1+\ddot{y}_3\,\varphi_1-$$

$$-\ddot{y}_3\,\psi_1)\sin\alpha_1]=Q_{z1}+Q'_{z1};$$

$$A_{1\theta}\ddot{\theta}_1+A_{2\theta}\ddot{\psi}_1\varphi_1+A_{3\theta}\dot{\varphi}_1\dot{\psi}_1+M_3(\ddot{z}_1\,y_3\cos\alpha_1+\ddot{x}_1\,y_3-$$

$$-\ddot{y}_1\,z_3+\ddot{z}_3\,y_3-\ddot{y}_3\,z_3)+A_{4\theta}\ddot{\psi}_3\varphi_1+A_{5\theta}\dot{\varphi}_3\dot{\psi}_3+A_{6\theta}\ddot{\varphi}_3\psi_1+$$

$$+A_{7\theta}\dot{\psi}_3\dot{\varphi}_1+A_{8\theta}(\ddot{\theta}_3+\ddot{\psi}_3\varphi_{01}+\ddot{\varphi}_3\psi_3-\ddot{\varphi}_3\psi_{01}-\ddot{\varphi}_3\psi)=Q_{\theta 1}+Q'_{\theta 1};$$

$$A_{1\psi}\ddot{\psi}_1+A_{2\psi}\ddot{\varphi}_1\theta_1+A_{3\psi}\ddot{\theta}_1\varphi_1+A_{4\psi}\dot{\theta}_1\dot{\varphi}_1+M_3[(\ddot{x}_1\,z_3-\ddot{z}_1\,x_3)\cos\alpha_1-(\ddot{z}_1\,z_3+$$

$$+\ddot{x}_1\,x_3)\sin\alpha_1+\ddot{x}_3\,z_3-\ddot{z}_3\,x_3]+A_{5\psi}\ddot{\theta}_3\varphi_1+A_{6\psi}\dot{\varphi}_1\dot{\theta}_3+A_{7\psi}\ddot{\varphi}_3\theta_1+A_{8\psi}\dot{\theta}_1\dot{\varphi}_3+$$

$$A_{9\psi}(\ddot{\psi}_3-\ddot{\theta}_3\varphi_{01}+\ddot{\varphi}_3\theta_{01}-\ddot{\varphi}_3\theta_3)+A_{10\psi}\ddot{\theta}_3\varphi_3=Q_{\psi 1}+Q'_{\psi 1};$$

$$A_{1\varphi}\ddot{\varphi}_1+A_{2\varphi}\ddot{\psi}_1\theta_1+A_{3\varphi}\dot{\psi}_1\dot{\theta}_1+M_3(\ddot{y}_1\,x_3-2\dot{y}_1\dot{x}_3+\ddot{y}_3\,x_3-\ddot{x}_3\,y_3-y_3\,\ddot{x}_1)\cos\alpha_1+$$

$$\ddot{z}_1\,y_3\sin\alpha_1)+A_{4\varphi}(\ddot{\theta}_3\psi_1-\ddot{\theta}_3\psi_{01}+A\dot{\theta}_1\dot{\varphi}_3-\dot{\theta}_3\psi_3+\ddot{\varphi}_3-\dot{\psi}_3\dot{\theta}_1-$$

$$+A_{6\varphi}\dot{\theta}_3\dot{\psi}_3+A_{7\varphi}\dot{\theta}_1\dot{\psi}_3=Q_{\varphi 1}+Q'_{\varphi 1}, \qquad \text{(I.29)}$$

where $A_{1\theta}, A_{2\theta}, ..., A_{7\varphi}$ - the functions of the sum moment of inertia relative tot he respective axes, for example

$$A_{1\theta}=J_{x1}^{O1}+J_{x3}^{O3};\quad A_{2\theta}=J_{x1}-J_{y1}+J_{z3}-J_{y3};$$
$$A_{3\theta}=J_{x1}-J_{y1}+J_{z3}-J_{y3}+J_{z1}+J_{z3};\ \text{da a. S.}$$

The terms on the right-hand side of the equation (I.29) contain inertial forces that are generated through the interaction of masses M_1 and M_3; at the same time, in the first three equations, the non-linear terms (products) arose due to the relative motion of the mass M_3 and taking into account the error (θ_{01}, ψ_{01}, φ_{03}, etc.) in the manufacture and installation of a real vibrating machine. In the event of $M_3 = 0$, the indicated terms will not be there. The following three equations contain non-linear terms as a result of both the rotational

motion of the mass M_3 and the proper motion of the mass M_1, which follows from the rule for constructing a mathematical expression for the motion of a rigid body [6].

The potential field of the position of the mass M_1 is associated with the state of the elastic systems I and II, which connect the masses M_1, M_2 and$M_3$and therefore, in the formation of the elastic forces that create a potential field, the coordinates of these masses will also appear; this is displayed on the right-hand side of the expression (1.34) by means of symbol Q_q ($Q_q = f\,(q_1)$, where i = 1, 2, 3.

The motion of the mass M_2 is described by the following system of differential equations

$$\begin{aligned} M_2\,\ddot{x}_2 &= Q_{x2} + Q'_{x2};\\ M_2\,\ddot{y}_2 &= Q_{y2} + Q'_{y2};\\ M_2\,\ddot{z}_2 &= Q_{z2} + Q'_{z2}; \end{aligned} \qquad \text{(I.30)}$$

$$B_{1\theta}\,\ddot{\theta}_2 + B_{2\theta}\,\ddot{\varphi}_2 + B_{3\theta}(\ddot{\theta}_2\,\varphi_2 + \dot{\theta}_2\,\dot{\varphi}_2) + B_{5\theta}\,\dot{\varphi}_2\,\dot{\psi}_2 = Q_{\theta 2} + Q'_{\theta 2};$$

$$B_{1\psi}\,\ddot{\psi}_2 + B_{2\psi}\,\ddot{\theta}_2\,\varphi_2 + B_{3\psi}\,\dot{\theta}_2\,\dot{\varphi}_2 + B_{4\psi}(\ddot{\theta}_2\,\theta_2 - \dot{\theta}_2^{\,2}) - B_{5\psi}\,\dot{\varphi}_2\,\theta_2 + B_{6\psi}(\ddot{\varphi}_2\,\varphi_2 + \dot{\varphi}_2^{\,2}) = Q_{\psi 2} + Q'_{\psi 2};$$

$$B_{1\varphi}\,\ddot{\varphi}_2 + B_{2\varphi}\,\ddot{\theta}_2 + B_{3\varphi}\,\ddot{\psi}_2\,\theta_2 - \dot{\theta}_2\,\dot{\psi}_2 + B_{5\varphi}\,\ddot{\psi}_2\,\varphi_2 = Q_{\varphi 2} + Q'_{\varphi 2};$$

Unlike the expressions (I.29), in these equations there are no components of such an inertial type that would connect the motion of the mass M_2 with the masses M_1 or M_3, but there are potential forces that connect the motion of the masses $M_1$and M_2 by means of coordinates ($Q_q = f\,(q_i)$, where i = 1, 2; $q = x_1, x_2, \ldots, \varphi_2$).

As noted above, the mass M_3 performs relative motion in the coordinate system $O_1 x_1 y_1 z_1$ and absolute motion in $Oxyz$; the differential equations of motion for the mass M_3 will have the form

$$\begin{aligned} M_3[&\ddot{x}_3 + (\ddot{x}_1 - \ddot{z}_1\,\varphi_{01} - \ddot{z}_1\,\psi_1)\cos\alpha_1 - (\ddot{x}_1\,\psi_{01} + \ddot{z}_1 + \ddot{x}_1\,\psi_1)\sin\alpha_1 +\\ &+ \ddot{y}_1\,\varphi_{01} + \ddot{y}_1\,\varphi_1 + \ddot{\psi}_1\,z_3 - 2\dot{z}_3\,\dot{\psi}_1 - \ddot{\varphi}_1\,y_3 - 2\dot{y}_3\,\dot{\varphi}_1] = Q_{x3} + Q'_{x3}; \end{aligned}$$

$$\begin{aligned} M_3[&\ddot{y}_3 + \ddot{y}_1 + (\ddot{z}_1\,\theta_1 - \ddot{x}_1\,\varphi_1 - \ddot{x}_1\,\varphi_{01} + \ddot{z}_1\,\theta_{01})\cos\alpha_1 +\\ &+ (\ddot{x}_1\,\theta_{01} + \ddot{x}_1\,\theta_1 + \ddot{z}_1\,\varphi_1)\sin\alpha_1 - \ddot{\theta}_1\,z_3 - 2\dot{z}_3\,\dot{\theta}_1 + \ddot{\varphi}_1\,x_3 - 2\dot{x}_3\,\dot{\varphi}_1] = Q_{y3} + Q'_{y3}; \end{aligned}$$

$$M_3[\ddot{z}_3+(\ddot{z}_1+\ddot{x}_1\psi_1+\ddot{x}_1\psi_{01})\cos\alpha_1-(-\ddot{z}_1\psi_{01}+\ddot{x}_1-\ddot{z}_1\psi_1)\sin\alpha_1-$$

$$-\ddot{y}_1\theta_1-\ddot{y}_1\theta_{01}+\ddot{\theta}_1 y_3+2\dot{y}_3\dot{\theta}_1-\ddot{\psi}_1 x_3-2\dot{x}_3\dot{\psi}_1]=Q_{z3}+Q'_{z3};$$

$$C_{1\theta}(\ddot{\theta}_3+\ddot{\theta}_1)+C_{2\theta}\ddot{\psi}_3\varphi_{01}+C_{3\theta}\varphi_1\ddot{\psi}_3+C_{4\theta}\dot{\psi}_3\dot{\varphi}_1-C_{5\theta}\ddot{\varphi}_3\psi_3+$$

$$C_{6\theta}\dot{\varphi}_3\dot{\psi}_3+C_{7\theta}\psi_{01}\ddot{\varphi}_3+C_{8\theta}\ddot{\varphi}_3\psi_1+C_{9\theta}\dot{\psi}_1\dot{\varphi}_3+C_{10\theta}\ddot{\psi}_1\varphi_1+C_{11\theta}\ddot{\varphi}_1\psi_1-$$

$$-C_{12\theta}\ddot{\psi}_1\varphi_{01}+C_{13\theta}(\psi_1\ddot{\varphi}_1-\ddot{\varphi}_1\psi_{01}-\ddot{\varphi}_1\psi_3)=Q_{\theta3}+Q'_{\theta3};$$

$$C_{1\psi}(\ddot{\psi}_3+\ddot{\psi}_1)+C_{2\psi}\ddot{\psi}_3\varphi_{01}+C_{3\psi}\varphi_1\ddot{\theta}_3+C_{4\psi}\dot{\theta}_3\dot{\varphi}_1+C_{5\psi}\ddot{\varphi}_3\theta_1+C_{6\psi}(\ddot{\varphi}_3\theta_1+\dot{\theta}_1\dot{\varphi}_3)-$$

$$-C_{7\psi}\theta_1\ddot{\varphi}_3-C_{8\psi}\dot{\theta}_3\dot{\varphi}_3+C_{9\psi}\ddot{\theta}_1\varphi_1+C_{10\psi}\dot{\varphi}_1\dot{\theta}_1-C_{11\psi}(\ddot{\varphi}_1\theta_1+\ddot{\varphi}_1\theta_{01})+$$

$$+C_{12\psi}\varphi_{01}\ddot{\theta}_1-C_{13\psi}\dot{\theta}_1\dot{\psi}_3=Q_{\psi3}+Q'_{\psi3};$$

$$C_{1\varphi}(\ddot{\varphi}_3+\ddot{\varphi}_1)+C_{2\varphi}\ddot{\theta}_3\psi_3+C_{3\varphi}\dot{\theta}_3\dot{\psi}_3+C_{4\varphi}\ddot{\theta}_3\psi_{01}+C_{5\varphi}\dot{\theta}_3\psi_1+C_{6\varphi}\dot{\theta}_3\dot{\psi}_3+$$

$$+C_{7\varphi}\theta_{01}\ddot{\psi}_3+C_{8\varphi}\ddot{\psi}_3\theta_1+C_{9\varphi}\dot{\theta}_1\dot{\psi}_3-C_{10\varphi}\dot{\psi}_3\dot{\theta}_3+C_{11\varphi}\ddot{\psi}_1\theta_1+C_{12\varphi}\dot{\psi}_1\dot{\theta}_1+C_{13\varphi}(\ddot{\psi}_1\theta_{01}-$$

$$-\ddot{\psi}_1\theta_3)+C_{14\varphi}(\ddot{\theta}_1\psi_3-\ddot{\theta}_1\psi_{01}-\ddot{\theta}_1\psi_1)=Q_{\theta3}+Q'_{\theta3}. \qquad \text{(I.31)}$$

Both here and in the above equations, the coefficients B_{iq} and C_{iq} are functions of the sums of the mass moments of inertia.

The equations (I.29) and (I.31) are connected to each other by non-linear terms of a potential and inertial nature, and the form of connections for both systems is similar; the difference between them is that in (I.29) there is the sum of the masses M_1 and M_3, while in the equation (I.31), there is only one mass M_3. It is in this form of dependence that the principle of vibrational movement of one body in relation to another one in the vibrating transport machines consists in.

It should be noted that the systems (I.29) and (I.31) describe the motion of the mass M_3 relative to M_1 with their constant interrelation (touching); the potential field in the form (on the right-hand side) is represented by the elastic-damping characteristics of M_3 (depending on its state: solid, body of finite rigidity, bulk material, etc.) and depending on its position relative to M_1,it may change until its complete disappearance. In addition, the dynamic relationship between M_1 and M_3 may be abrupt - in this case, the systems of equations (I.29) and (I.31) cannot be valid without appropriate adjustment.

1.3.2. Additional power factors

In the case of the generalized expressions (I.29), (I.30), (I.31) of mass motion, depending on the real mechanical system, there may arise both additional and accompanying power factors that would have been necessary to sustain and strengthenstability of movement.

Let us consider each of them.

a) The frictional forces between the mated surfaces of the masses M_1 and M_3.

Consider this problembased on an example of the vibrating transport machines (Fig. I.5): M_1 - the working member of the vibrating transport machines, M_3 - transportable (displaced) material. The working member is taken as an absolutely rigid body of various shapes (trough, bunker, pipe, etc.). Transportable materials may be the different types of materials.

At this time, the issue of friction force between the working member and the transportable material is elaborated insufficient detail for unit loads [7]; there have been examined details of the more frequent shapes (rectangular, spherical, cylindrical, etc.), as well as polygonal, with an overrolling nature, for which the friction force is realized only at points where the load is in contact with the working member.

The same does not go for issue of the massive materials with different granulometric compositions. Unlike the single (rigid) materials, there is no a fine line of contact betweenthe interacting bodies (the body M_3 refers tothe generalized model of operational load - Fig. I.4); It is related to the fact that for the dispersed (bulk) materials,separation or the attachment to the vibrating surface does not happen instantly,but takes placetogether with a transientelastic-damping process.

In order to describe the friction force between the bulk-type material and the surface of the working member, different approaches are used [1, 19, 23], the essence of which consists in the act that the response of load to the working member is proportional to the velocity of its displacement; in this case, there will be taken into account both the internal resistance of material and resistance of the medium (air, fluidity, etc.), where the motion is performed.

$$N_q = f(\dot{q}, q).$$

When considering the spatial motion (rectilinear or rotational) of TL, instead of the normal response, the moments of these forces appear on one or another part of the surface of the WM (though):

$$(F_{fr})_q = fN_q;\ (M_{fr})_q = (F_{fr})_q \cdot r_q,$$

where f -the friction coefficient of load on the surface of the WM (f is usually taken as variable in each cycle of motion, depending on a dynamic state - slip over the surface, stopping, etc.); r_q - the distance from the friction surface to the center of gravity in the direction of coordinates.

The frictional forces can be represented as follows:

$$F_{x3} = f_x N_x sign(\dot{x}_3);\quad F_{y3} = f_y N_y sign\ (\dot{y}_3);\quad F_{z3} = f_z N_z sign(\dot{z}_3),$$

where f_x, f_y and f_z are the friction coefficientsin the directions of$x$, $y$and z (henceforth, there are taken f_x, = f_y, = f_z = f); N_y - the normal response of load on the surface 2 (Fig. 10 – the lateral surfaces); N_z – the normal response of load on the surface 1 (to the bottom); *sign*is a non-linear function, which is determined depending on the sign of the transportation velocity V: *sign* = 1, when V< 0 and sign = -1, when V> 0.

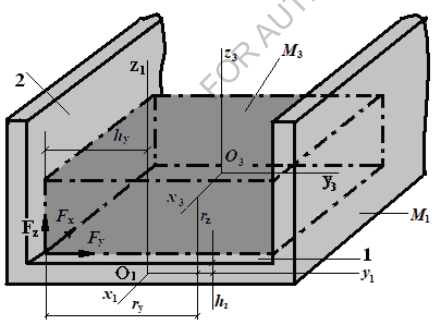

Fig. I.10. For determining the traction forces and moments of the traction force of TL with the working member

The moments of the friction forces relative to the coordinate axes have the form:

$$(M_{fr})_{x3} = (F_{z3} r_y - F_{y3} r_z) sign\ (\dot{\theta}_3);$$

$$(M_{fr})_{y3} = F_{x3} r_z sign(\dot{\psi}_3);$$

$$(M_{fr})_{z3} = F_{x3} r_y sign(\dot{\varphi}_3), \qquad \text{(I.32)}$$

where r_y, r_z - the distances from the friction surfaces to the coordinate axes of the system $O_3 x_3 y_3 z_3$.

The moments of thefriction forces relative to the coordinate axes of the system $O_1 x_1 y_1 z_1$ have the form:

$$(M_{fr})_{x1} = F_{z3} h_y - F_{y3} h_z;\ (M_{fr})_{y1} = F_{x3} h_z;\ (M_{fr})_{z1} = F_{x3} h_y, \qquad \text{(I.33)}$$

where h_y, h_z-the distances from the friction surfaces to the coordinate axes of the coordinate system $O_1 x_1 y_1 z_1$.

In this case, the WM is delimited on two sides by planes $O_1 x_1 y_1$ and $O_1 z_1 x_1$, while in the direction of $O_1 x_1$, it is open; in this case, the friction force on the surface of $O_1 y_1 z_1$ does not exist and, accordingly, the terms with the factors r_x, $h_x$in the expressions (I.32), (I.33) are equal to zero.

b) Gravity of TL.

Gravity of the material being transported, i.e. TL, plays a significant role in the vibratory transportation process formation, since the intensity of material movement depends heavily on the ratio of the gravity forces of OL and the WM inertia.

The force of gravity *P* of the mass M_3 relative to the axes of the system $O_1 x_1 y_1 z_1$ (WM) is expanded as follows:

$$P_{x_1} = -M_3 g\ [sin\alpha + (\psi_{01} + \psi_1) cos\alpha]; \qquad \text{(I.34)}$$

$$P_{y_1} = M_3 g\ [(\phi_{01} + \phi_1) sin\alpha + (\theta_{01} + \theta_1) cos\alpha]; \qquad \text{(I.35)}$$

$$P_{z_1} = M_3 g\ [cos\alpha - (\psi_{01} + \psi_1) sin\alpha]. \qquad \text{(I.36)}$$

Due to the fact that the location of the center of gravity of the mass M_3 in the coordinate system $O_1' x_1' y_1' z_1'$ is determined by coordinates x_3, y_3, z_3, therefore the moments of the force vector *P* relative to the coordinate axes can be expressed as follows:

$$(M_P)_{X_1} = P_{Z_1} y_3 - P_{Y_1} z_3;$$
$$(M_P)_{Y_1} = P_{X_1} z_3 - P_{Z_1} x_3; \qquad \text{(I.37)}$$
$$(M_P)_{Z_1} = P_{Y_1} x_3 - P_{X_1} y_3;$$

This notation is based on the assumption that the direction of the force P always corresponds to the direction of the axis Oz, while the coordinates of point O_3 located on the axis of$P$are known at any given time.

c) Exciting force.

The type of the exciting force will be identified depending on the type of the energy source (vibratory exciter). In any case, the direction of the force and the point of application are known for a particular mechanical system. With this in mind, let us assume that, in the best case, the direction of the exciting force corresponds to the direction of the axis of spring l_1 (Fig. I.1) and passes through the center of gravity of the mass M_1 (in most vibrating machines, the direction of the exciting force is determined by the location of the elastic system). At the same time, in the real machines, as a result of initial errors, the exciting force may not pass exactly through the center of gravity (this was also mentioned above) and will be deflected to eccentricities e_x, e_y and e_z; in addition, under the dynamic effect on the mass, it will deflect in relation to the external exciting force on the coordinates x_1, y_1, z_1, due to the deformation of the elastic system.

Consider the position of the mass M_1 before and after the application of the force Q, while we assume that the direction of the force remains unchanged (Fig. I.2). The mass M_1 is shown in three different positions - I, II, III; I corresponds to the initial position, when the direction of Qcorresponds to the direction of the axis of undeformable spring and passes through the center of gravity O_1; II corresponds to the real position of the mass M_1 [9, 11]. Figure I.2 shows deviations that are characterized by the angles and eccentricities. The existence of eccentricities is the cause of the occurrence of the moments of forces, which, together with the transverse and bending deformations, generate vibrations of the mass M_1 in space.

The projections of the force Q on the axes of the coordinate system will have the form as follows:

$$Q_{x_1} = Q[\sin\alpha_1(\psi_{0_1} + \psi_1) + \cos\alpha_1 - (\psi_{0_2} - \psi_2)\sin\alpha_1];$$
$$Q_{y_1} = Q[\varphi_{0_2} + \varphi_2 - \cos\alpha_1(\varphi_{0_1} + \varphi_1) - \sin\alpha_1(\theta_{0_1} + \theta_1)]; \qquad \text{(I.38)}$$

$$Q_{z_1} = Q[\cos\alpha_1(\psi_{0_1} + \psi_1) + \sin\alpha_1 - (\psi_{0_2} - \psi_2)\cos\alpha_1].$$

The moments of the force Q are determined by the formulas of the theory of vector algebra [6]; if we determine the coordinates of point N of the passage of the force vector Q, then the moments of this vector relative to the axes of the coordinate system $O_1 x_1 y_1 z_1$ will have the form as follows:

$$M_{x_1} = e_{y_1} Q_{z_1} - e_{z_1} Q_{y_1};$$
$$M_{y_1} = e_{z_1} Q_{x_1} - e_{x_1} Q_{z_1};$$
$$M_{z_1} = e_{x_1} Q_{y_1} - e_{y_1} Q_{x_1}.$$

If we take into account the aforementioned tolerance for the constant coincidence of the force Q with the axis $O_2 x_2$, its projections on the axes of the system will look like:

$$Q_{X2} = Q;\ Q_{Y2} = Q_{Z2} = 0;$$

accordingly, the moments will look like:

$$M_{X2} = M_{Y2} = M_{Z2} = 0.$$

On the basis of inertial, elastic and field damping forces acting on the considered three-mass system (Fig. I.5, I.6), as well as the external forces determined by the specificity of a particular machine, it is possible to obtain a system of the equations of a generalized form that will describe the dynamic state of the mentionedvibratory system.

For the mass M_1

$$\frac{d}{dt}\left(\frac{\partial T}{\partial \dot{q}_1} - \frac{\partial T}{\partial q_1}\right) + F_{q1} + \Phi_{q1} + F'_{q1} + \Phi'_{q1} + F''_{q1} + \Phi''_{q1} = Q_{q1} + F^*_{q3};$$

For the mass M_2

$$\frac{d}{dt}\left(\frac{\partial T}{\partial \dot{q}_2} - \frac{\partial T}{\partial q_2}\right) + F_{q2} + \Phi_{q2} + F'_{q2} + \Phi'_{q2} = Q'_{q2};$$

For the mass M_3

$$\frac{d}{dt}\left(\frac{\partial T}{\partial \dot{q}_3} - \frac{\partial T}{\partial q_3}\right) + F_{q3} + \Phi_{q3} = F_{q3},$$

where $q_1 = x_1, y_1, z_1, \theta_1, \psi_1, \varphi_1$; $q_2 = x_2, y_2, z_2, \theta_2, \psi_2, \varphi_2$; $q_3 = x_3, y_3, z_3, \theta_3, \psi_3, \varphi_3$;

$F_{q1},...,\Phi''_{q1}$; $F_{q2},...,\Phi'_{q2}$; $F_{q3},...,\Phi_{q3}$ is determined by (I.24), (I.26) - (I.28) and similar expressions; Q_{q1}, F^*_{q3} – the exciting force and forces of gravity and friction of TL acting on the mass M_1; Q'_{q2} – the exciting force acting on the mass M_2; F_{q3} – the frictional forces acting on the mass M_3.

Conclusions

1. For a loaded vibratory feeder, as a dynamic model of a three-mass asymmetric oscillatory system, a methodology was formulated for determining the coordinates of points of the centers of masses and connections (with elastic elements) for static and dynamic positions.
2. A total field of forces (potential, kinetic, internal and external) acting on the system is determined.
3. For each mass of the mentioned model, connected to each other by the elastic and inertial forces, a system of differential equations of spatial motion is obtained, the simplification of which is possible for any state of motion (plane, spatial, linear and non-linear)

1.4. Mathematical modeling of the process of spatial vibrating transportation along the rigid working plane

1.4.1. Areas of research

The dynamic (Fig. I.5, I.6) and mathematical models (I.29) – (I.31) developed in a systematic manner allow us to study the influence of basic dynamic and design parameters of a vibrating conveyor on the vibratory-technological process of different materials.

The studies can be carried out for the following parameters:

- design errors in the manufacture and installation of the vibration machines;
- the error-based occurrence of inactive three-dimensional vibrations;
- rigidity of the working (operating) member;
- characteristics of transported (processed) materials;
- design parameters of the vibrating machines;
- characteristics of a vibratory exciter;
- parameters of principalvibrationof the WM;
- other.

1.4.2. Possible design errors in the vibrating machines

In the mechanical parts of the vibrating machines, a significant role is played by the elastic components and related elements. Of very great significance are the specifics of the spring-operated elastic elements - they are vibrating not only in the direction of periodic force, but they also performtransverse and torsional vibrations. Usually, additional (parasitic) oscillations are small and are largely left out of research, in view of the fact that they do not significantly affect the accuracy of the results; on the other hand, in the case of larger oscillations (resonance
machines, etc.) such inaccuracies can producethe significant difference between the design and real parameters.

The second reason for the occurrence of inactive parasitic oscillations is thes for the accuracy of processing of the joint surfacesof the elastic elements and masses, performing active vibrations. Errors of processing, even within tolerance, at large amplitudes, cause parasitic oscillations, which affect the operating process [1, 2].

The next factor disturbing the operating process, is error in transferring the exciting forceto the working member. In this case, error may occur bothfrom the excitingand as a resultofimproper location ofthe elastic elements.

Examples of inaccuracies are given above in Figure 1.1.

1.4.3. Deviations of the directions of the exciting force and the coordinate axes of masses of thevibrating machines

Consider inaccuracies in the location of the rigid WM of the vibrating machine in space (Fig. I.11). The coordinate system is in perfect condition and is rigidly attached to the WM. The direction of the axis Ox is the same as the direction of the exciting force; due to possible inaccuracies in the manufacture and installation of the vibrating machine, the real application point O_1' of force to the WM is shifted away from the ideal O_1 to the eccentricities e_x, e_y, and $\boldsymbol{e}_z$ (Figure 1.11a); at the same time, the axes of the system $O_1'x_1'y_1'z_1'$ relative to the system $O_1x_1y_1z_1$ are inclinedat the angles $\theta_0, \psi_0, \varphi_0$ represented by the Euler angles (Figure I.11b).

Deviations of the exciting force $Q(t)$ are caused by the indicated inaccuracies, and their projections on the coordinate axes are determined using directional cosines:

$$Q_{x_1'} = Q(\psi_0 \sin\alpha_1 + \cos\alpha_1); \quad Q_{y_1'} = Q(\varphi_0 \cos\alpha_1 + \theta_0 \sin\alpha_1);$$
$$Q_{z_1'} = Q(\psi_0 \cos\alpha_1 + \sin\alpha_1), \qquad \text{(I.39)}$$

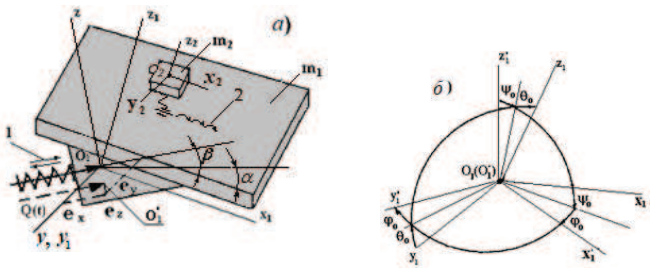

Fig.I.11. Deviations of the location of the working member caused by errors in the design

where $\alpha_1 = \alpha + \beta$; due to the smallness of angles $\theta_0, \psi_0, \varphi_0$ during expansion of directional cosines in a series, only the linear terms are taken into account;

The projections of the moment $M = Q.e$ on the coordinate axes $O_1x_1y_1z_1$ will have the form as follows:

$$M_{x_1'} = Q[e_y(\psi_0 \cos a_1 + \sin a_1) - e_z(\varphi_0 \cos a_1 - \theta_0 \sin a_1)];$$

$$M_{y_1'} = Q[e_x(\psi_0 \sin a_1 + \cos a_1) - e_z(\psi_0 \cos a_1 + \sin a_1)]; \qquad \text{(I.40)}$$

$$M_{z_1'} = Q[e_x(\varphi_0 \cos a_1 + \theta_0 \sin a_1) - e_z(\psi_0 \sin a_1 + \cos a_1)].$$

1.4.4. Simplified equations of spatial motion of WM and TL

The differential equations of translational and rotational motion of the WM, taking into account manufacturing errors, will have the form

$$M_1 \ddot{x}_1 + c_x \dot{x}_1 + k_x x_1 - k_x' \theta_1 = Q[(\psi_0 + \psi_1)\sin a_1 + \cos a_1];$$

$$M_1 \ddot{y}_1 + c_y \dot{y}_1 + k_y y_1 + k_y' \psi_1 = Q[(\varphi_0 + \varphi_1)\cos a_1 + (\theta_0 + \theta)\sin a_1];$$

$$M_1 \ddot{z}_1 + c_z \dot{z}_1 + k_z z_1 + k_z' \varphi_1 = Q[(\psi_0 + \psi_1)\cos a_1 + \sin a_1]; \qquad \text{(I.41)}$$

$$J_\theta \ddot{\theta}_1 + c_\theta \dot{\theta}_1 + k_\theta \theta_1 - k_\theta' x_1 = M_{x_1'};$$

$$J_\psi \ddot{\psi} + c_\psi \dot{\psi}_1 + k_\psi \psi_1 - k_\psi' y_1 = M_{y_1'};$$

$$J_\varphi \ddot{\varphi}_1 + c_\varphi \dot{\varphi}_1 + k_\varphi \varphi_1 - k_\varphi' z_1 = M_{z_1'},$$

where $k_x, k_y, k_z, k_\theta, k_\psi, k_\varphi$ and $c_x, c_y, c_z, c_\theta, c_\psi, c_\varphi$ are the elastic and damping coefficientsof the elastic system; $k_x', k_y', k_z', k_\theta', k_\psi', k_\varphi'$ - coefficients that link transverse-rotatory and longitudinal-torsional vibrations; $Q = Q_o f(t)$, Q_o – the exciting force coefficient, $f(t)$–law of variation of the exciting force; in the right-hand side of the equations (I.41), unlike the expressions (I.39) and (I.40), there are also taken into account the dynamic angular coordinates θ, ψ, φ.

The movement of TL in three forward directions is described by the equations as follows:

$$M_3 \ddot{y}_3 + \ddot{y}_1 + (\ddot{z}_1 \theta_1 - \ddot{x}_1 \varphi_1)\cos a_1 + (\ddot{x}_1 \theta_1 + \ddot{z}_1 \varphi_1)\sin a_1 - \theta_1 z_3 - 2\dot{\theta}_1 \dot{z}_3 +$$

$$+ 2\dot{\varphi}_1 \dot{x}_3 - \ddot{x}_1(\varphi \cos a_1 - \theta_0 \sin a_1) + \ddot{z}_1(\theta_0 \cos a_1 + \varphi_0 \sin a_1) + B\dot{y}_3 - C' y_3 =$$

$$= -fN_z sign(\dot{y}_3);$$

$$M_3 \ddot{z}_3 + (\ddot{z}_1 + \ddot{x}_1 \psi_1)\cos a_1 + (\ddot{x}_1 - \ddot{z}_1 \psi_1)\sin a_1 - \theta_1 \ddot{y}_1 + y_3 \ddot{\theta}_1 + 2\dot{y}_3 \dot{\theta}_1 -$$

$$- 2\dot{x}_3 \dot{\psi}_1 - \ddot{z}_1 \psi_0 \sin a_1 + \ddot{x}_1 \psi_0 \cos a_1 - \ddot{y}_1 \theta_0 + D_1 \dot{Z}_1 + E\dot{x}_1 + E' \dot{z}_3 + Cz_3 =$$

$$= -fN_y sign(\dot{z}_3) - g\cos a_1,$$

wherethe coefficientsA, B, B_1, C", D, E, E_1, and Ccharacterize the position of TL relative to the surface of the WM. The equations (1.4) are distinguished from general equations of motion of OL by the term arising as a result of errors $\theta_0, \psi_0, \varphi_0$.

The equations(I.41) and (I.42)are solved together with the equation of force of a vibratory exciter

$$Q = Q_o f(t) = Q_o \Phi^2,$$

whereΦ – magnetic flow, the change of which is determined by means of the expression [6].

$$\frac{d\Phi}{dt} = \frac{U_0}{W}\sin \omega t - \frac{(\delta - x_1)\, r}{\mu_0 S W^2}\, \Phi, \qquad \text{(I.43)}$$

whereU_o- the peak system voltage value, W – turn number, ω - circular frequency, δ – initial gap, r – ohmic resistance, μ - air magnetic conductivity h/m, S – core area,

When solving the system (I.41), (I.42) and the equations (I.43), errors varied within the following limit - for angular errors: $\theta_0, \psi_0, \varphi_0$ = (0 - 0,15) rad.; for transmission errors of the exciting force: e_x, e_y, e_z = (0 – 0,015) m. For better clarity of the influence of errors on the process, the vibrationshave been strengthened in one or another specific direction by resonating these vibrations with an exciting force (together with a change in errors).

1.4.5. Mathematical modeling of vibration transportation on changes in the initial design in accuracies of the vibrator

The influence of inaccuracies in the manufacture and installation of the vibrating machines on the vibration transportation process can be more noticeable for the resonant vibrating machines (for example, electromagnetic vibrating conveyors with a spring elastic system).

In normal operation of the vibrating machine, when the frequencies of inactive (spatial, the so-called parasitic) vibrations are far from resonant, inaccuracies within the limits presented in table. I.1, cannot have a notable impact on the transport and technological process; therefore, in simulation, for each spatial direction of vibrations, the vibrating machine is entereda resonance, and only after that, an increase in the magnitude of inaccuracies can cause disruptionin the transportation process. This approach reflects the true picture of the influence of inaccuracies on the technological process during the operation of the vibrating machine.

Below are some results of mathematical modeling of the system (I.41), (I.42), (I.43) when inaccuracies change within the limits presented in Table. I.1. Differential equations are solved by the Runge-Kutta method.

The simulation study was carried out at resonant active vibration with a frequency of 50 Hz.

In each case of a numerical experiment, the frequency of one or another inactive (parasitic) vibrationsY_1, Z_1, θ_1, ψ_1, $\varphi_1$is close to the resonant one (50 Hz), and when inaccuracies change within the limits presented in Table. 1.1, monitoring activity is performed over changes in the parameters (velocity, etc.) of the vibrational movement of TL.

Figures I.12 - I.16 illustrate the simulation results of vibrational transportation for an electromagnetic vibrating feeder operating in the resonant mode with a frequency of 50 Hz.

The influence of changes in inaccuracies in the manufacture of parts of a vibrating machine and in its installation on the velocity and trajectory of movement of bulk material was studied.

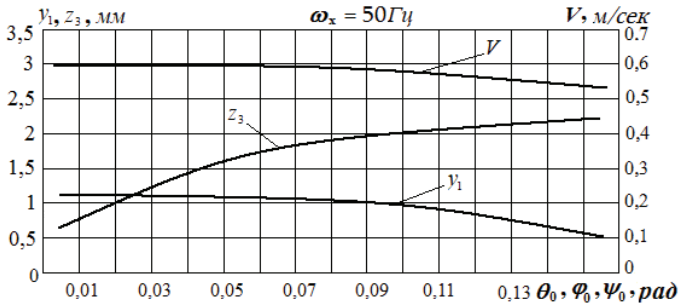

Fig. 1.12. The dependence of the velocity *(V)* and vertical trajectory (z_3) of TLon transverse vibrations (y_1) of WM on change in errors

Fig.

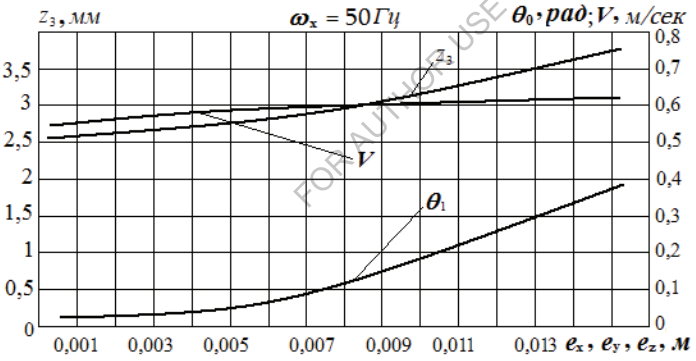

I.13. The dependence of the velocity *(V)* and vertical trajectory (z_3) of TL on rotary vibrations (θ1) of WM on change in errors

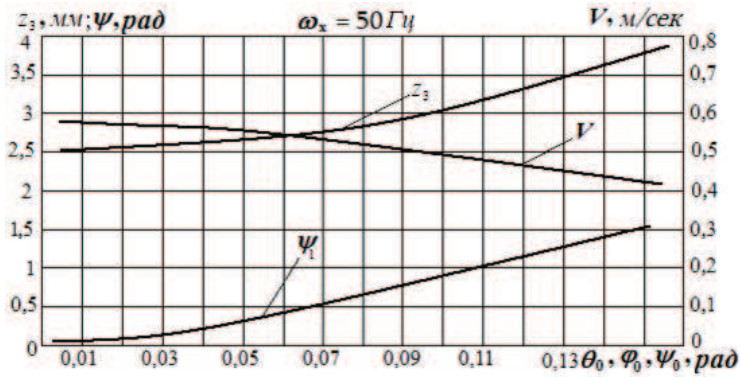

Fig. I.14. The dependence of the velocity *(V)* and vertical trajectory (z_3) of TL on torsional vibrations (ψ_1) of WM on change in errors

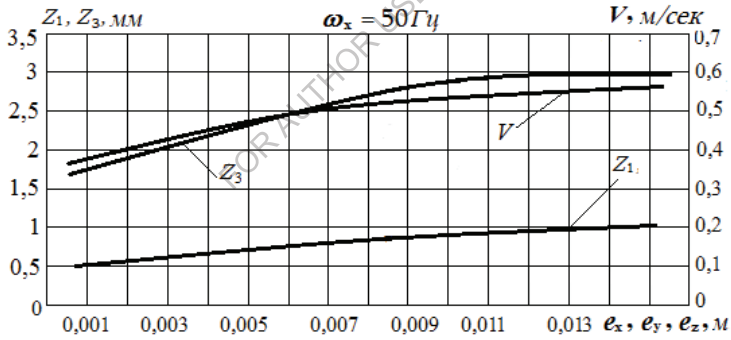

Fig. I.15. The dependence of the velocity *(V)* and vertical trajectory (z_3) of TL on vertical vibrations (z_1) of WM on change in errors

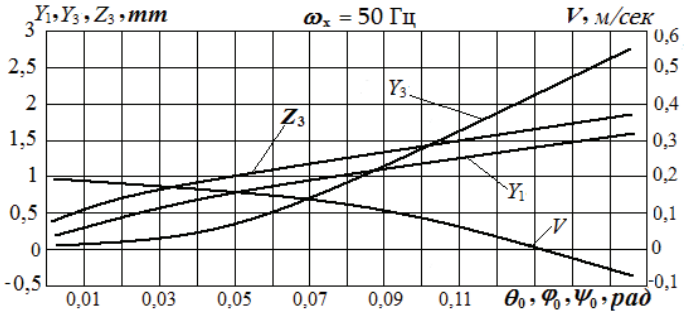

Fig.I.16. The dependence of the velocity *(V),* vertical trajectory (z_3), and transverse trajectory of TL on transverse vibrations (Y_1) of WM on change in errors

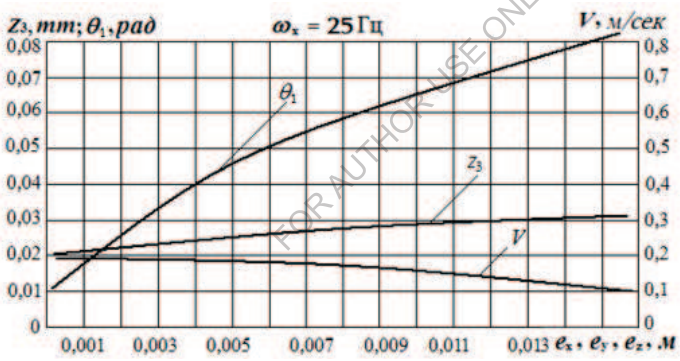

Fig. I.17. The dependence of the velocity *(V)* and vertical trajectory (z_3) of TL on turning vibrations (θl) of WM on change in errors

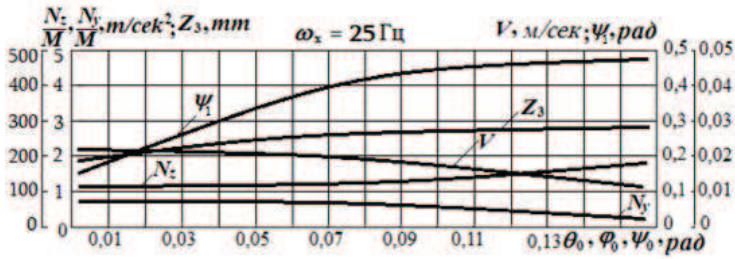

Fig. I.18. The dependencies of the velocity (V), vertical trajectory (z_3), reaction forcesof TL (N_z, N_y) on torsional vibrations (ψ_1) of WM on change in errors

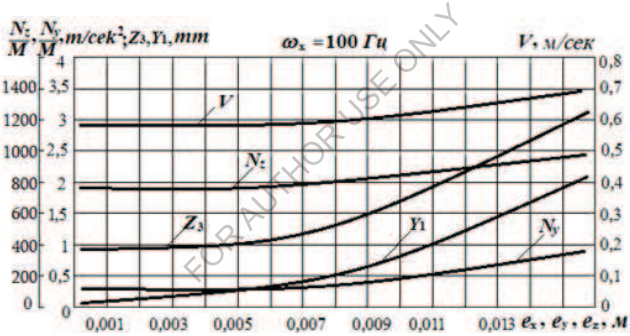

Fig. I.19. The dependencies of the velocity (V), vertical trajectory (z_3), reaction forces of TL (N_z, N_y) on transverse vibrations (y_1) of WM on change in errors

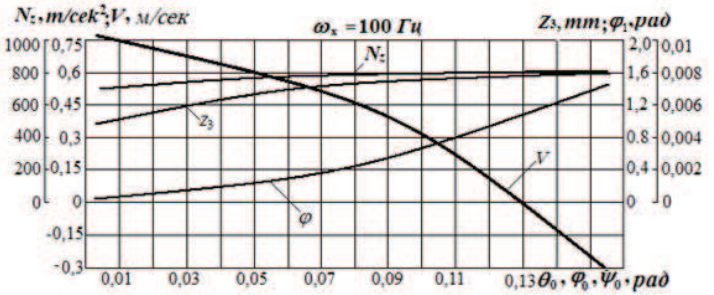

Fig. I.20. The dependencies of the velocity (V), vertical trajectory (z_3), reaction forces of TL (N_z) on turning vibrations (φ_1) of WM on change in errors

Three-dimensional vibrations, which are entereda resonance for strengthening them and, consequently, for studying their influence on the technological process, are mostlybelowresonance; their phases either coincide or differ little from the main active resonant vibration.

It is obvious that the same closely resonant vibrations, the frequencies of which are out of the resonance zone, will affect the technological process in a different way.

Figure I.14 illustratesthe graphs,which describe the dependenciesof the velocity and trajectory on error in the manufacture of the machine under conditions of the subharmonic resonant mode [11] of the operation of the machine.

The patterns of the influence of inaccuracies on the transportation process in the main (50 Hz) and subharmonic (25 Hz) modes are not the same (Figures I.13 and I.17).

Similar relationships for the superharmonic resonance mode (100 Hz) are shown in Figures I.19 and I.20. It should be noted that unlike the subharmonic electromagnetic vibrating machines [12,17], machines with the superharmonic resonant modes of operation have not found application; this is due to high dynamic loads, energy costs and metal consumption of the structure of such machines; therefore, research in this mode is of a theoretical nature.

Thus, the studies carried out have shown that errors in the manufacture and installation of the vibrating machines and parasitic vibrations, arising on their basis, disrupt the technological process and cause deterioration of the basic dynamic and operational parameters. However, there are cases when the transport speed remains constant, or tends to increase.

This suggests that in a few cases, instead of reducing the allowances for errors to a minimum (which is a quite a complicated task), it would be advisable to create such a

design of a vibratory exciter, where it would be possible to control the exciting force and its moment.

1.4.6. Development of a new design of the vibratory feeder with an adjustable mode of the vibratory exciter

On the basis of theoretical (simulated) and experimental studies, the design of an electromagnetic vibratory exciter with an adjustable vibration direction was developed; the design is based on changing the direction of the exciting force relative to the direction of the axis of the elastic system (spring).

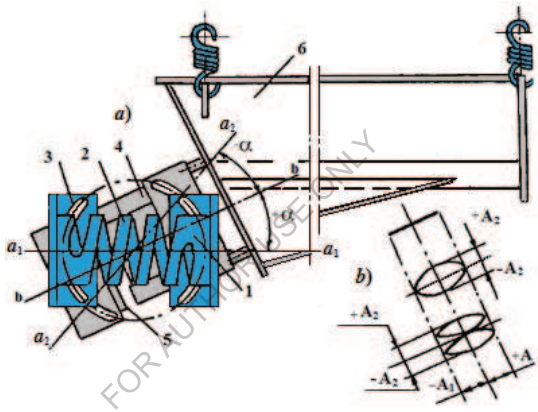

Fig. I.21. The electromagnetic vibratory exciter with a variable tilting angle and various types of vibrations

The elastic system is represented by helical cutting-through springs 2, which are connected to the electromagnet 4 by a bracket system on one side, and to the armature 5 on the other side. In this case, the bracket system 3 with a slotted groove provides rotation of longitudinal axis $a_1 - a_1$ ($a_2 - a_2$)of the elastic system (springs) by an angle $\pm\alpha$ relative to the axis of action of the electromagnetic exciting force $b - b$.

The electromagnetic vibrator connectedto the through 6 is on the whole a vibratory feeder designed for supplying bulk, lump or separate materials from the bunkers or other collecton chambers; it was developed on the basis of themass-produced electro-vibratory feeder PEV1A - 065 × 1.8. The new electromagnetic vibrator makes it possible to excite elliptical vibrations of the working member and to adjust the axes of the ellipse, which

in turn allows to adjust the performance of the machine in accordance with the characteristics of material to be processed.

The vibration exciter makes it possible to excite vibrations in the working member (the through, sieve, etc.) of the machine: rectilinear ones, when $\alpha = 0$, elliptical, when $\alpha \neq 0$, biharmonic, when the frequencies of the longitudinal (ω_l) and transverse (ω_{tr}) vibrations are equal($\omega_{tr}/ \omega_l = 1$), as well aseight-shaped vibrations, when $\omega_{tr}/ \omega_l = 1/2$; the said forms of vibration are obtained without the use of the additional vibratory exciters.

Change in the angle αallows for adjusting the machine to the optimal operating mode depending on the material to be processed, increasingits productivity and broadening the applicability of the machine in various technological processes.

The findings suggest that the combination of some inactive spatial vibrations with the main active vibrations can be useful, and they must be taken into account when designing the vibrating machines.

Chapter 2.
The movement of bulk materials along the spatially vibrating plane of the finite rigidity

Introduction

One of the significant factors affecting the process of vibration transportation is the elasticity of the working member, which is more or less apparent depending on its structural dimensions.

In the theory of vibration transportation, the working member is usually considered to be a rigid body; on this basis, a number of studies have been carried out, where as a model of the transported material there are adopted either the individual lump parts (material point) or massive cargo (bulk materials) [1, 3, 7, 8].

The sources of research on the interaction of TL and the elastic surface of the working member of the vibrating machine are few in number. The impacts of dynamic (moving) loads on the elastic structures are considered in the papers [2, 15, 18, 22]. There are considered problems of the action of movable loads on the elastic planes and rods without the reverse impact. In work [22], the subject of research is a vibratory conveyor with a long working member; when considering bending vibrations of the working member, the external forces are represented by harmonic force and harmonic moment, which arise as a result of eccentric transmission of the exciting force, as well as by force coming from the elastic elements.

Figure 1.22 illustrates graphical form of solving this problem, where u – is the displacement of the point of the working member in an absolute system of coordinates; y– the displacement of the conveyor through during transverse vibration.

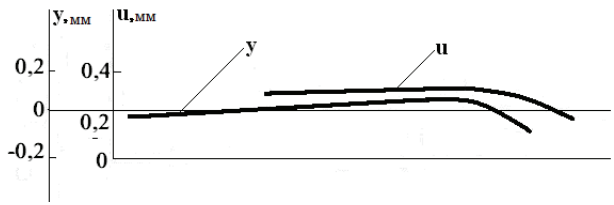

Fig.I.22. Bending deformation (*u*) of the working member and the vibration amplitude (*y*)

In works [4, 20], an elastic working member was used for wave transportation with a phenomenological model of a bulk cargo. The elastic band is located on the transported surface, and transverse and longitudinal waves propagate on it; by varying their parameters, it is possible to form various combinations of traveling waves, which derives the nature of the transportation process from.

2.1. The movement of the system "mobile load - elastic WM"

We represent the working member in the form of an elastic plane, which has a constant cross-section (Fig. I.23).

Consider the system “elastic working plane- TL-vibratory exciter”; it is assumed hereinafter that with an increase in the length of the working member, its elasticity is increasingly affecting the process of vibration transportation, and it is possible to choose parameters (dimensions) that will contribute to the intensification of the operating modes of the vibration machine.

Figure I.23 illustrates that the vibration plane *m* is a working member connected to the vibratory exciter of the elastic system *k*. Operational (movable) load can be represented by both bulk material and single lump materials with double-sided movements at the velocities of V_x, V_y and in the sliding or tossing modes.

During the operation, the working memberconducts two types of movement: vibrational movement, when *m* is represented in the form of an absolutely rigid body (i.e., it vibrates with the frame) suspended on the elastic elements *k,* and deformative movement, when the working member is considered to be a plate with the distributed mass.

The movement of the mass *M* (TL) is conducted under the influence of the vibrational plane *m*, from which the above two types of movement (vibrations) are transmitted.

In the formation of the elastic strains of the working member, like plates, there take part:

1) The elastic force coming from the elastic system of the vibratory exciter (from springs or bow springs)

$$Q_1 = \sum_{i=1}^{n} A_i k q_i(t), \qquad (i = 1,...,n), \tag{I.44}$$

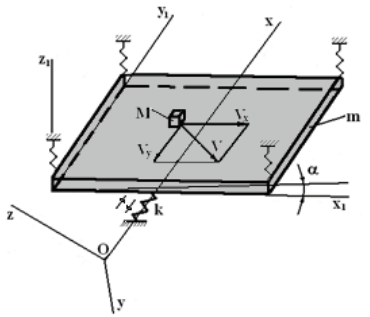

Fig.I.23. The system: Elastic vibratory system – TL–Vibratory exciter

where$y$is a generalized coordinate of the though (plane); n –the number of the generalized coordinates; k – rigidity of the elastic system of the vibrating machine; A_i - coefficient that takes account of rigidity decomposition of the elastic system on the coordinates q_i;

2) The exciting force coming from the vibratory exciter

$$Q_2 = Q_0 f(t,x), \tag{I.45}$$

where Q – coefficient determined by parameters of the vibratory exciter; $f(t, x)$ – in the general case, non-linear and periodic law of the exciting force variation;

3) The distributed force of the though (plate)

$$Q_3 = \mu \sum_{i=1}^{n} \ddot{q}_i(t), \tag{I.46}$$

whereμ- the mass of the unit capacity of the though;

4) Cargo reaction force on the surface of the vibrating plane

$$Q_4 = Q_z f(x, y, z), \tag{I.47}$$

where Q_z – in the case of an operational bulk load, it is a function of the coordinates of cargo movement relative to the surface of the though [1]; in the case of unit load, Q_z is determinedfrom the condition of pullout and attachment of cargo relative to the surface of transportation [1, 11].

If the deformations of the plate remain within the elastic range, the vibration equation will have the form

$$\frac{\partial^4\omega}{\partial x^4}+2\frac{\partial^4\omega}{\partial x^2\partial y^2}+\frac{\partial^4\omega}{\partial y^4}+\frac{\mu h}{D}\frac{\partial^2\omega}{\partial t^2}=\frac{1}{D}F(x,y,t), \qquad \text{(I.48)}$$

where$h$ – is a plate thickness; $D=Eh^3/12(1-\nu^2)$ - bending rigidity; ν - Poisson's ratio; $\omega(x,y,t)$ - divergence of a point from equilibrium.

For a plate freely supported by its edges, the form of the solution for the homogeneous part of the equation (I.48) has the form

$$\omega=\frac{4Mga^3}{BD\pi^4}\sum_{i=1}^{\infty}\sum_{j=1}^{\infty}\delta_{ij}\sin\frac{i\pi x}{a}\sin\frac{j\pi y}{b}, \qquad \text{(I.49)}$$

where δ_{ij} - is a generalized coordinate of deformation.

The external force can be decomposed in a series

$$F=\sum_{i=1}^{\infty}\sum_{j=1}^{\infty}Q_{ij}\sin\frac{i\pi x}{a}\sin\frac{j\pi y}{b}, \qquad \text{(I.50)}$$

where Q_{ij} represents the sum of forces (I.44) (I.45) (I.46) (I.47).

If the displacement of a material point is considered, the equation (I.50) will have the form [3]

$$Q_z=N_z\sin\frac{i\pi V_x t}{a}\sin\frac{i\pi V_y t}{b}. \qquad \text{(1.51)}$$

If we put (1.50) and (1.52) into the equation of vibrations (1.44) and take into account (1.51), we obtain the equation for the coordinates δ_{ij}

$$\delta_{ij}+p_{ij}^2\delta_{ij}=\frac{4BD}{\rho hMga^3}[A_i k q_i(t)+Q_o f(t)+\mu q_i(t)+\frac{4N_z}{ab}\sin\frac{i\pi V_x t}{a}\sin\frac{j\pi V_y t}{b}], \qquad \text{(1.52)}$$

where $p_{ij}=\frac{i^2a^2+j^2b^2}{a^2b^2}\sqrt{\frac{D}{\rho h}}$.

The right-hand side of the equation (I.52) involves the coordinates of the movement of the though as a rigid body, and the coordinates of the movement of TL; therefore, when solving, the equation (I.52) must be considered together with the equations of the through as a rigid body and with the equations of the displacement of TL. For its part, the influence of the elastic forces from the elastic strains should be reflected in the equations of motion of the though and TL.

2. 2. A spatial dynamic model of loaded vibrating transport machine with the elastic WM

Let us represent the working member in the form of a rectangular plate with the corresponding dimensions and elastic characteristics (Fig. I.24). The coordinate system $Oxyz$ describes the movement of the working member (m), as a rigid body, the axis of which coincides with the direction of the exciting force inclined to the inertial system $Ouvw$ at an angle β. The movement of technological load (M), represented by a cubic body, in which the entire mass of load is concentrated, is described in a coordinate system $EXYZ$ immovably attached to the working member.

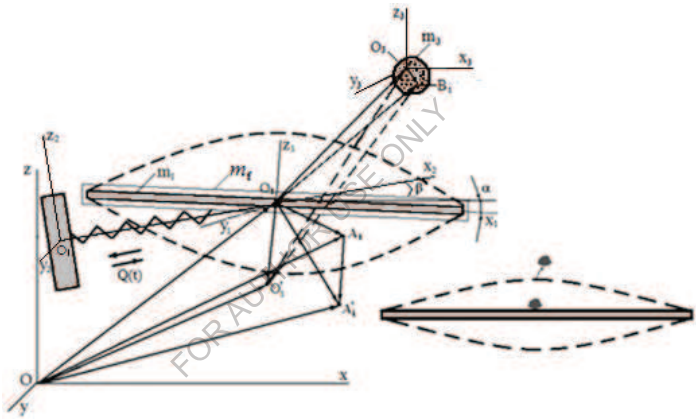

Fig.I.24. The motion of the loaded working member ib space

To describe the rotational motions of the mass M, a coordinate system is attached to it. The movements of the working member and TL will be described by the Euler angles $\theta_1, \psi_1, \varphi_1$ and $\theta_2, \psi_2, \varphi_2$, respectively.

As noted above, in the case under consideration, an attempt is made to take into account the elastic strains of the bottom of the working member in a mathematical model of the system "vibratory exciter - WM - TL". In this case, instead of a separate consideration of the active and reactive parts of the electromagnetic vibrating machine, one thing is considered - the reduced mass of the working member.

The working member of the vibrating machine will be affected by the exciting force Q_{ex} coming from the vibratory exciter, the elastic force from the elastic systemQ_{el}, and a normal reaction of TL N_z. The stiffness of the vibrator suspension is taken to be equal to zero.

Due to a deformation in the working plane of the vibrating machine, points O_1 and A_i will be in the positions O_1' and A_i' (Fig. I.24); the vectors O_1O_3, O_1A_i and O_2O_1, respectively, will be replaced by the expressions

$$\vec{O_1'O_3} = \vec{O_1O_3} - \vec{O_1O_1'}; \quad \vec{O_1'A_i'} = \vec{r_i} + \vec{A_iA_i'}; \quad \vec{OO_1'} = \vec{OO_1} + \vec{O_1O_1'} \tag{I.53}$$

In what follows, let us accept that the working member is deformed only in the direction of the minimum rigidity of the plate (bottom). Then, the first expression of the system (I.53) takes the form

$$(O_1'O_3)_x = x_3;\ (O_1'O_3)_y = y_3;\ (O_1'O_3)_z = \delta - z_3, \tag{I.54}$$

where $\delta = \delta_0 \sin\frac{i\pi x_1}{a} \sin\frac{i\pi y_1}{b}$ is the elastic deformation in the direction to O_3z_3; a and b— the length and width of the plate; the projections of the second and third expressions (I.53) will be obtained in the same way

$$(O_1A_i')_x = r_{ix};\ (O_1A_i')_y = r_{iy};\ (O_1A_i')_z = r_{iz} + \delta;$$

$$(OO_1')_x = x_1;\ (OO_1')_y = y_1;\ (OO_1')_z = z_1 + \delta\cos\alpha, \tag{I.55}$$

where $\alpha_1 = \alpha + \beta$; α is the angle of the plate to the axis Ox.

The projections of the fixing points of the elastic elements and changes in the rotations of the angles of the coordinate axes connected to the working member will be expressed in a similar form. Due to their smallness, these changes are not taken into account in a mathematical model considered in this work.

2.2.1. The kinetic and potential energies of the system "vibratory exciter – elastic elements - WM of the vibrating machine - TL", taking into account the elasticity of WM.

In the case of the kinetic energy expression with account for (I.53) (Fig.I.24), the determination is carried out in the same sequence as in the case with the active working member (see Chapter I, paragraph 1.2.2.)

$$T_1 = \frac{1}{2}\sum_{i=1}^{n_1} M_i[\vec{V}_{O_1'} + \vec{\omega}_{O_1} \times (\vec{O_1O_3} - \vec{O_1O_1'}) + \vec{\omega}_{O_1'} \times \vec{r_i} + \vec{V}_{O_3'} + \vec{\omega}_{O_3'} \times \vec{r_i'}]^2, \text{(I.56)}$$

where M_i - M_i – the mass of load particulate B_i; $V_{O_1'}$ - the velocity of a point O_1'; ω_{O_1} - the angular velocity of a point O_1; $\omega_{O_1'}$ - the angular velocity of a point O_1; r_i – the radius-vector of particulate A_i; V_{O_3} - the velocity of a point O_3; ω_{O_3} - the angular velocity of a point O_3; r_i' - the radius-vector of particulate B_i.

The kinetic energy expression with account for (I.53) of the working member will have the form

$$T_2 = \frac{1}{2}\sum_{i=1}^{n_1} m_i[\vec{V}_{O_1} + \vec{\omega}_{O_1} \times (\vec{r_i} + \vec{O_1O_1'})]^2, \qquad \text{(I.57)}$$

wherem_i – is the mass of particulate A_i.

In order to determine the potential energy of the linear elastic systemof the vibratory exciter and a deformation of the working member, it is possible to use the expression

$$U = \frac{1}{2}\sum[k_x(\Delta l_{ix})^2 + k_y(\Delta l_{iy})^2 + k_z(\Delta l_{iz})^2], \qquad \text{(I.58)}$$

where, unlike the adopted method (Chapter I), the coefficients of rigidity k_z, k_y, k_z are determined by taking into account the bending rigidity of the working member, while the projections Δl_{ix}, Δl_{iy}, Δl_{iz} are determined by taking into account the expression (I.53). The potential energy of TL and the system's dissipative functions are determined analogously.

The projections of the kinetic energy system on the coordinate axes are determinedas in the case with the active working member (Chapter I) with account for (I.54) and (I.55) and will be the sum of the kinetic energies of two masses m_1 and m_3.

Given that deformations of the through as anelastic body are considered in the direction of its vertical displacement, the same external forces will be put into the differential equations of deformations of the body, taking into account (I.54) and (I.55), which were the part of the equation of vertical motion of the elastic working member. As a rigid body (Chapter I).

According to the expressions (I.56) (I.57) (I.58), and using the Lagrange's equation of the second kind, we'll obtain the differential equations of the associated movements of the working member and TL; this case because of space limitation will not be considered here; we would just note that in the general equations, the components with elastic deformations will be of a type of $\ddot{\delta}\psi_1$, $\dot{\delta}\dot{\varphi}_1$ and so on. In addition, the equation of the bottom deformation will be added to the total number of the equations of the working member, like a plate (Fig. I.23), taking into account the spatial movements of transported material and the working member, which has the form as follows

$$
\begin{aligned}
&[m\cos^2\alpha - M(\sin^2\alpha + \cos\alpha_1\cos\alpha)]\ddot{\delta} + [m\cos\alpha_1 + M(\cos\alpha_1 - \cos\alpha)]\ddot{z}_1 + \\
&+ M[\cos\alpha_1\cos\alpha(\ddot{Z} + \dot{\theta}_1\dot{Y} - 2\dot{X}\ \dot{\psi}_1 + \ddot{X} - \ddot{X}\psi_1 - \ddot{Y}\theta_1) - \ddot{Z} - \ddot{\theta}_1 Y - \cos\alpha\ddot{x}_1\psi_1 - \\
&- (\cos\alpha - 1)\dot{x}_1\dot{\psi}_1 - \ddot{x}_1 + \sin\alpha\ddot{z}_1\psi_1 + (\sin\alpha - 1)\dot{z}_1\dot{\psi}_1 + \ddot{y}_1\theta_1 + \\
&+ \cos\alpha_1\sin\alpha(\ddot{\psi}_1\delta + \ddot{\psi}_1 Z - \dot{Z}\dot{\psi}_1 + \ddot{\varphi}_1 Y + 2\dot{\varphi}_1\dot{Y} + \ddot{Y}\varphi_1 + 2\dot{\delta}_1\psi_1 + \dot{\psi}_1\dot{\delta}) - \\
&- \cos\alpha_1\dot{\delta}\dot{\psi}_1] + b_x x_1 - b_y y_1 + b_z(z_1 - \delta\cos\alpha_1) + b_\theta\theta_1 + b_\psi\psi_1 + b_\varphi\varphi_1 + \\
&+ a_z(\dot{z}_1 + \dot{\delta}\cos\alpha_1) + a_\theta\dot{\theta}_1 + a_\psi\dot{\psi}_1 + a_\varphi\dot{\varphi}_1 + c_z'[d_{64}\dot{X} + d_{65}\dot{Y} + d_{66}(\dot{Z} - \dot{\delta}) + \\
&+ d_{70}\dot{\theta}_2 + d_{71}\dot{\psi}_2 + d_{72}\dot{\varphi}_2] + k_z'[d_{65}Y + d_{66}(Z - \delta) + d_{70}\theta_2 + d_{71}\psi_2 + \qquad \text{(I.59)} \\
&+ d_{72}\varphi_2] + a_x\dot{x}_1 + a_y\dot{y}_1 = Q(\psi_1\cos\alpha_1 + \sin\alpha_1) + Q_z;
\end{aligned}
$$

where X, Y, Z – displacements of the friable material (TL - M_3), the coefficients b_x, b_y,…, d_{71}, d_{72} at the displacements and velocities characterize the spatial elastic and damping properties of the vibratory exciter and the conventional elastic system of TL, and they are determined by the coordinates of fixing the elastic elements to the masses and their elastic-damping characteristics [5]; Q is an exciting force, determined depending on the type of the vibratory exciter.

If we exclude nonlinear inertial forces) in the form of the product of coordinates and their derivatives from the equation (I.59, as well as those elastic and damping forces that are small compared to the forces acting mostly in the vibration (active) direction, we

have the equation (I.52) obtained from the general equation of a plate with a movable load (Fig. I.23)

When solving the equations (I.59) together with other equations of the working member and TL, the reaction of a single load on the surface of the WM must be considered depending on the type of deformation of the bottom (plate), that is, in the equation (I.59), the response of load will have the form:

$$Q_z = N_z[\sin\frac{i\pi X}{a}\sin\frac{j\pi Y}{b}]; \qquad \text{(I.60)}$$

When bulk material moves across the surface of the through (plate) with the same thickness, then

$$Q_z = N_z, \qquad \text{(I.61)}$$

that is, it is assumed that the transported material is continuously fed onto the WM, and the bottom of the WM is being constantly under the dynamic load.

2. 3. A mathematical model of spatial motion of the system "vibratory exciter-WM of the vibrating machine with an elastic bottom - TL"

To simplify the equation of the associated motion of TL and the elastic WM, it is advisable to make some assumptions: 1) in the equations of the WM, not to take into account the responseof TL to the WM; 2) in each equation, the forces of elasticity and damping are taken into account only on those coordinates along which the motion is considered; 3) due to the smallness of the rotational movement of the TL, its movement is considered only in three linear directions; 4) nonlinear components in the form of a product and the components of an inertial nature, not higher than the second order, are taken into account in the equations of motion of TL.

These assumptions,in normal operation of the vibrating machineallow to obtain a true qualitative and sufficiently quantitative picture of the transportation process on the elastic WM.

The equations of spatial motion of the WM, as a rigid body will have the form:

$$\ddot{x}_1+\frac{c_x}{m}\dot{x}_1+\frac{k_x}{m}x_1=\frac{1}{m}Q_x(t);\ \ddot{y}_1+\frac{c_y}{m}\dot{y}_1+\frac{k_y}{m}y_1=\frac{1}{m}Q_y(t);\ \ddot{z}_1+\frac{c_z}{m}\dot{z}_1+\frac{k_z}{m}z_1=\frac{1}{m}Q_z(t);$$

$$\ddot{\theta}_1+\frac{c_\theta}{J_\theta}\dot{\theta}_1+\frac{k_\theta}{J_\theta}=\frac{1}{J_\theta}Q_\theta(t);\ \ddot{\psi}_1+\frac{c_\psi}{J_\psi}\dot{\psi}_1+\frac{k_\psi}{J_\psi}\psi_1=\frac{1}{J_\psi}Q_\psi(t);\ \ddot{\varphi}_1+\frac{c_\varphi}{J_\varphi}\dot{\varphi}_1+\frac{k_\varphi}{J_\varphi}\varphi_1=\frac{1}{J_\varphi}Q_\varphi(t), \qquad \text{(I.62)}$$

where J_θ, J_ψ, J_φ - the moments of mass *m*relative to the axes of a coordinate system $Oxyz$.

Elastic deformations of the non-rigid WMare describing by the equations

$$\ddot{\delta}+p_\delta^2\delta=-\ddot{z}_1\cos\alpha_1-\frac{1}{\rho h\cos^2\alpha_1}\left[b_z z_1+b_x x_1+Q_\delta(t)+Q_z\right], \qquad \text{(I.63)}$$

where $$p_\delta=\frac{i^2a^2+j^2b^2}{a^2b^2}\sqrt{\frac{D}{\rho h}};\quad i=1,2,\ldots,n_1;\ j=1,2,\ldots,n_2;$$

b_x and b_z are determined taking into account rigidity of the elastic system of the vibrating machine and the bottom of the WM; Q_δ - exciting force coming from the vibratory exciter; Q_z - a normal response of load to the bottom of the WM; in the case with unit loads Q_z wil*l* have the form (I.60) .

The movement of technological load is described by the differential equation system

$$\begin{aligned}
&\ddot{X}+(\ddot{x}_1-\ddot{\delta}\psi_1\cos\alpha_1-\dot{\delta}\dot{\psi}_1\cos\alpha_1-\ddot{z}_1\psi_1(\cos\alpha-(\ddot{x}_1\psi_1-\ddot{\delta}\cos\alpha_1+\ddot{z}_1)\sin\alpha+\ddot{y}_1\varphi_1-\\
&-\ddot{\psi}_1\delta-\ddot{\psi}_1 Z-\ddot{\varphi}_1 Y-2\dot{\varphi}_1\dot{Y}+A\dot{x}_1-B\dot{Y}+B_1X=-(N_z-N_y)sign(\dot{X})+gsjn\alpha;\\
&\ddot{Y}+\ddot{y}_1+(\ddot{z}_1\theta_1-\ddot{x}_1\varphi_1+\ddot{\delta}\theta_1\cos\alpha_1+\dot{\delta}\dot{\theta}_1\cos\alpha_1)\cos\alpha_1+(\ddot{x}_1\theta_1+\ddot{z}_1\varphi_1+\ddot{\delta}\varphi_1\cos\alpha_1+\\
&+\dot{\delta}\dot{\varphi}_1\cos\alpha_1)\sin\alpha-\ddot{\theta}_1 Z-2\dot{\theta}_1\dot{Z}+\ddot{\theta}_1\delta+\dot{\theta}_1\dot{\delta}+2\dot{\varphi}_1\dot{X}+B\dot{Y}+B_2Y=-N_z sign(\dot{Y});\\
&\ddot{Y}+(\ddot{z}_1+\ddot{x}_1\psi_1+\ddot{\delta}\cos\alpha_1)\cos\alpha+(\ddot{x}_1-\ddot{z}_1\psi_1-\ddot{\delta}\psi_1\cos\alpha_1-\dot{\delta}\dot{\psi}_1\cos\alpha_1)\sin\alpha-\ddot{y}_1\theta_1-\\
&-\ddot{\theta}_1 Y-2\dot{\theta}_1\dot{Y}-2\dot{\psi}_1\dot{X}+D_1 z_1+E\dot{x}_1+E_1\dot{Z}-CZ=-N_z sign(\dot{Z})-g\cos\alpha;
\end{aligned} \qquad \text{(I.64)}$$

where A, *B*, B_1, B_2, *D*, *E*, E_1, *C* – the coefficients describing the properties of transported material; among them, *B*, *D*, *E*, E_1, and *C* – vary according to the position of load relative to the WM [1, 11] .

In the equations (I.64), the influence of the WM elasticity is taken into account by the coordinate δ included in other, linear or non-linear components in the form of a product with other coordinates. Among them, a dominant impact is exerted by the

components, where the acceleration of the elastic deformations (inertial terms) enter in a linear form, for example, $\ddot{\delta}\cos\alpha_1\cos\alpha$ in the first equation and $\ddot{\delta}\cos\alpha_1\sin\alpha$ in the second one.

2. 4. Mathematical modeling of the process of spatial vibrating transportation along the elastic plane

The subject of the research was an electromagnetic vibratory feeder with a vibratory exciter C-920, with a resonance frequency of 50 Hz [11].

The vibro-transportation process on the elastic surface is described by the equations (I.62) - (I.63) with respect to the WM and TL of a certain type. To study the impact of different rigidities of the bottom of the elastic WM on the transportation process, it is necessary to change rigidity of the bottom surface, i.e. its dimensions, and in order to simplify the problem, it can be represented as a set of homogeneous plates. By changing the rigidity of such WM, it is possible to obtain different frequencies of the elastic deformations.

This approach provides the opportunity to study the impact of different rigidities of the bottom of the WM, as well as the impact of the linear and nonlinear elastic deformations on the transportation process. The occurrence of the resonant elastic deformations of platinum is based on the transfer of a nonlinear electromagnetic force or nonlinear elastic force from the elastic system of the vibratory feeder (equation (I.63).

When studying parasitic spatial vibrations (Chapter 1), with a view to identifying the nature and features of their impact on the transportation process, it was possible to confine ourselves to change in the frequency of the exciting force near resonance in a relatively small range (for example, at three points - before resonance, in resonance and after resonance in increments of 1, 5 - 2 Hz); the same approach will also be used in this study.

Similarly, as stated above, when studying the impact of resonant vibrations, with a view to saving machine time, there is no need to consider change in rigidity of the plate within wide limits, since during resonance withdrawal, for example, in the zone and above, the amplitude decreases significantly. Therefore, by solving the equations (I.62) - (I.64) in the zones of $\omega \pm 2$ Hz, the obtained results can be used to providesome indications of trendsin the influence of the amplitude (frequency) of the elastic deformations of the WM on the process of vibro-transportation.

Below (Fig. I.25 - I.32) are dependency graphs of the velocity and trajectory of the vibratorydisplacement of bulk TL on a combination of various resonant (25, 50, 100 Hz)

activevibrations of the WM frame and the corresponding resonant elastic deformations of the WM's bottom.

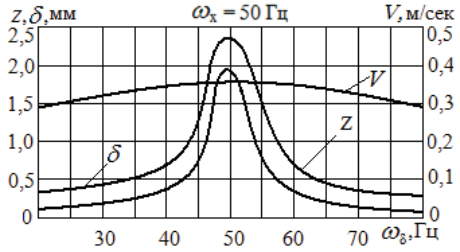

Fig.I.25. The dependence of the velocity and trajectory of TL *V* and *Z* on the amplitude and the frequency of deformation of the WM's bottom during the phase coincidence with operating vibration of WM

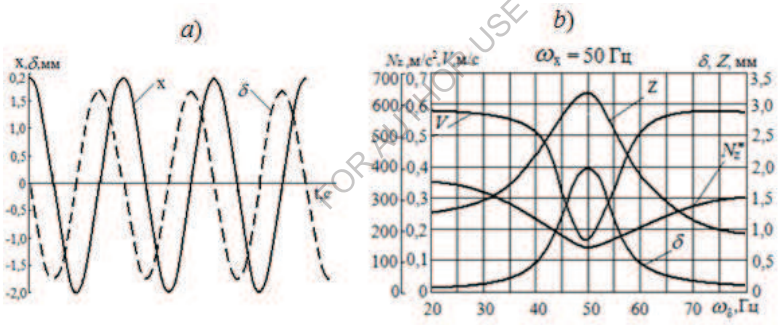

Fig.I.26. The dependence of the velocity and trajectory of TL *V* and *Z*on the amplitude and the frequency of deformation (δ) of the WM's bottom (Fig.I.26*b*) during the phase non-coincidence with operating vibration of WM (Fig. I.26*a*)

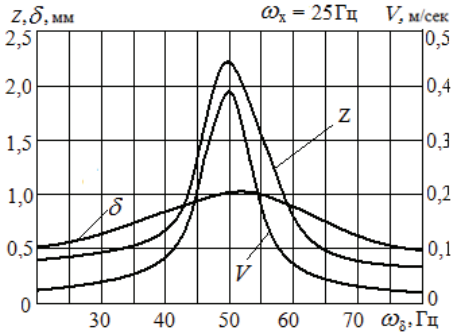

Fig.I.27. The dependence of the velocity and trajectory of TL *V* and *Z* on the amplitude and the frequency of deformation (δ) of the WM's bottomin the subharmonic (ω_x=25 Hz)resonant mode of machine operation during the phase coincidence

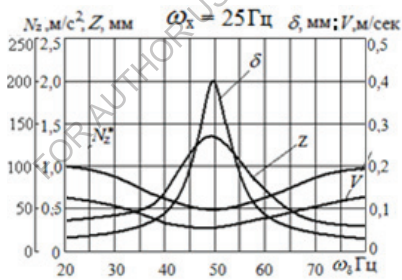

Fig.I.28. Зависимость скорости, траектории и нормально реакции от амплитуды и частоты деформации (δ) дна РО при субгармоническом (ω_x=25 Гц) резонансном режиме работы машины при сдвиге фаз.

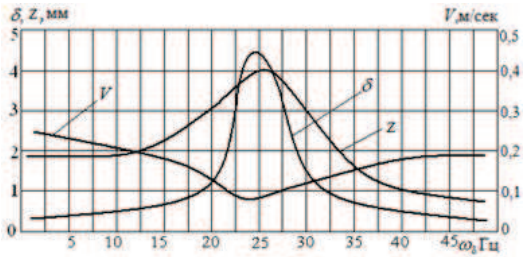

Рис.I.29. The dependence of the velocity and trajectory of TL *V* and *Z* on the amplitude and the frequency of deformation (δ) of the WM's bottom in the subharmonic (ω_x=25Hz) resonant mode of machine operation during the phase displacement*δ*and *x*

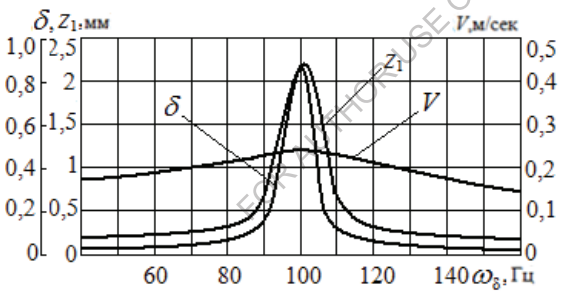

Fig.I.30. The dependence of the velocity and trajectory of TL *V* and *Z* on the amplitude and the frequency of deformation (δ) of the WM's bottom in the subharmonic (ω_x=25 Hz) resonant mode of machine operation during the phase coincidence *δ*and *x* .

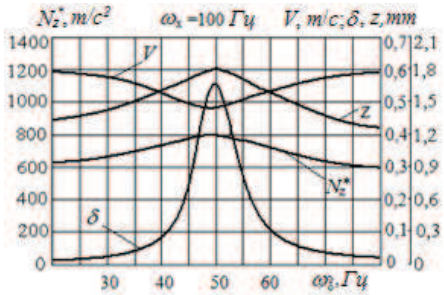

Fig.I.31. The dependence of the velocity, trajectory and normal response on the amplitude and the frequency of deformation (δ) of the WM's bottom in the subharmonic (ω_x=25 Hz) resonant mode of machine operation during phase displacement δ and x

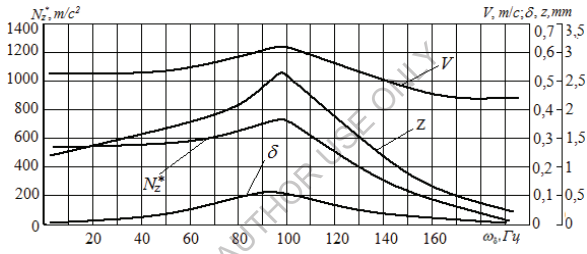

Fig.I.32. The dependence of the velocity and trajectory of TL V and Z on the amplitude and the frequency of deformation (δ) of the WM's bottom in the subharmonic (ω_x=100 Hz) resonant mode of machine operation during the phase coincidence δ and x

2. 5. Development of new designs of the vibratory feeders with an elastic bottom of the WM

The simulation results show that the WM with finite rigidity can make major differencesin the patterns of the vibration technological process in comparison with the rigid WMs.

The need to take into account rigidity is primarily basedon the need forincreasing the dimensions of the WM of the vibrating machines without increasing their thickness, as well as by the application of a concentrated exciting force to a certain point of the working member, which is not evenly redistributed over the entire surface.

Another consideration for taking into account rigidity is that low rigidity of the WM can have a positive impact on execution of technological process; this assumption is based on the possibility of increasing the total amplitude, which consists of two types of vibration: 1) the vibration amplitude of the WM as a rigid body (in the form of an oscillator) and 2) the amplitude of the elastic deformations of the bottom of the WM as an elastic deformed body.

A certain combination of the mentioned amplitudes can give a positive effect in vibration treatment of materials, or in other technological processes. In particular, an increase in the total amplitude of the vibrating conveyor will contribute to an increase in the displacement velocity of material; in addition, the elastic deformations of various shapes can be successfully applied to cleaning the vibration tanks, vessels, wagons, etc. The effect can be increased if deformation of the elastic surface enters resonance with the exciting force or with vibration of the WM body. It should be noted that for the large-size WM and heavy operational load, this is found to be difficult to implement, since it requires the reduction in the thickness of the working surfaces to the dimensions that are unacceptable in technological processes with heavy loads.

Obtaining an increased total amplitude of the WM is prevented by its inertia (Fig.33b), since, under the effect of the force Q, the WM moves together with the frame to the amplitude A_k, and simultaneously itself deforms (in the first form) to the amplitude A_n or A'_nin the direction opposite to the force Q, which can reduce the total amplitude.

One way to achieve the desired effect is to use counterweights at the ends or contours of the plane; for other forms of deformation (n > 1), the solution can be different both in design and depending on the technological process.

Based on the analysis of various designs of the elastic working members and theoretical studies, the design of a vibratory feeder with the elastic WM was developed (Fig. I.33a).

The originality of the elastic vibrating through 3 is that the plate 4 is connected to it and its elastic rotation (deformation) is carried out in-phase with respect to vibrations of the through 3, that is, in the direction of transportation of technological bulk cargo. The plate is rigidly connected to the wall of the through 3, while the loads are attached to the plates 5, and the frequencies of natural rotational vibration of the plate are multiple to the frequency of the exciting force.

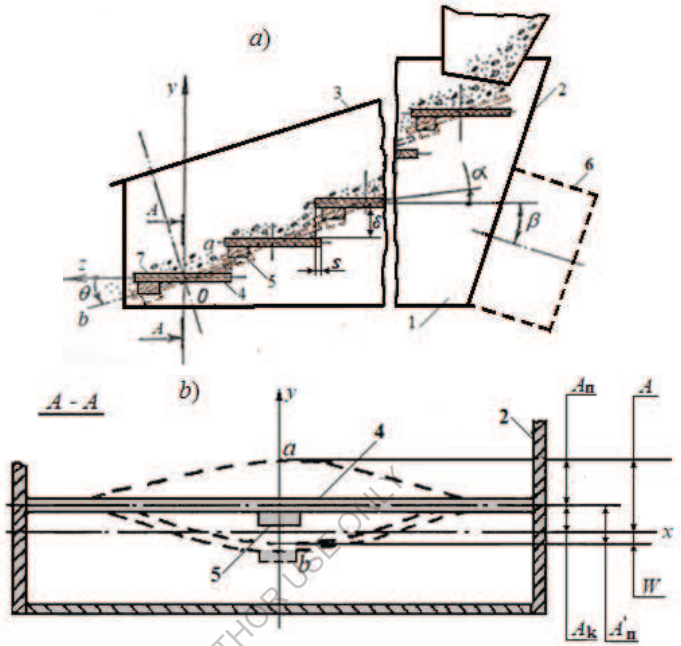

Fig.I.33. *a*) – The working member with;
b) – section *A-A*: a counterweighted elastic plate.

$$\omega_{пл} = \omega_{возб.} / n; \qquad (n = 1,2,3), \tag{I.65}$$

The parameters of the plate and the counterweight are determined by their design and inertial characteristics, which provide the occurrence of resonant rotational vibrations of the platinum relative to the exciting force. δ and s are the distances between the plates, while β and α are the angles of vibration and tilt of the working member.

The vertical amplitude of the extreme point „*a*“ of the plate 4, vibrating in-phase relative to the stationary flat system *Oxy*, is equal to:

$$A = A_{кр} + A_{пл},$$

where $A'_{пл.}$ - is the amplitude of vertical vibration of the through (the working member's frame), $A_{пл.}$ - is the amplitude of the elastic deformation of the extreme point „*a*“ of the

plate. The vibration amplitude of the extreme point „*b*“, which is become out of phase relative to the counterweight 5 of the plate, is equal to:

$$W = A \quad + A' \quad ,$$

where $A'_{\text{пл.}}$ - is the amplitude of vertical vibration of a point „*b*“ from the side of the counterweight attachment.

Thus, in the process of vibration, the plate 4 from the side of the upper part 7 rotates at an angle θ towards the direction of transportation, which contributes to an increase in productivity.

By choosing the parameters of the plate 4 and mass 5, it is possible to adjust natural torsional vibrations of the plate to a certain frequencythat is multiple to the frequency of the vibratory exciter and thereby achieve vibrations of one edge of the plate in the in-phase mode with the vibratory exciter.

By tilting the through at an angle $0 \le \alpha \le \theta$ towards the movement of material, it is possible to carry out additional regulation of productivity and technological parameters and at the same time to exclude the rotation of the portable surface 7 in the opposite direction to the movement of material.

The presented design of the through will allow to significantly increase the productivity of the vibrating machines (vibrating feeders, vibrating conveyors), and by increasing the vertical component of the vibration amplitude in the transportation process with stratification, drying, mixing, etc., to increase the mobility of hardly transportable materials (wet, finely dispersed, etc.).

Conclusions

1. Possible deviations in the transmission of the exciting force to the working member and in the design arrangement of the coordinate systems of masses due to errors in the manufacture and installation of the vibrating machine and the specifics of the elastic system are considered.

These deviations were taken into account in the interrelated equations of motion of the system "vibratory exciter - working - operational load", and the nature of the influence of spatial "parasitic" vibrations of the working member on the behavior of operational load was investigated.

The simulation results showed that the combination of some spatial vibrations with operating vibrationis having a positive effect, and in the future they can be used for practical purposes.

2. The equations of spatial motion of the system "vibratory exciter - working member with an elastic bottom - operational load" have been composed and the effect of the bottom deformation on the behavior of operational load has been investigated.

Studies have shown that it is possible to increase the total vibration amplitude of the elastic bottom of the working member, as well as to increase the intensity and velocity of the movement of bulk material along the elastic surface. The structural changes of the existing working members are outlined to improve the technological process characteristics.

References

1. Goncharevich I. Theory of Vibratory Technology. Hemisphere Publisher, 1990.
2. Filippov A.P. Oscillations of deformable systems. M.: Mashinostroenie, 1970, 736 p. (in Russian).
3. Gritsiuk V.E. A mathematical model of body motion along the deformable rough shape surface. Applied Mechanics, Kiev, No. 6, 1983, pp. 63-64. (in Russian).
4. Ganiev R., Kononenko V. Oscillations of solids. M. Nauka, 1976 (in Russian).
5. Suslov G.K. Theoretical mechanics. OGIZ publishers, 1946, 655 p. (in Russian).
6. Blekhman I. I. Vibration Mechanics and Vibration Rheology. Theory and applications. M., Fizmatlit, 2018 (in Russian).
7. Blekhman I. I. Theory of Vibration Processes and Devices. Vibration mechanics and vibration technology, Ore and metals, SPB, 2013 (in Russian).
8. Kryukov B. I. Forced oscillations of essentially nonlinear systems. Mashinostroenie, Moscow, 1984, (in Russian)
9. Khvingia M.V., Zviadauri V.S. The movement of bulk material along the spatial vibrating plane. M., Mashinostroenie, No. 3, 1981, pp. 42-49 (in Russian)..
10. Panovko G.I. Dynamics of the Vibratory Technological Processes. RCD. M.-Izhevsk. 2006 (in Russian).
11. Zviadauri V. Dynamics of the vibratory transportation and technological machines; "Mecniereba", 2001 (in Russian)
12. Khvingia M.V. Dynamics and strength of vibration machines with electromagnetic excitation. Mashinosroenie, 1980 (in Russian).
13. Sorokin S.A. The influence of the amplitude-frequency characteristics of the vibratory doser on uniformity of mixture discharge. // Agriculture, forestry and water industry. 2012. No.5 [Electronic media]. URL: http://agro.snauka.ru/2012/05/329 (reference date: 26.01.2017) (in Russian).
14. L.A. Vaisberg, I.V. Demidov, K.S. Ivanov. Mechanics of granular media under the vibration impacts: Methods for description and mathematical modeling. Institute of Mechanical Engineering Problems of the RAS, Russian Federation), "Ore Concentration", 2015. No. 4 (in Russian).
15. Poturayev V.N. Mechanics of the vibrating machine with the elastic working members / V.N. Poturayev, V.P. Nadutiy, A.V. Yurchenko; The AS of USSR. Institute of Geo-Technical Mechanics – Kiev: Naukova Dumka, 1991. – 152 p (in Russian).

16. Blekhman I. I. Vibration Mechanics and Vibration Rheology. Theory and applications. M., Fizmatlit, 2018 (in Russian). [2]. Blekhman I. I. Theory of Vibration Processes and Devices. Vibration mechanics and vibration technology, Ore and metals, SPB, 2013 (in Russian).
17. Chelomey V.N. (Red.) Vibrations in the technique. Handbook in six volumes, Vol. 4, vibration processes and machines, 1981, p. 13-132 (In Russian).
18. Poturayev V.N. Problems of the vibrating transport and technological machines. In the book "Problems of Vibration Engineering" – Kiev, Naukova Dumka, 1970.- pp. 3-9 (in Russian).
19. Stefan J Linz. Model for transport of granular matter on an annular vibratory conveyor Journal of Statistical Mechanics: Theory and Experiment; 2005.
20. Brodskiy Yu.A., Kolosov S.L., Shalunov B.S. Vibrating conveyors – technolgically pure type of industrial transport."Heavy Engineering Industry", No. 1, 2004. pp. 35-37 (in Russian).
21. Shiron E.G. Cause of galloping motion of though. Proceedings oft he AS of Latvian SSR, No. 3, 1964, pp. 85-92 (in Russian).
22. Yeliseyev A.V., Selvinskiy V.V., Yeliseyev S.V. Dynamics of vibrating interactions of the lelements of technological systems with account for unilateral constraints. Monograph, Printing office of IrGUPS, Irkutsk, 2015, 400 p. (in Russian).

PART II
CALCULATION AND MODELING FOR DYNAMICAL STABILITY OF THE ELECTROMEGNETIC VIBRATING MACHINES

Introduction

The vibrators are having many industrial applications and can be used to obtain mechanical vibrations used in vibration technologies, for example: for shaking concrete and other mixtures, vibration transfer of bulk and viscous substances, activation of chemical processes in liquid and bulk media, and so on. The resonant vibrators are the most efficient energy consumers when converting electrical energy into mechanical energy. The vibratory exciters can have different designs and constructions, but the basic principle of their operation is the same - generating the vibration in the movement of two masses, one of which is a working member.

For all vibrators, one of the integral parts is the elastic element. In the vibrating machines, there are mainly used cylindrical helical springs with a circular cross-section (II.1) and the flat spring systems (II.2), whose rigidity is calculated according to the following formulas.

$$k_{\text{пр}} = \frac{Gd^4}{8D^3 l_{\text{пр}}} \qquad \text{(II.1)}$$

$$k_{\text{рес}} = \frac{192EI\xi}{l^3}\ , \qquad \text{(II.2)}$$

where D - the average diameter of coil, d - the wire diameter, G - elastic shear modulus, l_w- the wire length, E - the elastic modulus, I – the second area moment; l - the length of bow springs.

Figure 2.1 illustrates the design model of the double-sided clamped spring arrangement.

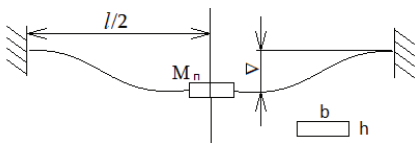

Fig. II.1. The double-sided clamped spring Arrangement

The type of the elastic systems and their damping coefficients are of great importance, since they play an important role in the dynamic stability of the vibrating

machines during operation. The elastic elements can have both linear and non-linear characteristics. In terms of nonlinearity, they can have hard or soft characteristics.

Although the electromagnetic vibrators have a very simple design, their theory and, therefore, the mathematical description of their dynamic and sustainable conditions is quite complex and involves fundamental issues of vibrational theory.

1. The torsional electromagnetic vibrating machine

Among the vibrating machines with various elastic systems, in practice, machines are used whose elastic elements work under torsion. Along with flat bow springs and coil springs, the torsion bars are the main type of the elastic elements used in the vibrating machines, exciters and bunkers [1, 2]. The torsional elastic elements springs have several advantages over other elastic elements such as leaf springs or coil springs.

These advantages include the manufactur ability of the torsion bars, greater compactness and design ability, increased durability and stability in operation, the improved availability per unit weight of the torsion shaft, due to the specificity of the stress state during torsion, which enables, other things being equal, to reduce the weight of the torsion bars by 30 - 35%; the absence of additional stresses caused by inaccuracies in the manufacture of the torsion bars (typical of the processes of winding coil springs or leaf spring pressing). The torsional elastic elements are characterized by lower losses due to structural friction in the fixturings compared to the spring arrangements and a lower noise level than in the spring systems [3, 4, and 5].

A simplified diagram of the torsional electromagnetic vibrating machine is shown in Figure II.2. It consists of an active mass (AM) 1 with a through 2 and a reactive mass (RM) 3, which are interconnected by means of the torsional elastic elements 4, and a bicyclic electromagnet 5, which excites and maintains vibrations.

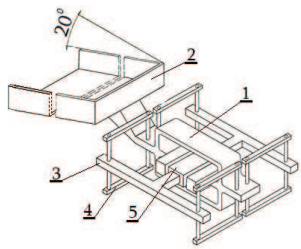

Fig.II.2 A simplified diagram of the torsional electromagnetic vibratory exciter

The torsional elastic system I used in the electro-vibrating machines is an elastic frame (Fig. II.3) and consists of two torsional bars 1 and one connecting lever 2, which connects free ends of the torsion bars. The frame is loaded with torsional and bending moments as well as with a shear force. Such flat and elastic frames, the number of which is equal to eight, are located in space symmetrically relative to the longitudinal and transverse axes of the machine. Each frame has series-connected two torsion bars and one lever; therefore, the total pliancy is equal to the sum of pliancy of the individual elements. [6, 7].

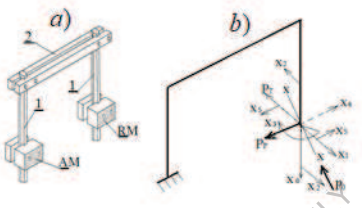

Fig.II.3.The elastic system of the vibrating machine: *a*) torsional frame; *b*) forces operating in the fixturing

In the process of vibrations, the torsional elastic frames are in a complex deformed state of torsion and bending [6, 8].

2. Calculating the rigidity of the elastic frames at small deformations

During vibrations, the displacement of AM relative to RM, associated with torsion of the torsion bar, due to the equally-spaced location of the elastic frames, takes place in the direction of longitudinal axis of the machine, i.e. in the thrust line of the electromagnet and inertial loads. The design scheme, by the type of the effect of force is planar-spatial and statically indefinite [6, 9].

In the planar-spatial systems, the internal power factors in the section of plane of the frame are equal to zero; therefore, in order to unveil static uncertainty, it is sufficient to identify the internal power factors acting in the plane perpendicular to the frame section. Static indeterminacy is unveiled by the force method. The canonical equations obtained in this case have the form as follows:

$$\begin{aligned} \delta_{11} x_1+\delta_{11} x_2+\delta_{11} x_3=-\delta_1 P_t; \\ \delta_{21} x_1+\delta_{22} x_2+\delta_{23} x_3=-\delta_2 P_t; \\ \delta_{31} x_1+\delta_{32} x_2+\delta_{33} x_3=-\delta_3 P_t; \end{aligned} \qquad \text{(II.3)}$$

where δ_{ji} are coefficients denoting the mutual displacement of points of the system, the first index corresponds to the direction of movement, the second one - to the force number that caused this movement; X_k - unknown power factors; δ_k P_t – the displacements from an external force.

There is no connection on the frame that would prevent the movement in the direction of X_1 (the external force P_o acts along the x-x line (Fig. II.2.b). Therefore, X_1, δ_{11}, δ_{12}, δ_{13} are equal to zero.

Table II.1 shows the values of coefficients of possible displacements δ and $\delta\overline{o}$ obtained by the Vereshchagin rule, where I is an axial torque of the torsion bar section, I_0- is the second area moment of the lever section on a torsion, I_k is the moment of inertia of the section of the torsion for torsion, I_{ko} is the moment of inertia of the section of the torsion for torsion, P_t - longitudinal component of the external force P_o, l - the torsion length, r - the lever arm, E - the elasticity modulus, G - the transverse modulus of elasticity, μ - Poisson's ratio.

Table II.1.

δ_{22}	$\frac{2l}{GI_k}+\frac{r}{EI_0}$
$\delta_{23}=\delta_{32}$	0
δ_{33}	$\frac{2l}{EI}+\frac{r}{GI_{ko}}$
δ_2 P_t	$-\frac{P_t r}{2}(\frac{2l}{GI_k}+\frac{r}{EI})$
δ_2 P_t	$-P_t(\frac{2l}{GI_k}+\frac{rl}{GI_{ko}})$

After unveiling static uncertainty from the equations (2.1), we get

$$X_2 = M_k = K_1 P_t r;\ X_3 = M_u = K_2 P_t l; \qquad \text{(II.4)}$$

$$K_1 = 0.5; \quad K_2 = \frac{0{,}5m+1}{m+1}; \quad m = \frac{I_{ko} l}{(1-\mu) I r}$$

where M_k- torsional moment, M_u- bending moment.

By multiplying the total force moment diagram, (Fig. II.4) by the diagram of the moment of a unit force applied to the pinch point, we get the displacement of AM relative to RM in the plane perpendicular to the frame section, i.e. in the direction of *P*:

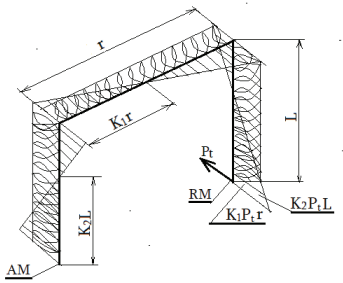

Fig. II.4. The total force moment diagram

$$\lambda = \frac{K_1 P_t r^2 l}{GI_k} + \frac{2-3K_2+2k_2^3}{3}\frac{P_t l^3}{EI} + \frac{k_1^2+2k_1^3}{3}\frac{P_t r^3}{EI_o} + (1+k_2)\frac{P_t r l^2}{GI_{ko}} \qquad \text{(II.5)}$$

Linear rigidity of the torsional elastic frame equals

$$k_t = \frac{GI_k}{k_1 r^2 l(1+z_1+z_2+z_3)} \qquad \text{(II.6)}$$

where

$$z_1 = \frac{2-3K_2+2k_2^3}{3}\frac{GI_k l^2}{EIr^2} \; z_2 = \frac{k_1^2+2k_1^3}{3}\frac{GI_k r}{EI_o l} \; z_3 = +\frac{(1+k_2}{k_1}\frac{I_k l}{Iko\, r} \qquad \text{(II.7)}$$

Coefficients Z_1, Z_2 and Z_3 show, respectively, the influence of a bend in the torsion bar, a ben in the lever and its rotation on linear rigidity of the frame.

Despite the fact that, according to initial assumptions, the equations (II.5) and (II.6) are linear, however, both experimentally and theoretically it is proved that due to the opening of the torsion pinching nodes, rigidity of the elastic system is a nonlinear function of the vibration amplitude. In this design, the connecting arm consists of two beams rigidly packed together by means of the fastening bolts. At low vibration amplitudes, the beams work on torsion and bending as a monolithic system. An increase in the load leads to a gradual slippage at the beams' fixing points, as a result of which the torsional and bending rigidity of the lever goes down (GI_{ko}, EI_o). In the process of vibration, changes in the parameters I_{ko}, l affect the magnitude of the coefficient K_2. For

example, with an increase in the displacement of the masses of the vibratory exciter from zero to $1{,}2.10^{-3}$ m, K_2 varies in the range of 0.5÷0.95. In the process of deformation, the rigidity is mostly affected by the varying (by about 25%) active working length l of the torsional bar. As is clear from the equations (II.5), (II.6), (II.7), rigidity of the system is mainly associated with the first term, therefore, change in l directly, and not through Z_1, Z_2, Z_3, affects rigidity K_t and creates a noticeable nonlinearity, which is the reason that $K_t \neq$ const.

3. Determination of the lateral force during deformation of the torsional elastic frame

The rectilinear parallel displacement of AM relative to RM, and curvilinear (along the arc) motion of the lever ends, at high vibration amplitudes (Fig. II.3), cause deformities of the elastic elements in the plane of the frame section, and therefore lateral force P_r appears.

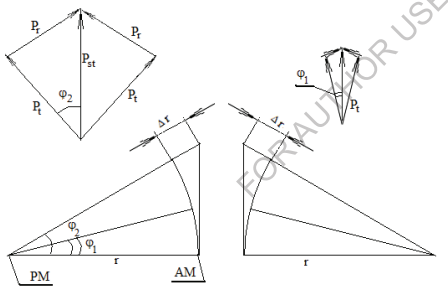

Fig.II.5a. The diagram of the summation of longitudinal (P_t) and transverse (P_r) forces

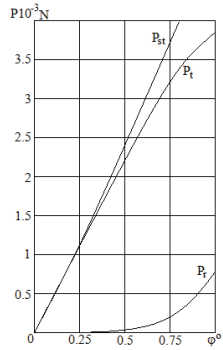

Fig.II.5b. Variation in the magnitude of longitudinal and transverse forces depending on the torsional angle of the torsion bar

Flexural rigidity of the torsional elastic system in the plane perpendicular to the direction of the motion of masses further prevents the displacement of AM relative to the RM. Thus, the traction force of the electromagnet and inertial loads from the acceleration of longitudinal motion of AM and RM decompose into the longitudinal P_t and P_r components, which change direction and magnitude with an increase in the vibration amplitude (Fig. II.5a).

As evidenced in Figure II.5a, when AM moves relative to the RM by the value λ, the distance between the masses increases by Δr. This increase is offset partially by the lateral bending of the torsion bars. Thus, without the torsion bar deflection, the movement associated with a torsion of the torsion bar and the lever cannot be realized.

Figure II.3 shows that

$$\Delta r = r_i - r\,, \tag{II.8}$$

where $\Delta r = P_r l^3/3EI_0$ the deflection of the torsion bars caused by lateral force.

After substituting the values Δr and r_i = r/cosφ for (II.8), we get an expression connecting the lateral force P_r with an angle of torsion (rotation) of the torsion bar $\varphi = \lambda/r$

$$P_r = \frac{3EIr}{l^3}\left(\frac{1}{\cos\varphi} - 1\right) \tag{II.9}$$

To facilitate the further use, we expand [(1/cosφ) -1] in a series

$$\frac{1}{\cos\varphi} - 1 = 1 + \frac{1}{2}\varphi^2 + \frac{5}{24}\varphi^4 + \cdots - 1$$

Due to the smallness of φ (for the vibratory exciter with a capacity of 1 kW at λ=5.10^{-4} *m*, (φ = 0.002 rad), it is advisable to write (II.9) in the form as follows

$$P_r = \frac{3EIr}{2l^3}\varphi^2 \tag{II.10}$$

It can be seen from (II.10) that the lateral force is a nonlinear function of the vibration amplitude φ. The non-linearity of lateral rigidity has an impact on the torsional rigidity characteristic. Therefore, the nonlinear rigidity characteristic of a torsional elastic system (due to a change *K*2, *l*) increases with allowance for lateral force.

The ratio of stresses corresponding to the acting forces equals

$$\frac{\sigma_1}{\sigma_2} = \frac{P_t l W_2}{P_r l W_1} = \frac{2\lambda l^2 I_k W_2}{3K_1 r^3 EIW_1(1+Z_1+Z_2+Z_3)\varphi^2}\,, \tag{II.11}$$

where W_1, W_2 – the torsion bar section module under bending from the acting forces P_1 and P_2, respectively. For a torsion bar with a hexagonal cross-section, the expression (II.8) takes the form

$$\frac{\sigma_1}{\sigma_2} = 0{,}426\frac{\lambda l^2}{K_1 r^3(1+Z_1+Z_2+Z_3)\varphi^2} \qquad \text{(II.12)}$$

4. Analysis of the rigidity characteristics of the torsional elastic frame

Despite the fact that longitudinal and lateral rigidities have separately the linear characteristics, the overall rigidity of the machine, without considering the impact of slippage in the pinching points of the torsion bars, at the large vibration amplitudes turns out to be nonlinear. This is caused by a nonlinear force P_r (Figure 2.5a), which, due to the relationship between the lateral and longitudinal rigidities of the torsional frame, gives the elastic system a nonlinear rigidity characteristic.

Based on the analysis, it turns out that the nonlinear characteristic of the torsional elastic frame is due to both slippage in the fixturings and the lateral force P_r.

At low vibration amplitudes, the rigidity characteristic of the torsion frame is soft, caused by slippage in pinching. At large vibration amplitudes, a transverse force *P*r appears which compensates for the effect of slippage. With a further increase in the displacement, the effect of Pr increases noticeably in comparison with slip into pinches. Thus, the torsional elastic frame is a nonlinear system and has a soft characteristic at small amplitudes, and rigid one at large amplitudes.

Due to the fact that the torsional frame does not have a connection that prevents the AM displacement along the transverse axis of the machine, transverse vibrations may appear in the system together with longitudinal ones. However, transverse vibrations do not progress at the specified operating frequencies, since the rigidity *K*r is one level higher than K_t [6, 8]. In expression (2.5), we denote by $K_{KT} = GI_k/L$ и $K_{ut}=3EI/L^3$ the torsional and bending rigidities of the torsion bar. After the agreed notations, (2.5) takes the form

$$K_{Kt} = K_t K_1 r^2(1 + z_1 + z_2 + z_3); \qquad \text{(II.13)}$$

Taking into account

$$K = m_b\omega^2, \qquad \text{(II.14)}$$

we get

$$K_{Kt} = 4nm_b\pi^2 f_1^2 r^2(1 + z_1 + z_2 + z_3); \qquad \text{(II.15)}$$

where m_b – reduced mass; ω - free circular frequency in radians; f_1, - vibration frequency of the vibratory exciter in hertz; n – the number of the torsional elastic frames.

By means of the equations (II.15), the geometric parameters of the torsional elastic frame are directly determined, which provide the required rigidity and frequency for the remaining parameters of the machine, specified out of concern for the design considerations.

At vibrations, the elastic element performs a complex movement in space [10], which is transmitted to the working member of the machine. Additional vibrations (transverse, vertical, rotary) are amplified when symmetry, i.e. the equality of individual rigidities of the torsional elastic frames relative to the axes of the machine is broken, When the free frequencies of individual vibrations coincide with the exciting frequency (or with frequencies multiple to it), additional resonances may arise in the system. These vibrations can both reduce and increase the productivity of the machine [1].

5. Design of the torsional elastic frame for the rigidity taking into account strength in a 25-Hz vibratory mode

When calculating the rigidity of the torsional elastic system of the vibratory exciter providing the 25-Hz mode, it is advisable preliminary to estimate the utilization rate of the elastic element material [2].

$$k_y = \int_0^M Md\varphi = \frac{K_1 r^2 V}{4G}(1 + z_1 + z_2 + z_3); \qquad \text{(II.16)}$$

where V is the volume of material.

Taking into account the consumption of the expensive spring steel and based on the design considerations (especially in relation to compactness of the machine), the length of the levers and the torsion bars specifies the parameters. Further, the overall dimensions of the elastic elements are adjusted taking into account the plaices of the clamped parts of the torsion bars, and their diameters are determined.

Considering that the torsional moment of inertia of the polygonal torsion bar is equal to $I_k = K_i d^4$, where d is a diameter of an incircle inside the polygon, K_i is the dimensionless coefficient.

$$d = \sqrt[4]{\frac{K_t l}{K_i G}} = \sqrt[4]{\frac{4m_b \pi^2 f_1^2 r^2 l(1+z_1+z_2+z_3)}{K_i G}} \qquad \text{(II.17)}$$

It should be noted that the calculatory rigidity and weight of the elastic system of the low-frequency 25-Hz vibratory exciters are 4 times less than in the main resonance mode

(50 Hz). However, in order to avoid affecting the performance of the machine, it is necessary to increase the vibration amplitude of the working member (in the case of the same velocities). This causes an increase in stresses of the elastic elements of the torsional frame. Therefore, it is necessary to test the torsion bars to destruction to calculate the parts that work simultaneously in torsion and bending.

$$\tau = \frac{M_k}{W_k}; \qquad \sigma = \frac{M_u}{W_u}; \qquad \sigma_b = \sqrt{4\tau^2 + \sigma^2}. \tag{II.18}$$

Further, the torsional, flexural and overall strength margins are determined taking into account the maximum stresses,

$$n_\tau = \frac{\tau_{-1}(\varepsilon_\tau)d}{\tau}; \qquad n_\tau = \frac{\sigma_{-1}(\varepsilon_\sigma)d}{\sigma}; \qquad n_b = \frac{n_\tau n_\sigma}{\sqrt{n_\tau^2 + n_\sigma^2}}, \tag{II.19}$$

where σ_{-1}, τ_{-1} are the endurance limit stresses of material under bending and torsion, respectively; $(\varepsilon_\tau)_d$ $(\varepsilon_\sigma)_d$ – the influence coefficients of the absolute dimensions (scaling factor) under torsion and bending, respectively, for a smooth shaft with a diameter *d*.

Thus, when calculating the elastic element of the 25-Hz and sub harmonic vibratory exciters, the following requirements are met: doubling the vibration amplitude of the working member with a view to ensuring the required average transportation velocity $\lambda = \lambda_o/2$, reducing the rigidity by 4 times $K_{to} = K_t/4$, and adjusting the obtained values [2].

Using the equations (II.5), (II.6), (II.7), we obtain

$$\frac{d^4}{r^2 l(1+z_1+z_2+z_3)} = 4\frac{d_o^4 n_o}{r_o^2 l_o(1+z_{1o}+z_{2o}+z_{3o})} \tag{II.20}$$

$$\frac{\pi r}{d}(1 + z_1 + z_2 + z_3) = \frac{\tau_o l_o r_o}{2d_o}(1 + z_{1o} + z_{2o} + z_{3o}), \tag{II.21}$$

where the index *o* is put for the parameters of the elastic elements providing 25-Hz and sub harmonic resonances.

While maintaining the values $r=r_o$; $L=L_o$; $d=d_o$, according to (2.20), we'll obtain that $n_o = n/4$,, and from (II.21) – $\tau_o = 2\tau$, that is, the mass of the elastic elements decreases by 4 times, however, an increase in τ by 2 times causes a decline in the reliability of the machine due to an increase in the operating stresses of the torsion bars.

Consider the case when $n=4n_o$, $\tau = \tau_o$, for $\lambda_o=2\lambda$. Based on the design considerations, we will make the ratio of the lever lengths and the torsion bar a constant (usually i=1.5÷1.7), in the main and subharmonic modes

$$\frac{r}{l} = \frac{r_o}{l_o} = i \qquad \text{(II.22)}$$

After solving the system of the equations (II.20), (II.21) (II.22), we obtain $d_o = 1{,}5d$; $l_o=1{,}74$ l; $r_o=il_o$. Thus, after adjustment, the mass of the elastic element decreases 2.2 times. If condition (II.22) is replaced by the condition $L/L_o=1$, we obtain $do=2d$; $r_o= 4r$, i.e. the mass of the elastic element decreases 1.5 times.

Analysis of the equations (II.5) ÷ (II.7) shows that the decline in the torsional rigidity of the lever increases the pliancy of the torsional frame. Consequently, the stresses on the frame are reduced. This allows reducing further the mass of the elastic system without reducing the strength margin. Based on the studies, it can be concluded that from the viewpoint of savings of material of the elastic system, the torsional frame is effective in comparison with springs and bow springs [2, 6].

6. Determination of the damping coefficient

The elastic elements of the frame are twisted and bent under the effect of a periodic exciting force. In this regard, as a result of joint action by the forces of elasticity and dry friction, energy dissipation occurs in the places where the elastic elements are pinched (Fig.2.6 a, b).

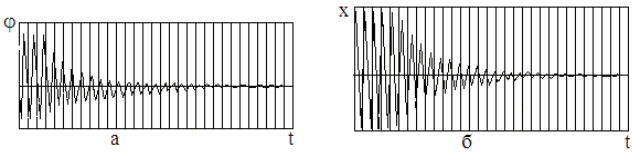

Fig. II.6. Oscillograms of damping of free vibrations of the torsion bar: a) torsional; b) bending

The structural damping coefficients of torsion and bending can be experimentally obtained using the energy method, after processing the oscillogram of free damped vibrations [11].

$$\psi = \frac{2}{m_s} = \frac{A_s - A_{s+m_0}}{A_s}, \qquad \text{(II.23)}$$

where m_0 –the number of periods, A_s and A_{s+mo}- the vibration amplitudes at the beginning and at the end of cycle.

7. Calculation of elastic frictional forces generating in the connection "shaft-bushing"

In the resonant vibrating machines, including those with a torsional elastic frame, an accurate determination of the vibration amplitude of the working member by calculation is possible only if losses in the design are known. All attachment fittings of the torsion bars are the conventionally fixed joints of the "shaft-bushing" type, loaded simultaneously with torque and bending moments, as well as with radial and axial forces.

At vibrations, the elastic elements of the frame are subjected to torsion and bending both in the direction of the acting force and in the plane of the frame; these deformities cause energy dissipation in the fixturing. In addition, along with longitudinal (main) vibrations, the machine can also perform transverse (lateral) and rotary vibrations, which are connected, mostly, with flexural deformation of the torsion bar. It is practically impossible to determine experimentally the structural damping coefficient separately for the corresponding vibrations in a real machine. Therefore, it is advisable to determine them theoretically when considering the geometric scheme of pinching of the torsion bar, which is affected by moments and forces, simultaneously.

This approach is also advisable due to the fact that the structural damping coefficient and the nonlinearity of the elastic system are interconnected, and both are caused by imperfection in the articulated parts. With an increase in loading, a gradual slippage occurs in the pinched places, as a result of which the rigidity of the system decreases and dissipative forces appear, causing energy dissipation during vibrations.

These issues have not yet been sufficiently studied for a connection in which the contact of the mating surfaces is carried out along a smooth non-circular surface that is, in a wedge-shaped elastic-frictional connection loaded simultaneously with torsional and flexural moments. At the same time, for the theoretical study of these systems, it is desirable to have, in addition to the numerical value of the damping coefficient, also the functional dependences showing the relationship between the vibration amplitude both with the damping coefficient and with the rigidity of the torsional elastic system.

8. Determination of dissipative forces under torsion and bending

Figure II.7 illustrates geometry of the clamped part of the torsion bar to determine the structural damping coefficient [12].

The bushing virtually is not subject to torsional deformation due to its large transverse dimension in relation to the torsion bar diameter (for example, usually for such connections of the bushing with the shaft, the ratio of their moments of inertia during torsion is $I_в/I_т \geq 15$).

As Figure. II.7 shows, the pressure ρ, caused by the torque M_k has an uneven effect along the width of the torsion bar, that is, from the side of the rib, the pressure ρ decomposes into the normal σ_n and shear σ_t stresses, while in the middle of the width of the side plane *B*, the pressure ρ causes only the shear stress σ_t. This is due to the fact that, in the plane of the cross section of the torsion bar, the distances from the points lying along the width of the side plane to the center *O*, are different in magnitude.

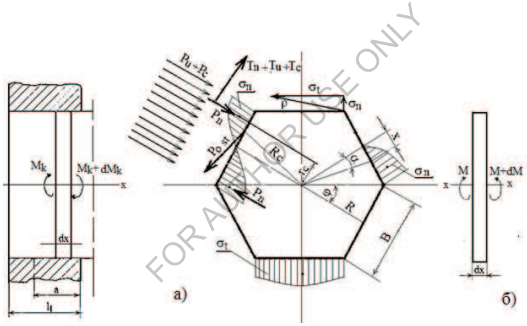

Fig.II.7. The geometric conditions of the clamped part of the torsion bar for determining the structural damping coefficient of torsion under the combined effect of the torsional and bending moments: a) forces acting on the clamped part of the torsion bar; b) the condition of equilibrium of the elementary section of the torsion bar under torsion

The average value of the line pressure over the width of the side plane of the polygonal torsion bar caused by the torque is

$$\rho = \frac{2M_k}{n'BR_c} \qquad \text{(II.24)}$$

Where n′ is the number of the side planes, $B_c = \frac{B}{4\sqrt{1+4ctg^2\frac{\pi}{n'}}}$ - the arm of force at a point $B/4$.

Under the influence of the elastic linkages, normal and tangential stresses appear, which exert an uneven effect along the width of the side plane B, the values of which are respectively equal to:

$$\sigma_n = \rho sin\alpha;$$
$$\sigma_t = \rho\, cos\alpha; \qquad \text{(II.25)}$$

where $\alpha = 2\pi x/Bn$ - is an angle between the torsion bar perpendicular to the side plane and the current value

$0 \le \alpha \le \pi/n.x$ – the current coordinate $0 \le x \le B/2$.

After integrating the stress diagrams along x, we obtain the normal and tangential forces that act on the side planes of the torsion bar:

$$P_n = \int_0^{D/2} \rho \cos\left(\frac{2\pi x}{Bn'}\right) dx = \frac{k_1}{n'R_c} M_k;$$
$$P_t = \int_0^{D/2} \rho \sin\left(\frac{2\pi x}{Bn'}\right) dx = \frac{k_2}{n'R_c} M_k, \qquad \text{(II.26)}$$

where $k_1 = \frac{n'}{\pi}\left(1 - \cos\frac{\pi}{n'}\right)$; $k_2 = \frac{n'}{\pi}\sin\frac{\pi}{n'}$ are the constant coefficients obtained when performing the integration.

The static moment of the diagram of normal stresses relative to the ribs of the torsion bar was determined as follows:

$$S_y = \int_F x dF = \int_0^{B/2} x\rho \sin\left(\frac{2\pi x}{Bn'}\right) dx = k_3 \rho B^2,$$
$$F = \frac{\sigma_n B}{2} = P_n, \qquad \text{(II.27)}$$

where $k_3 = \frac{n'}{4\pi}\left(\frac{n'}{\pi}\sin\frac{\pi}{n'} - \cos\frac{\pi}{n'}\right)$,- is a constant coefficient obtained when performing the integration.

It should be noted that the obtained static moment is a moment caused by the normal stresses, which can also be determined through the normal force P_n.

$$M_n = P_n r_c = \boldsymbol{S}_y \qquad \text{(II.28)}$$

where $r_c = \frac{S_y}{P_n} = \frac{2k_3B}{4}$ is the arm of a normal force P_n applied to the center of gravity of the diagram of the normal stresses σ_n.

The torque associated with the frictional forces is

$$M_t = p_t R, \qquad \text{(II.29)}$$

where $R = \frac{B}{2} ctg \frac{\pi}{n'}$ is the arm of frictional forces (the minimum distance from the center O to the side plane).

And finally, for the n'-facetted torsion bar, we obtain the following expression:

$$\begin{aligned} M_n &= 2\frac{k_3}{R_c} B M_k = k_4 B M_k; \\ M_t &= 2\frac{k_2 R}{R_c} M_k = k_5 M_k; \\ M_k &= M_n + M_t \end{aligned} \qquad \text{(II.30)}$$

Table II.2 shows the values of the coefficients $k_1 \div k_5$ for the multifaceted torsion bar, taking into account the number of ribs and the values of R and R_c for different n' while keeping the width B of the side plane unchanged. Therefore, with increasing n', the radius r of the circumscribed circle increases. If an increase in the number of the side planes occurs due to a decrease in the width B while keeping the diameter of the circumscribed circle unchanged, then R and R_c tend to r. Unveiling the $0.\infty$-type uncertainty results in

$$\lim_{n' \to \infty} R = \lim \frac{2r\sin\frac{\pi}{n'}}{2} ctg \frac{\pi}{n'} = r\,. \qquad \text{(II.31)}$$

From table II.2 it can be seen that при $n \geq 8$, the elastic-frictional connection of the multifaceted torsion bar practically turns out to be a frictional connection.

Table II.2

Number of side planes n'	k1	k2	k3	k4	k5	Kc.B	R.B
3	0.477	0.827	0.078	0.409	0.625	0.381	0.289
4	0.373	0.901	0.615	0.22	0.809	0.558	0.5
5	0.304	0.935	0.051	0.135	0.879	0.732	0.688
6	0.256	0.955	0.042	0.094	0.917	0.901	0.866

8	0.194	0.975	0.032	0.052	0.955	1.233	1.207
∞	0	1	0	0	1	∞	∞

The rotational displacement (slippage) in an elastic-frictional connection is possible only under deformation of the elastic joints. Based on the geometrical considerations (Figure II.8), the relationship between linear compression and the torsion angle of the torsion bar in the pinched places is expressed by the following relationship:

$$ao = (ob + bc)\cos\left(\frac{\pi}{n'} - \varphi_k\right) \tag{II.32}$$

After the value substitution

$$\text{ao} = \text{R} = \frac{\text{B}}{2}\text{ctg}\frac{\pi}{\text{n}'}; \qquad \text{ob} = \frac{\text{B}}{2}\sin\frac{\pi}{\text{n}'}; \qquad \text{br} = \frac{\Delta\text{h}}{\cos\left(\frac{\pi}{\text{n}'} - \varphi_\text{k}\right)}, \tag{II.33}$$

In (II.33) and after some transformations we obtain

$$\Delta\text{h} = \frac{\text{B}}{2\sin\frac{\pi}{\text{n}}}\cos\left(\frac{\pi}{\text{n}'} - \varphi_\text{k}\right) - \frac{\text{B}}{2}\text{ctg}\frac{\pi}{\text{n}'} \tag{II.34}$$

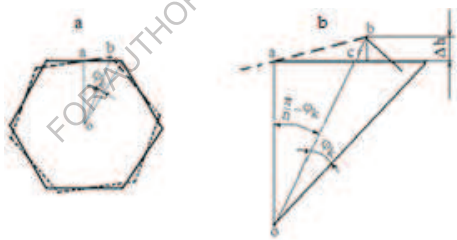

Fig. II.8. Deformation pattern of the clamped part of the torsion bar

Let us write (2.34) as a Maclaurin power series with respect to the variable φ_k.

$$\text{h} = \text{B}[0.5\varphi_\text{k} - 0.25\text{ctg}\left(\frac{\pi}{\text{n}'}\right)\varphi_\text{k}^2 - \frac{1}{12}\varphi_\text{k}^3 \ldots] \tag{II.35}$$

Due to the fact that the torsion angle φ_k in the fixturing is small, henceforth, the variable quantities higher than the first degree are not taken into account and finally

$$\Delta h = 0.5B\varphi_k. \tag{II.36}$$

The magnitude of the reaction of the elastic joints of the clamped part of the torsion bar is equal to the normal force P_n.

$$P_n = 0.5k_1c_k a_k \varphi_k, \quad \text{(II.37)}$$

where a_k is the length of the slip region of the clamped part of the torsion bar, c_k[Н/м] - the rigidity coefficient of the elastic joints, taking into account the pliancy of the fastening bolts.

As a result of a serial connection in the clamping unit of the bushing, torsion bar and fastening bolts, the total torsional clamping rigidity will be equal to:

$$\frac{1}{c_k} = \frac{1}{c_B} + \frac{1}{c_\tau} + \frac{1}{c_\sigma}; \quad \text{(II.38)}$$

where C_T, C_B and C_σ are the compressive rigidities of the torsion bar and bushings, and the tensile rigidity of bolts, respectively.

After the substitution of the corresponding rigidities for (II.38), we obtain

$$c_k = \frac{Ebb_1B}{2Rb_1 + R_B + l_1'b}, \quad \text{(II.39)}$$

where 0.5 B is the width of the contact surface of the mating, R_b- the bushing width l_1'- the bolt length; b_1 - the fictitious parameter of the cross-section of the bolts, determined from the condition of equality of the total sectional area of the bolts $F=b_l l_l$ (l1 is the pinch length of the torsion bar).

The frictional force from the action of normal force is

$$T_n = 0.5fk_2c_k a_k \varphi_k, \quad \text{(II.40)}$$

where f is coefficient of friction.

The magnitude of the frictional force from compression acting on one side plane equals

$$T_{ci} = f\rho_o B a_k \cos\beta_i, \quad \text{(II.41)}$$

where =1, 2, ... n' is the number of the side plane, β_i - an angle between the perpendicular to the compression force P_o and the appropriate i side plane; $\rho_{o=}P_o/\sum_{i=1}^{n'} l_1 B cos\,\beta_i$ – the value of specific pressure exerted on the side planes of the torsion bar.

For the n'-faceted torsion bar, the T_c value is:

$$T_c = \frac{f P_o a_k}{l_1} \qquad \text{(II.42)}$$

The frictional force from flexural moment is:

$$T_u = f c_u Q_u y, \qquad \text{(II.43)}$$

where Q_u is the slippage length from flexural moment, Y - the torsion bar flexing, c_u [N/m] - the coefficient of pinching rigidity under bending, which is determined similarly to (II.38), (II.39).

$$c_u = \frac{E b_1 b}{2Rb_1 + R_B b_1 + lb}, \qquad \text{(II.44)}$$

According to Figure II.8, the equation of moment scattering relative to the axis of the torsion bar X-X has the form

$$M_k = 0.5 k_1 c_k a_k \varphi_k - (T_n + T_c + T_u)R - P_o r_o - C_u l y z_o = 0, \qquad \text{(II.45)}$$

where z_o - is the arm of forces.

Figure II.9 illustrates geometry of the clamped part of the torsion bar to determine the structural damping coefficient of bending under the combined action of flexural and torsional moments.

The elastic force caused by the moment M_u, is

$$P_u = C_u \alpha_u y. \qquad \text{(II.45a)}$$

The frictional moment from the bending force is

$$m_u = f \sum_{i=1}^{n} c_u \alpha_u R_{oi} y, \qquad \text{(II.46)}$$

where R_{oi} is the arm of force acting on the *i* side plane, determined according to Figure II.9.

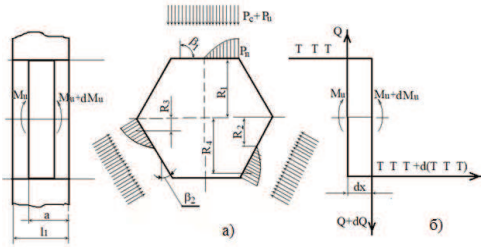

Fig.II.9. The geometric conditions of the clamped part of the torsion bar for determining the structural damping coefficient of bending under the combined effect of the torsional and bending moments: *a*) forces acting on the clamped part of the torsion bar; *b*) the condition of equilibrium of the elementary section of the torsion bar under bending

The frictional force from the action of compression force is

$$m_u = f\sum_{i=1}^{n}\frac{P_o a_u}{l}R_{oi}. \qquad \text{(II.47)}$$

The frictional force from torsion

$$m = 0.5 f c_k a_k \varphi_k. \qquad \text{(II.48)}$$

The shearing force of the clamped part of the torsion bar (Fig. II.3*b*) caused by flexural moment is balanced by the elastic and frictional forces acting in the direction of flexing. Thus, the equation of equilibrium of moments relative to the point O for bending (Figure 4.3) has the form:

$$Q = c_u y a_u + (T_n + T_c + T_u)cos\beta_i \qquad \text{(II.49)}$$

The equation of equilibrium of moments relative to a point *O* for bending (Fig.4.3) has the form:

$$M_u - Q l_1 - m_c + m_u + m_k = 0. \qquad \text{(II.50)}$$

Due to the fact that the torsion angle φ_k of the torsion bar in the fixturing is small, the pressure from the compression and bending forces T_c, T_u are practically unchanged. This

assumption allows to believe that the displacement of the corresponding resultant relative to the point *o* (Fig. II.1) is equal to zero. Due to the smallness of *y*, the frictional moment from the force T_u is also very small compared with the moment from the force T_c. Also, the frictional forces T_n and T_u from Figure II.3 turn out to be much smaller in comparison with the magnitude of the force T_c. Thus, the equations (II.22), (II.28) are simplified and take the form [12]:

$$M_k - 0.5k_1 c_k l_1 \varphi_k - T_n R + T_c R = 0;$$
$$M_u - c_u l_1^2 y - f \sum_{i=1}^{n} c_{ul_1} R_{oi} y - f \frac{P_o l_1}{l_1} R_{oi} = 0. \qquad \text{(II.51)}$$

9. Determination of the structural damping coefficient using the polygonal hysteresis loop

In the case when the diameter of the torsion bar is much greater than the pinching length ($d/l_1>5$), or the compression force is small ($P_o/q<I/2.5$), the fixturing of a part of the torsion bar, in order to simplify the calculation, is considered to be an absolutely rigid in torsion and bending. Taking into account the above, it can be assumed that the slippage of all parts of the torsion bar along the length of fixturing begins simultaneously [12].

The equations for constructing the hysteresis loop separately for torsion and bending are as follows:

$$\alpha M_k = A_1 l_1 \varphi_k \pm B_1 l_1 \varphi_k \pm q_1 l_1$$
$$\alpha M_u = A_2 l_1 y \pm B_2 l_1 y \pm q_2 l_1 \ , \qquad \text{(II.52)}$$

where $A_i (I = 1, 2)$ is a coefficient that takes account of the intensity of the reaction of the elastic joints; B_i is a coefficient that takes into account the friction forces of the elastic joints, α is a variable dimensionless load parameter, which, under a symmetric load, varies within $-1 \le \alpha \le 1$, q_i - the limiting friction moment per unit of the fixturing length from the force P_o.. The ± sign in (II.52) is taken depending on loading or unloading.

The hysteresis loops constructed using the equations (II.52) have the polygonal shapes (Fig. II.10).

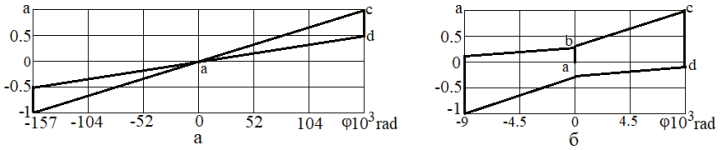

Fig.II.10 The polygonal hysteresis loops: a) Полигональные петли гистерезиса: a) – triangular; b) trapezoidal

In the complete absence of q_i, the kinematic connections of the fixturing are not violated due to the presence of the elastic joints. Owing to the coefficient B_i, the hysteresis loops have the triangular shapes (Fig. II.10a), in the presence of q, the hysteresis loops have the trapezoidal (polygonal) shapes (Fig. II.10b). The angle of inclination of the section *cd* to the ordinate depends on the fixturing geometry and the value of the friction coefficient.

When q_i, is completely absent, or when it is small, the rigidity of the system decreases significantly. A small variation in the magnitude of q_i significantly affects the system's rigidity.

The structural damping coefficients are equal to the ratio of the areas of the torsional or bending hysteresis loops to the areas corresponding to the potential energies of the system [13]

$$\psi_k = \frac{s_k}{U_k + S_{uk}};$$

$$\psi_u = \frac{s_u}{U_u + S_{uu}}; \qquad \text{(II.53)}$$

where S_k, S_u – areas corresponding to the torsional and bending hysteresis loops; V_k, V_u - areas corresponding to the potential energies of torsion and bending under deformations of the unrestrained parts of the torsion bar; S_{vk}, S_{vu} - areas corresponding to the potential energies of torsion and bending under deformations of the clamped parts of the torsion bar,

The obtained coefficients ψ_k and ψ_u express the energy dissipation of independent torsional and bending vibrations of the vibratory exciter.

The determination of the aggregate damping coefficient in the presence of combined transverse and longitudinal vibrations, taking into account ψ_k and ψ_u, is described in detail in [14].

Let us consider vibrations with a small amplitude, when only longitudinal vibrations practically take place in the torsional vibratory exciter. According to expression (II.5),

the longitudinal displacement of AM relative to RM is caused by joint torsion and bending of the torsional elastic frame. The total potential energy based on (II.5) and (II.6) is equal to:

$$U = \frac{1}{2}K_t\lambda_t^2 = \frac{P^2}{2}\left(\frac{k_1 r^2 l}{GI_k} + \frac{k_1' l^3}{3FI} + \frac{k_2' r^3}{3FI_o} + \frac{k_3' r l^2}{GI_{ko}}\right), \quad \text{(II.54)}$$

where $k_1' = 2 - 3k_2 + 2k_2^3; \quad k_2' = k_1^2 + 2k_1^3; \quad k_3' = (1 - k_2)$.

According to (II.54), the total potential energy of the torsional elastic frame can be represented as the sum of two quantities:

Potential energy under torsion

$$U_k = \frac{P^2}{2}\left[\frac{k_1 r^2 l}{GI_k} + \frac{k_3' r l^2}{GI_{ko}}\right] \quad \text{(II.55)}$$

and potential energy under bending

$$U_u = \frac{P^2}{2}\left[\frac{k_1' l^3}{3FI} + \frac{k_2' r^3}{3FI_o}\right] \quad \text{(II.56)}$$

Since in this case only longitudinal displacements are considered, the individual structural damping coefficients under torsion ψ_{ko} and under bending ψ_{uo} are equal to the ratio of the corresponding areas of work of the dissipative restraint forces to the area of total potential energy of the system;

$$\psi_{ko} = \frac{s_k}{U + S_{uk}} = \frac{s_k}{U_k + U_u + S_{uk}};$$

$$\psi_u = \frac{s_u}{U + S_{uu}} = \frac{s_u}{U_k + U_u + S_{uu}}. \quad \text{(II.57)}$$

Figure II.11 shows the graphs of variance in torsional damping, obtained using the equations (58) and plotted in the coordinates of the double amplitude of vibrations $2A$, $q = (0 \div 7000)N$, $G_{ik} = 33.10^3\ N.m^2$, $EI = 42.10^3 N.m$, $M_u = 400\ N.m$, $r = 25.10^2 m$. In the presence of asymmetric vibrations (asymmetric movement), the hysteresis loop also has an asymmetric shape.

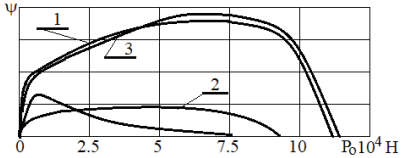

Fig.II.11. The graphs of variance in the dependence of the design damping coefficients on the compressive force, obtained by using the polygonal loops: 1 – of torsion; 2 – common; 3 – of bending.

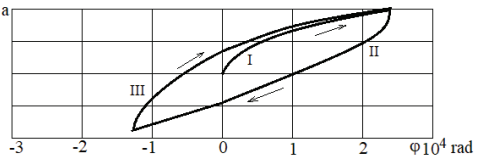

Fig.II.12. The hysteresis loop created by two curves under torsion of the torsion bar

The aggregate structural damping coefficient of the torsional vibratory exciter at longitudinal displacement is equal to the ratio of the total work of the frictional forces of torsion and bending S (of the hysteresis loop) to the area of the total potential energy of the system;

$$\psi = \frac{s}{U+S_{uk}+S_{uu}} = \frac{s_k+s_u}{U_k+U_u+S_{uk}+S_{uu}}; \qquad \text{(II.58)}$$

$$\psi = \psi_{ko} + \psi_{uo}$$

10. Determination of the slip length and structural damping coefficient using the differential equations of the hysteresis loop

In cases when the clamping length is of the same order of magnitude as a diameter of the torsion bar or exceeds it in the presence of a large limit moment of friction q_i, the structural damping coefficients obtained from the equation (II.52) are inaccurate. In this case, the assumption that the slippage of the torsion bar along the entire clamping length begins simultaneously, does not correspond to reality, since in the area of the section l_l (Fig. II.7), there is a gradual slippage of the clamped parts of the torsion bar relative to the bushing caused by the torsion of the torsion bar that generates the distributed dissipative forces [12].

When the lengths of the slip sections $\alpha_к$ and α_u from the effect of M_k and M_u do not exceed the clamping length l_l,, the individual branches of the hysteresis loop are constructed after solving the differential equations, for the derivation of which we

consider the equilibrium conditions for the torsion bar elements in the zone of its deformation (for torsion, see Fig. II .7*b*, for bending, see Fig. II.9*b*).

The equilibrium equations (II.51) for the elementary moments have the form as follows:

$$\frac{dM_k}{dx} = (A_1 + B_1)\varphi_k \pm q_1; \tag{II.59}$$

$$\frac{dM_u}{dx} = (A_2 + B_2)y \pm q_2,$$

where $q_1 = fP_o/l_1, q_{21} = fP_o/2l_1$.

Differentiating the known expressions

$$M_k = GI_k d\varphi_k/dx;$$

$$M_u = EId^2y/dx^2, \tag{II.60}$$

by *x*, and replacing dM_k/dx and d^2M_k/dx^2 by $GI_k d^2\varphi_k/dx^2$ and EId^4y/dx^4 in the equations (II.59), we'll get the differential equations for constructing the hysteresis loops followed the curve lines

$$\varphi_k'' - \beta^2\varphi_k = \pm\frac{q_1}{GI_k}; \tag{II.61}$$

$$\varphi_k^{iv} - k^4 y = \pm\frac{q_2}{EI}, \tag{II.62}$$

where $\beta^2 = (A_1 + B_1)/GI_k, k^4 = (A_2 + B_2)/EI$.

Solutions of the equations (4.39) and (4.40) can be written as follows:

$$\varphi_k = c_1 e^{-\beta x} + c_1 e^{-\beta x} \pm \frac{q_1}{GI_k}; \tag{II.63}$$

$$y = 0.5D_1(chkx + coskx) + 0.5D_2(shkx + sinkx) + 0.5D_3(chkx - coskx) +$$

$$+0.5D_4(shkx - sinkx) \pm \frac{q_2}{k^4 EI}. \tag{II.64}$$

To determine the unknown quantities in the expression (II.63), by means of which the hysteresis loops are constructed followed the curved lines (Fig. II.12), the following stage-by-stage boundary conditions must be observed taking into account loading and unloading [9, 11, 13, 15]; in this case, with a view to reducing the number of boundary

conditions, it is assumed that $\beta^2 = (\beta_1^2 + \beta_2^2)/2$. With a symmetrical load, the area of the hysteresis loop corresponding to the energy dissipated in one cycle is

$$S_k = \int_{-1}^{1} \varphi_{k2} d\alpha - \int_{-1}^{1} \varphi_{k3} d\alpha = \frac{M_k}{GI_k\beta}\sqrt{1 + (\frac{q_1}{\beta M_k})^2} + \frac{q_1}{GI_k\beta^2} - \frac{M_k}{GI_k\beta}(2K - \frac{m_1 - 1}{2} ln \frac{K+2}{K-2}),$$

(II.65)

$$\mathrm{m_1} = 1 + (2\mathrm{q_1}/\beta\mathrm{M_k})^2, \quad K = \sqrt{m_1 + 3.}$$

Potential energy from the deformation of the clamped part of the torsion bar is

$$S_{uk} = \int_{-1}^{0} a_{k1max} d\alpha - \int_{-1}^{0} \varphi_{k1} d\alpha = \frac{M_k}{GI_k\beta}\sqrt{1 + b^2} - \frac{M_k}{2GI_k\beta}(\sqrt{1 + b^2} + b^2 ln \frac{b}{\sqrt{1+b^2}-1}),$$

(II.66)

where $b = \frac{q_1}{\beta M_k}$.

At the low vibration amplitudes (up to about 1 mm), due to the absence of the transverse displacements, the structural damping coefficient can be determined according to the expression (II.53). Since the movement of masses in the torsional vibratory exciter is mostly associated with torsional deformations of the frame, the difference between the structural damping coefficients ψ_k and ψ_{ko} is small. Figure II.13 shows the graph of variance in the structural torsional damping coefficient at coordinates M_k, λ. (q_1=$10^4 H$, M_k= =$3.7.10^2 H.m$).

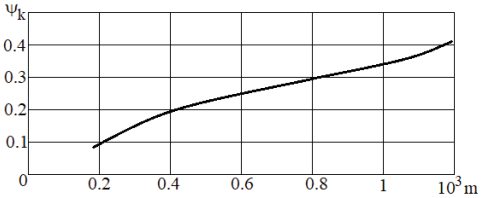

Fig.II.13. The graph of variance in the structural damping coefficient under torsion of the torsion bar

It is known that as a result of bending, the upper layer of the beam is lengthened, and the lower layer is shortened. This results in the emergence of tensions

$$\sigma = M_u \frac{y}{I_x}, \tag{II.67}$$

where I_x is the current distance from the layer being considered to the neutral one (Fig.II.14).

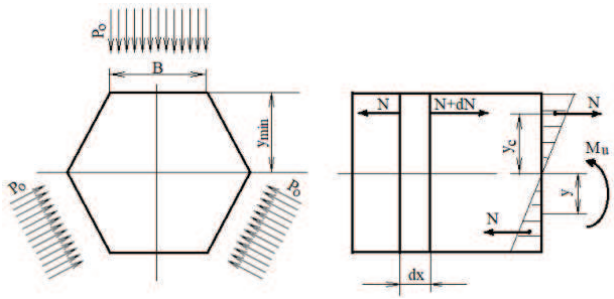

Fig.II.14. The geometric conditions for determining the structural damping coefficient under bending

Integrating the equations (II.67) over the upper and lower cross-sectional areas from the neutral layer of the torsion bar, we generate the tensile force N_1 of the upper half and the compressive force N_2 of the lower half of the cross-section. These surface displacements (deformations) are resisted by frictional forces acting in the fixturing, as a result of which energy dissipates during vibrations. In this case, there is no axial displacement of the torsion bar relative to the bushing, because the total normal force N, caused by the rotational movements of the beam cross-sections under bending, is known to be zero under pure bending and is small under transverse bending [9].

Thus, in connection with the surfaces of the beam cross-sections under bending, the surface compressive and tensile forces appear [1, 15], the values of which, with certain assumption for a hexagonal torsional bar, are

$$N_1 = 0.5B^3 \frac{M_u}{I_x}. \tag{II.68}$$

Finally, the simplified differential equation, by means of which the hysteresis loops for bending at a purely frictional connection of nodes are constructed, has the form:

$$u'' = \pm \frac{q_3}{EF}, \tag{II.69}$$

where u – is the displacement of an arbitrary section in the direction of the tensile or compressive force, $q_3 = 0.5fP_o/l_1$ is the ultimate friction force.

Thus, the structural damping coefficient under bending of the torsion bar can be determined approximately through the longitudinal deformations of the torsion in the fixturing caused by the surface tensile and compressive forces.

11. Determination of the lengths of slip zones and structural damping coefficients for purely frictional group connection

With the increasing number of the side planes of the torsion bar $n > 8$,, the elastic-frictional connection under torsion approaches the purely frictional one (the coefficients A_1 and B_1 in the equation (II.61) become insignificant, and it can be set to $\beta = 0$). The picture is similar at sufficiently high q_1 ($\geq 2.10^4 H$).

In view of the above, the equation (61) takes on the form;

$$\varphi_k'' = \pm\frac{q}{GI_p}, \qquad \text{(II.70)}$$

where I_p - is the polar moment of inertia of the torsion bar cross-section; $q = fP_oR/l_1$ - the limit frictional moment per unit length. The solution to the equation (70) has the form:

$$\varphi_k = c_{1+}c_2x \pm \frac{qx^2}{2GI_p}, \qquad \text{(II.71)}$$

where the "+" sign is put at loading, and the "-" sign - at unloading. Depending on the stage loading and unloading, taking into account the boundary conditions [11, 12] and some transformations, we will obtain the equations for the slippage lengths and the torsion angle of the torsion bar in the fixturing:

$$a_{k1} = \frac{\alpha M_k}{q}; \quad \varphi_{k1} = \frac{\alpha^2 M_k^2}{2qGI_p}; \quad \varphi_{k2} = \frac{1+2\alpha-\alpha^2}{4qGI_p}M_k^2; \quad \varphi_{k3} = \frac{1-2\alpha r+2r+\alpha^2}{4qGI_p}M_k^2. \qquad \text{(II.72)}$$

For a symmetric cycle with r = -1, the angle of torsion: $\varphi_{k3} = \frac{-1+2\alpha+\alpha^2}{4qGI_p}M_k^2$.

The hysteresis loop for a purely-frictional connection is shown in Figure II.15.

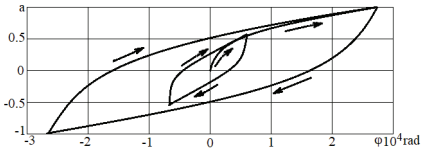

Fig. II.15. The hysteresis loops with a purely frictional connection under torsion of the torsion bar

At the symmetrical load, the area of the hysteresis loop of a purely frictional connection, corresponding to the energy dissipated in one cycle, is

$$S_k = \int_{-1}^{1} \varphi_{k2} d\alpha - \int_{-1}^{1} \varphi_{k3} d\alpha = \frac{2M_k^2}{3qGI_p}. \quad \text{(II.73)}$$

The potential energy of the deformed clamped part of the torsion bar under torsion is

$$S_{uk} = \int_{-1}^{0} a_{k1max} d\alpha - \int_{-1}^{0} \varphi_{k1} d\alpha = \frac{M_k^2}{3qGI_p}. \quad \text{(II.74)}$$

The damping coefficient for a purely frictional connection is determined similarly to an elastic-frictional connection, using (II.53), (II.57).

Figure II.16 illustrates the graph of variance of the structural damping coefficient under torsion of a purely frictional connection at coordinates M_k, q.

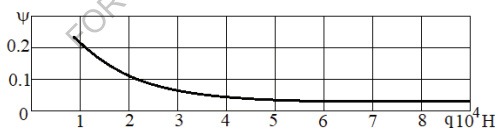

Fig. II.16. The graph of variance in the structural damping coefficient under torsion of the purely frictional connection

The obtained structural damping coefficients under torsion of the purely frictional or elastically frictional fixturing have almost the same values. This is because the elastic connections of the hexagonal torsion bar at relatively large q do not have a noticeable effect on the process of opening the clamped parts. It should also be noted that when expanding the torsional expressions of the torsion bar in the fixturing of an elastic-frictional connection by αM in a Maclaurin power series up to the third term, we obtain the expressions of the purely frictional connections. Based on this, in order to simplify

the calculation, it is possible in some cases to consider the elastic-frictional connections as purely frictional (Table 2), and instead of the expression (II.65), (II.66), to use (II.73), (II. 74).

The solution to the differential equation (2.69), which determines the work of dissipative forces under bending, is mathematically described similarly to (II.70) [11]. The expressions used to construct the hysteresis loops under bending deformation (Fig. II.17), in accordance with the stages of loading and unloading of a symmetrical cycle, are as follows:

$$u_1 = \frac{\alpha^2 M_u^2}{2.10^6 P_o}; \quad u_2 = \frac{1+2\alpha-\alpha^2}{410^6 P_o} M_u^2; \quad u_3 = \frac{-1+2\alpha+\alpha^2}{410^6 P_o} M_u^2 . \qquad \text{(II.75)}$$

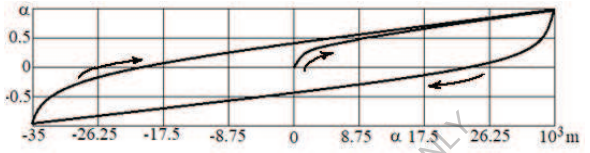

Fig.II.17. The hysteresis loop under bending of the torsion bar

The area of the work of the frictional forces and the potential energy from deformation of the clamped part of the torsion bar under bending are respectively equal to:

$$S_u = \frac{M_u^2}{3.10^6 P_o} . S_{uu} = \frac{M_u^2}{3.10^6 P_o} \qquad \text{(II.76)}$$

The structural damping coefficients under bending ψ_u, and ψ_{uo} are determined using the expression (II.53), (II.57). Figure II.18 illustrates the graph of variance of the structural damping coefficient under torsion of the torsion bar at coordinates M_u, q.

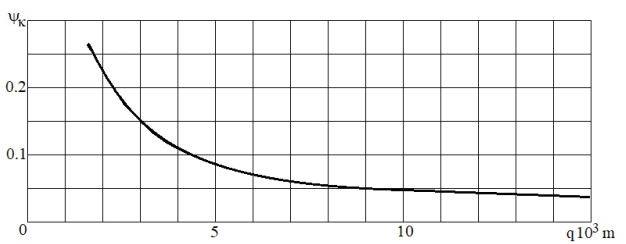

Fig. II.18. The graph of variance in the structural damping coefficient under bending of the torsion bar

Taking into account the potential torsional energy U_k of the torsion frame, in contrast to the coefficients ψ_u and ψ_{uo}, makes a great difference between ψ_u and ψ_{uo}. This is due to the fact that

the main longitudinal movement of masses and the corresponding potential energy of the torsional vibratory exciter are associated with the torsion of the elastic frame.

12. Determination of the non-linear rigidity of the elastic system associated with slippage in the fixturing points of the torsion bar

In paragraph II.4, it was noted that the system's rigidity, determined without taking into account the pliancies of the fixturings, using the expression (II.15), is in error.

No matter how perfect the termination is, with increasing loading, its elasticity allows the built-in end of the torsion bar to obtain linear and angular displacements. The effect of the built-in end is especially significant for the relatively short torsion bars [16, 17], without taking into account the slip length αk in the fixturing, at a given vibration amplitude of 10^{-3} m, the natural frequency of the system is 5-7 Hz lower.

To specify the natural frequency and the system's overall rigidity, a certain length Δl from the place of the built-in end is added to the free length l of the elastic element [8].

$$l l_o = l + 0.5 l_2 + 0.25 l_3, \qquad \text{(II.77)}$$

where l_2–is the length of the fixturing of the torsion bar with the lever, l_3– is the length of the fixturing of the torsion bar with AM or RM.

In the torsional vibratory exciters, usually $l_3 \approx l_2$.

Formula (II.77), specifying the design frequency, nevertheless does not give a true picture of the dependence of the frequency on the vibration amplitude, and, therefore, cannot explain the origin of the soft characteristic of the elastic system. Formula (II.77) also does not take into account the magnitude of the compression force, the diameter, length and geometry of the clamped part of the torsion bar, as well as the magnitude of torsional moment.

Due to the fact that the connection between the bushing and the torsion bar is imperfect, the reaction of the moment acting between the bushing and the torsion bar is expressed as the sum of the moment arising from deformation and from the frictional bonds [18]. Based on this, the total value of the torsional angle of the torsion elastic system, with account for the fixturing, is

$$\varphi = \varphi_k + \varphi_{ko}, \tag{II.78}$$

where φ_k is a torsional angle of the torsion bar in the presence of imperfect connection, φ_{ko} – a torsional angle of the clamped part of the torsion bar.

Taking into account (II.72), the equation (II.77) after some transformations takes on the form:

$$M(\varphi) = M_k - \frac{\alpha M_k^2}{2ql}, \tag{II.79}$$

where $M(\varphi)$ is the aggregate elastic-frictional moment,
M_k – the moment acting on the torsion bar.

Since the traction force of the electromagnet is much less than the inertial loads, during the dynamic study of the vibratory exciter in the expressions for determining the twisting angle of the free and clamped part of the torsion bar, the AM displacement relative to the RM, the rigidity of the elastic system, structural damping coefficients and other characteristics, it is necessary to replace the static force by the dynamic one. To this end, we use the well-known expressions, by means of which we define the single-frequency inertial loads, which we use to determine the single-frequency inertial loads (dynamic forces) depending on the value of the twisting angle $M_k = I_m \ddot{\varphi}$, where $\ddot{\varphi} = \omega^2 \varphi$ - is the angular acceleration, from which

$$M(\varphi) = I_m \omega^2 \varphi - \frac{I_m^2 \omega^4}{2ql} \omega^2 \varphi^2. \tag{II.81}$$

Taking into account (II.79), the expression (II.78) takes on the form as follows:

$$M(\varphi) = I_m \omega^2 \varphi - \frac{I_m^2 \omega^4}{2ql} \omega^2 \varphi^2. \tag{II.82}$$

Using the well-known expression e $c = M/\varphi$ [9], we find the rigidity of the torsional elastic system taking into account slippage in in the fixturing, which is a function of the vibration amplitude:

$$c_1 = \frac{GI_k}{l} - \frac{I_m^2 \omega^4}{2ql} \alpha^2 \varphi. \tag{II.83}$$

13. Analysis of structural damping characteristics

It should be noted that the similar expression can be obtained by increasing the free length of the torsion bar by the amount of slip, using (II.72).

Similarly, we obtain the expressions for the rigidities, which are the functions of the vibration amplitude for the following loading steps:

$$c_1 = \frac{GI_k}{l} - \frac{I_m^2\omega^4}{4ql} - \frac{I_m^2\omega^4}{2ql}\alpha\varphi + \frac{I_m^2\omega^4}{4ql}\alpha^2\varphi. \qquad \text{(II.83)}$$

Figure II.19 illustrates curves of the total rigidity of the elastic system, depending on the magnitude of the vibration amplitude; they are the non-linear functions of the displacements. When determining the rigidity (II.79), the value of the torsional angle φ_k of the torsion bar in the place of the fixturing must be doubled, because the torsion bar is clamped at both ends. Curve $q = 0$ corresponds to the system's rigidity without taking into account the pliancy of the fixturing in the presence of different values of the compressive forces.

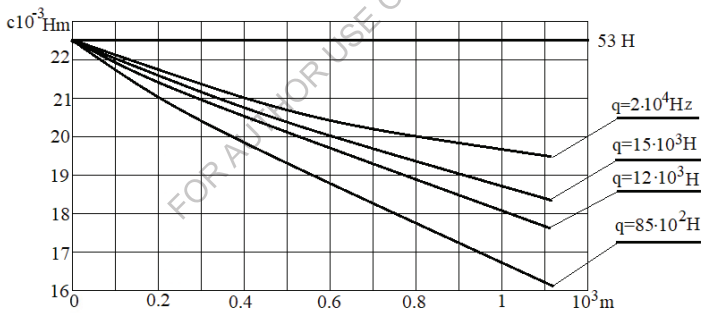

Fig. II.19. The dependence of the system's rigidity on variation in the magnitude of the vibration amplitude under the effect of different compressive forces

Thus, taking into account the slippage of the torsion bar in the fixturing in the expressions for the rigidity of the elastic system (II.81) and (II.82) leads to a nonlinear system with a soft characteristic of rigidity, which is in good agreement with the experiment.

The equations used to construct the individual sections of the hysteresis loop were obtained in the proposal that the friction forces are independent of the strain rate; they are valid for the low rates of velocity variation of loads acting on the torsion bar. However,

the obtained damping coefficient can be used at higher strain rates, since it practically is a little dependent on the vibration frequency [11, 19, 20, 21].

Figure II.20 illustrates the values of the structural damping coefficients, depending on the vibration amplitudes under torsion ψ_k, under bending ψ_u and at the longitudinal displacement, taking into account the bending and torsional deformation ψ. As Figure shows, the damping coefficients are the non-linear functions of the vibration amplitude.

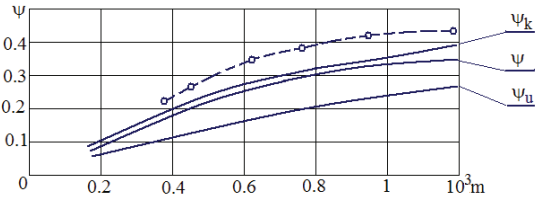

Fig.II.20. The dependence of the damping coefficients of torsion, bending and common one on the magnitudes of the vibration amplitude

Certain discrepancy between the theoretical and experimental (dashed line) values of the damping coefficients is due to the fact that in the dynamic modes, the energy dissipation occurs both due to the structural hysteresis and as a result of internal friction at the interval of aerodynamic resistances. However, this difference is small and can be neglected.

Figure II.21 illustrates the graph of variance in the structural damping coefficient under torsion, depending on change in the magnitude of the force clamping the torsion bar. In the absence of q_1, in view of the presence of the coefficients $A_1 \neq 0$ and $B_1 \neq 0$ in the equation (II.52), the energy dissipation takes place; with the increasing q_1, the damping coefficient increases to a certain maximum; the subsequent increase in q_1 causes a decrease in the damping coefficient, but further it is necessary to use the equation (II.61) instead of (II.52). The dotted curve corresponds to the purely frictional connection (II.70) and shows that at $q_1 \geq 3.10^4$H, the damping coefficients of the elastic-frictional and purely frictional connections are the same, while at $7.10^3\text{H} \leq q_1 \leq 8.10^3$H, the discrepancy between them reaches a noticeable value, and with further decrease in q_1, there are no kinematic joints in the purely frictional connections, and the torsion bar rotates in in the fixturing, while with an elastic-frictional connection, the fixturing of the torsion bar is not violated, despite a noticeable decrease in the system's rigidity.

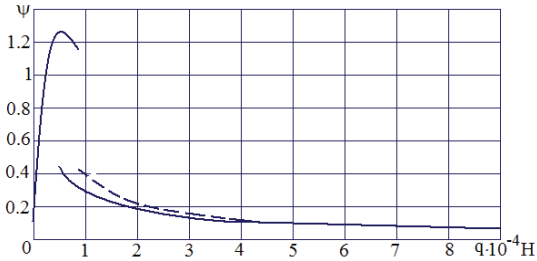

Fig.II.21. The structural damping coefficient under torsion depending on the value of compressive force

The structural damping coefficient for the purely frictional clamping of the torsion bar, taking into account (II.73), (II.74), is

$$\psi_k = \frac{8K_1M_k}{3ql+2K_1M_k}. \qquad \text{(II.84)}$$

In some cases, when calculating the structural damping coefficient, one can ignore the energy S_{uk} according to the formula (II.74), since it is much less than the potential energy of the entire elastic system (II.54), for example, $U_k/S_{uk} = 25$. Based on this, we obtain a simple expression that can be used to pre-determine the structural damping coefficient:

$$\psi_k = \frac{8K_1}{3ql}M_k. \qquad \text{(II.85)}$$

The expression (II.84) with account for (II.80), has the form as follows:

$$\psi_k = \frac{8K_1I_m\omega^2}{3ql}\varphi, \qquad \text{(II.85)}$$

14. Mathematical modeling of the electromagnetic vibrators

In programming with a mathematical model of an electromagnetic vibrator, some difficulties and unpredictable consequences appear. Unlike other vibratory exciters, which are excited by harmonic forces, the electromagnetic vibrators are mathematically described by two equations: the equation (II.86) describes the mechanical oscillatory process with an exciting force having a quadratic degree, and the equation (II.87) describes an electromagnetic circuit, in which an electromagnetic flux (force) is formed [24, 26, 26].

$$\ddot{x} + 2h\dot{x} + \omega_o^2 x = a\Phi^2 \quad \text{(II.86)}$$

$$\dot{\Phi} = b\sin(\omega t) - d(\delta - x)\Phi \quad \text{(II.87)}$$

where $2h$, a, b, d are the coefficients of proportionality, respectively, of dissipative forces, exciting forces, electric intensity, magnetic permeability; ω_0 – a natural circular frequency of the vibrator; δ - the initial air-gap clearance; Φ - the magnetic flux, x - the vibration amplitude of the mechanical system.

Figure II.22 illustrates oscillograms of a single-stroke electromagnetic vibrator with an exciting force sinωt. Oscillatory process of readings in Figure II.22*a* corresponds to the power supply of the vibrator with a frequency of 50 Hz, and Figure II.22*b* shows oscillogram of the vibrational process of the vibrator with a frequency of 25 Hz. We can say that the transient processes in both modes are far from reality [27]. The amplitudes of mechanical vibrations at the beginning of the vibrator starting increase sharply, and then gradually decrease or stabilize. As for the magnetic fluxes, they are initially completely displaced from the zero axes, and then gradually cross the zero axis, while the vibration amplitude of the exciting force does remains unchanged.

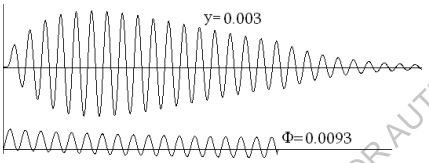

Fig.II.22a. Oscillograms of the transient process with a frequency of 50 Hz.

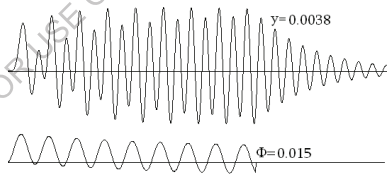

Fig.II.22b. Oscillograms of the transient process with a frequency of 25 Hz.

The electromagnetic vibrators based on the principle of excitations are single-stroke (single-gap) and two-stroke (two-gap) [27, 28]. In the two-stroke vibratory exciters, depending on the half-periods, the traction force is realized from one or another side of the gap clearance, and thus the excitation frequency of the vibrator corresponds to the frequency of the industrial electric power network. The design of the single-stroke vibratory exciters is the simplest and most reliable in operation, however, the disturbing frequency of these vibratory exciters is doubled in comparison with the frequency of the industrial electric power network, since the electromagnet generates the force of attraction in both periods of alternating current. To halve the disturbing frequency of these vibrators, semiconductor diode is connected to the power circuit [22].

In the scientific literature (existing on the Internet and available in libraries), the mathematical description of the action of a semiconductor diode in the supply circuit of the electromagnetic vibrators is rather scarce and in principle is untrue.

The assumption that at a half-period rectification of the alternating electric current, the cut-off half-periods in the equation (II.87) are equal to zero, that is the term bsin(ωt) is set equal to zero is not true. This approach in mathematical modeling causes a gradual accumulation of magnetic flux in the system, which is equivalent to the one-sided deflection of the elastic system of the vibrator (Fig. II.23a). Some researchers, in order to overcome the gradual increase in the exciting force and the one-sided deflection of the elastic system, unreasonably increase magnetoresistance coefficient or dissipation of the magnetic flux, that is, if the power consumption is too high, they artificially reduce the tractive force of the electromagnet. Figure II.23b shows the oscillatory process with the unreasonably increased power consumption, which does not correspond with experimental results.

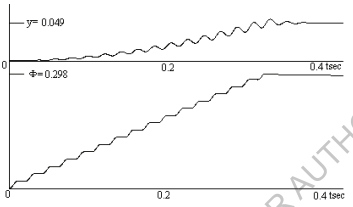

Fig.II.23*a*. Oscillogram in the nulling of sinωt

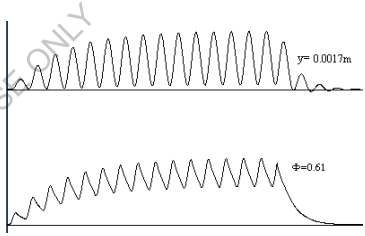

Fig.II.23*b*. Oscillograms of vibration of the vibrator during the large dispersion of the magnetic flux

To clarify this problem, we will analytically solve the equation (II.87), provided that the vibrations of the air-gap clearance are so small as to be negligible [29]. In this case, the analytical solution of the equation (II.87) can be represented as a product of two functions $\Phi = u(t)\cdot v(t)$ [25], where one of them is given arbitrarily, and the other one is determined based on the equation (II.87).

$$\Phi = b\frac{c\delta sin\omega t - \omega cos\omega t}{(c\delta)^2+\omega^2} + C_1 e^{-c\delta t} \qquad \text{(II.88)}$$

According to the initial conditions $t = 0$, $\Phi = 0$, the coefficient C_1 will equal

$$C_1 = \frac{b\omega}{(c\delta)^2 C* + \omega^2} \quad \text{(II.89)}$$

After the substitution of (II.89) for (II.88), we get the magnetic flux in the electromagnet core

$$\Phi = \frac{b\omega}{(c\delta)^2+\omega^2} e^{-c\delta t} + b\frac{c\delta \sin\omega t - \omega \cos\omega t}{(c\delta)^2+\omega^2} \quad \text{(II.90)}$$

The analysis of the equations (II.88) shows [29,30] that when the electromagnet is supplied with direct current ω=0, that is $b\sin\omega t = u_0$, the magnetic flux will equal $\Phi = u_0/\delta$, while the force of attraction of the magnet is $F = a\Phi^2$. For $\omega \neq 0$ and $\delta = 0$, we obtain

$$\Phi = \frac{b}{\omega} - \frac{b}{\omega}\cos\omega t \quad \text{(II.91)}$$

The first term of the equations (II.90) and (II.91) disappears, and the second term remains and is responsible for the vibrating process. Based on the equations (II.91), it can be seen that the magnetic flux in the supply circuit of the magnet coil strongly depends on the frequency of the supply current.

With half-periodic inherent rectification, the term b·sinωt in the equation (II.87) exists only in the positive half-periods, but in the negative half-periods, this term becomes zero, which means that it is absent and the equation (II.87) takes on the form

$$\dot{\Phi} = -c\delta\Phi \quad \text{(II.92)}$$

from which

$$\Phi = C_2 e^{-c\delta t} \quad \text{(II.93)}$$

For the initial conditions $t = 0$, $\Phi = \Phi_0$, the analytical solution of the equation (II.93) has the form

$$\Phi = \Phi_0 e^{-c\delta t} \quad \text{(II.94)}$$

It is easily seen that exponential decay Φ occurs over an extremely long period of time and does not at all reflect the real disappearance of the magnetic flux.

Indeed, when t = 0, 01 *s*, which corresponds to a half-period of 50 Hz, Φ will not disappear to nothing. If $t = 0$, the magnetic flux is equal to $\Phi = \Phi_0 = 1$, then for $t = 0{,}01$, Φ becomes equal to $\Phi = 0.99005$. As a result, after *n* cycles, according to (II.87), the massive energy of the false magnetic flux Φ is accumulating, which cannot be explained in any way in terms of electrical engineering [29, 30, 31]. The inadmissibility of

replacing the equation (II.87) by the equation (II.92) is also seen from considering the balance of voltages in the power circuit.

$$ir = u \cdot sin\omega t + W\dot{\Phi}\ , \qquad \text{(II.95)}$$

Where u - is the voltage amplitude; r - active resistance; W - the number of the turns of the coil.

In accordance with the equation (II.95) after the termination of the voltage $u \cdot sin\omega t$, the electric current i, the magnetic flux Φ and the inductive reactance $W\,d\Phi / dt$ (Ldi / dt) of the electric circuit (where L is the inductance) cannot exist [28, 29]. The absence of the term $u \cdot sin\omega t$ in the equation (II.95) results in the equation

$$\dot{\Phi} = \frac{ri}{W} \qquad \text{(II.96)}$$

According to the equation (II.96), when the alternating current voltage stops, the electric current i in the circuit may exist only during the disappearance period of Φ. Otherwise, (95) loses its significance as an equation for describing the electromagnetic circuit.

Based on the aforementioned study, in the negative AC half-periods, that is, during the periods when the current is closed by the diode, the equation (II.87) should be replaced by the equation describing the magnetic flux damping. To simplify the calculation, taking into account a tolerance for the negligible error in the negative half-periods, it is possible to set Φ to zero, which is equivalent to the action of a semiconductor diode at negative voltage [30].

$$\text{when} \quad \sin(\omega t) < 0 \qquad \text{then } \Phi = 0 \qquad \text{(II.97)}$$

When describing the action of a semiconductor diode in a mathematical model, it should be borne in mind that a semiconductor diode does not cut off the so-called negative peaks of an AC voltage; it cuts off the negative AC peaks [30]. Based on this, when using the Runge Kutta software, it is necessary to set to zero not the operator $y[i]$, which forms the magnetic flux Φ, but the operator $w[i]$, which, at the end of the cycle, is equated to $y[i]$ and transfers the values to the beginning of the cycle. Figure II.24a shows the corresponding oscillogram. By the time when the vibrator is disconnected, the operator w $[i]$ must also be set to zero, so as not to get a false long process of gradual magnetic flux depression (Fig. II.24b).

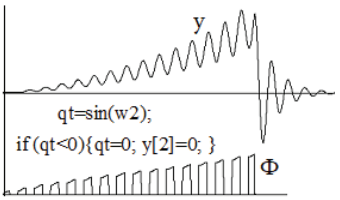

Fig.II.24a. The process of magnetic flux accumulation in the nulling of operator $y[i]$

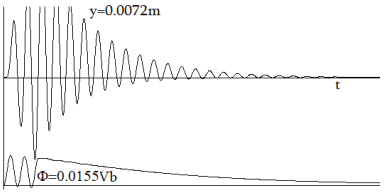

Рис.II.24б. The process of vibration damping when the vibrator is switched on without nulling of operator $w[i]$

Taking into account the above adjustments, we get the oscillatory process of the electromagnetic vibratory exciter with the half-period inherent rectifications, which is in good agreement with the results of experimental studies of a real electromagnetic vibratory exciter (Fig. II.25).

Figure II.25*a* illustrates the resonant oscillatory process with a frequency of 50 Hz with a disturbance of a half-period rectified current with a frequency of 50 Hz, and Figure II.8b shows an oscillatory process with a disturbance at a frequency of 25 Hz with the appearance of an insignificant subharmonic resonance. It should be noted that when the vibrator is driven by the half-periodic rectified current, the role of the phase shift of $\pi/2$ is no longer crucial. The oscillatory (vibrating) processes are the same both due to $sin(\omega t-\pi/2)$ and $sin(\omega t)$. The matter is that with a half-period of the rectified current, rectified asymmetric pulses make the system nonlinear with a soft characteristic and cause asymmetric vibrations of the elastic system.

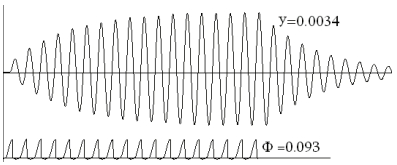

Fig.II.25a. The main resonant mode with a half-periodic rectification

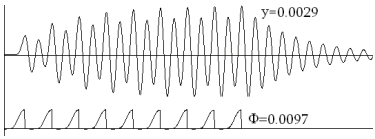

Fig. II.25b. The subharmonic resonant mode with a half-periodic rectification

The expansion of the second term of the equation (II.88) into a power series on t has the form as follows [30]

$$\Phi = \frac{b\omega}{w_0} cos\omega t + \frac{bc\delta\omega t}{w_0} \cos\omega t + \frac{bc\delta\omega^2 t^2 \cdot}{2w_0} cos\omega t - \cdots, \quad \text{(II.98)}$$

where $w_0 = (c\delta)^2 + \omega^2$

Based on (II.88), it follows that the oscillatory process practically occurs due to cosωt = sin(α - π/2), that is the vibration amplitudes of the mechanical system lag behind the oscillatory process of the electric power network (exciting force) in phase with π/2.

It should be noted that the first terms of the equation (II.98) can also be obtained through analytical solution of the equation of forced vibrations

$$\ddot{x} + 2h\dot{x} + \omega_o^2 x = a \cdot sin\omega t, \quad \text{(II.99)}$$

the analytical solution of which is

$$x = Ae^{\omega t} \sin\left(\omega_0 t + \varphi_0\right) + A_{(\omega)} \sin(\omega t + \varphi), \quad \text{(II.100)}$$

where $A_{(\omega)} = \frac{a}{m\sqrt{(\omega_0^2 - \varphi^2)^2 + a^2\omega^2}}$

The substitution of the analytical solution for the equation (II.87) and expansion of the resulting equation in a power series and its subsequent integration, also result in a power equation, the first terms of which coincide with the equation (98). Based on a comparison of the equations (II.87), (II.98) and (II.100), it is also proved that the magnetic flux and the alternating electric current circulate in accordance with sin(ωt - π/2) =cosωt and lag in angle π/2 behind the supply voltage b·sinωt. Squaring of the equation (II.15) gives a simulating harmonic exciting force of the electromagnetic vibrator [30].

$$\phi^2 = \frac{b^2\omega^2}{w_0^2} cos^2\omega t + 2\frac{b^2\omega^2 c\delta t}{w_0^4} cos^2\omega t + \cdots \quad \text{(II.101)}$$

On the basis of research, in a number of cases, it becomes possible to replace the system of differential equations (II.86) and (II.87) by one differential equation without particular errors, in the right-hand side of which there is only one main term of the equation (II.101) that simulates a nonlinear exciting magnetic force [30]. With this

approach, the calculations are simplified and the above problems of the half-periodic inherent rectification and phase shift in mathematical simulation (modeling) disappear.

$$\ddot{x} + 2h\dot{x} + \omega_o^2 x = a\frac{b^2\omega^2}{w_0^2}cos^2\omega t \qquad \text{(II.102)}$$

Figure II.26 illustrates the modes of vibrational resonance of the electromagnetic vibrator obtained using the equation (II.102). Figure II.26a shows the oscillatory regime of a non-rectified exciting force with a frequency of 50 Hz, and Figure II.26b shows the same with a half-periodic inherent rectification with a frequency of 50 Hz.

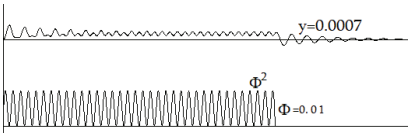

Fig.II.26a. The resonant mode with excitation by the frequency of 50Hz

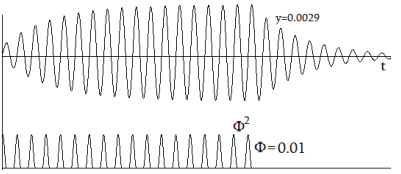

Fig.II.26b. The resonant mode with high-periodic rectified excitation by the frequency of 50Hz

Figures illustrate that due to the absence of diode rectification, the disturbance frequency is doubled (instead of 50Hz, we actually have 100Hz), therefore, the oscillatory regime does not arise (Fig. II.26*a*), and in accordance with Figure II.26*b*, due to the half-periodic inherent rectification, the disturbance frequency is not doubled and, therefore, the resonance regime appears.

When the vibrator is excited by the non-rectified electric current with a disturbance frequency of 25 Hz, the resonance regime appears again, since in this case the frequency is doubled again and becomes the resonant frequency (Fig. II.27).

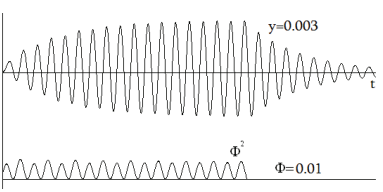

Fig.II.27. The resonant mode with harmonic excitation by the frequency of 25Hz

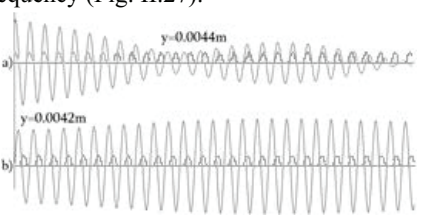

Fig. II.28. The transient frequency mode from 52 Hz to 52 Hz. *a*) without adjustment; *b*) with adjustment.

The oscillatory processes obtained by model simulations using the equation (II.102) are almost indistinguishable from the oscillatory processes obtained by model simulations in accordance with the system of the equations (II.86) and (II.87) and the experimental studies of the electromagnetic vibratory exciters. It should be noted that the simulated magnetic flux Φ based on the equations (II.102), is not formed by integrating sinφ, and therefore it is symmetrical about the zero axis. Therefore, in the last figures, the magnetic flux is presented in the form of the exciting force of the electromagnet through Φ^2, which changes in time according to the law of $\cos^2 \omega t$.

During digital modeling (the discrete increase or decrease in the excitation frequency) of the nonlinear systems (for example, using the Runge-Kutta method) it is very difficult to obtain the amplitude-frequency characteristic (AFC) that would fully reflect the nonlinear dynamic properties of the system. Moreover, in some cases it is practically impossible. This is especially noticeable, when there are the low damping coefficients ϕ < zero,1 [32, 33, 34]. To set the stable amplitudes in the nonlinear systems, which are described by formula (II.103), it takes too much time (oscillatory cycles), while when there are the low damping coefficients, a small spacing h < 0.1 is required in the disturbance frequency. In spite of this, however, there is no guarantee that the set amplitudes will not end up on the lower branches of the resonant mode. With discrete switching from one excitation frequency to another, there is a phase imbalance between the electromagnetic excitation and the potential (or kinetic) forces of the vibrator, which leads to instability of the mechanical vibration mode (Fig. II.28*a*).

$$\ddot{x} + 2h\dot{x} + \omega_o^2(x + \eta x^3) = a\frac{b^2\omega^2}{w_0^2}cos^2\omega t \qquad \text{(II.103)}$$

When the excitation frequency changes discretely in a nonlinear system, the process of a sharp increase or decrease in the amplitudes of stationary vibrations occurs. For example, when in a nonlinear oscillatory system with a rigid characteristic (II.103), the vibration frequency increases, the peak of the resonance system shifts towards higher frequencies, while in the systems with a soft characteristic, the opposite is true. A sharp increase or decrease in the amplitudes of the transient process causes a bump up in the amplitudes on the lower stable branch of resonance, that is, the small vibration amplitudes are set.

This correction creates the condition for a stable transient process, and we obtain the AFC for the nonlinear systems even with a transition increment of 2–3 Hz.

Based on the research carried out, a mathematical model was created for carrying out the numerical experiments (modeling) of the dynamics and dynamic stability of the nonlinear wide-range vibrators, including the electromagnetic vibrators.

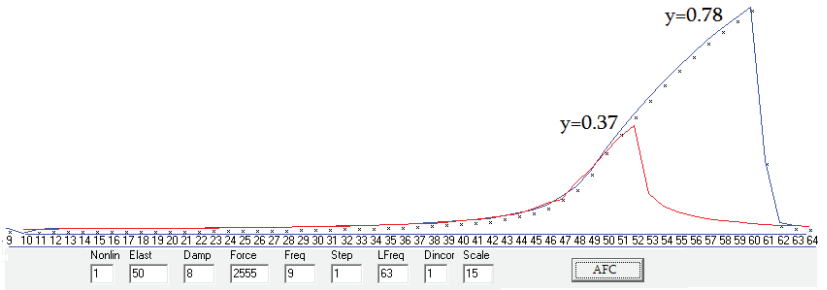

Fig.II.29 The AFC (frequency response) of the harmonically excited, debalance-type, pneumatic, hydraulic and other vibrators with the non-linear elastic systems having the rigid characteristic

Figure II.29 shows the AFC (frequency response) of a harmonically excited nonlinear non-electromagnetic vibratory exciter with a rigid response in the frequency range of 9÷64 Hz, taking into account the above correction, while Figure II.30 shows the same, but without correction in accordance with the equation (104)

$$\ddot{x} + 2h\dot{x} + \omega_o^2(x + \eta x^3) = a \cdot sin\omega t \qquad \text{(II.104)}$$

As Figure II.30 shows, with an increment of 1 Hz, changing the frequency without correction, two stable branches typical of the nonlinear systems are not fixed during the numerical experiments.

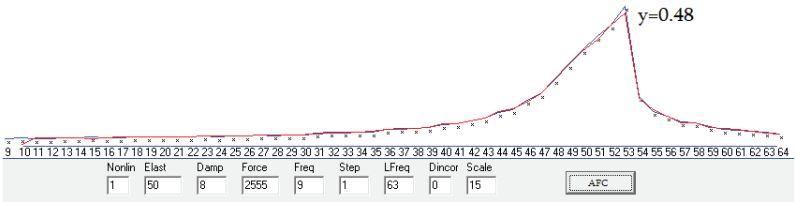

Fig.II.30. The AFC (frequency response) of the harmonically excited vibrators with the non-linear elastic systems without adjustment

It should be noted that in mathematical modeling of the nonlinear systems, it is desirable to use a floating-point number, otherwise in most cases, the influence of non-linearities is lost, since when measuring in the *SI* system, we deal with too small numbers. For example, with an amplitude of vibrations $y = (0{,}001\ m)^3 = 0{,}000000001\ m^3 = 10^{-9}\ m^3$. It should also be noted here that in the equation (20), the non-linear effect of the air-gap clearance is expressed in the denominator in the thrust coefficient of the electromagnet, as described in [35].

Figure II.31 shows the AFC (frequency response) of the nonlinear electromagnetic vibratory exciter, excited by the half-periodically rectified current in the excitation section of 7÷61 Hz, taking into account (II.103) and corrections. The magnitude of the amplitude of the exciting force is the same in all cases.

Comparison of the obtained AFC with the previous ones shows that the AFC of the electromagnetic vibrator differs from the previous non-electromagnetic vibrator in that the latter has several low-frequency multiple resonances, the so-called subharmonics, while in the previous AFC, the low-frequency multiple resonances are not visible.

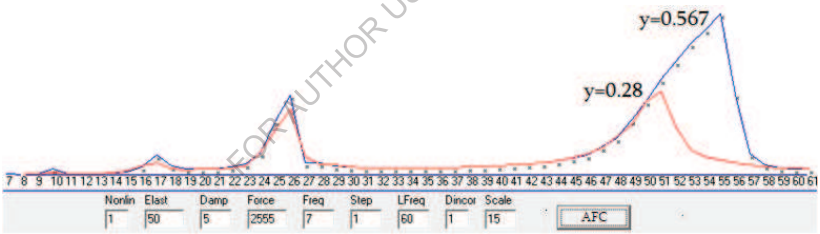

Fig.II.31. The AFC (frequency response) of the vibrators with the non-linear elastic systems having the rigid characteristic excited with a half-periodic rectified current

Based on the comparison of the last two frequency characteristics (responses), it can be concluded that the half-periodic rectification of alternating current in the system causes the appearance of additional non-linear effects. With a tractive force of the electromagnet with a rectified half-period of the electric current, in addition to the main frequency, other frequencies appear, including the multiple frequencies, which under certain conditions can cause the corresponding resonant vibrations.

Conclusions

A method has been developed to calculate the rigidity of a spatial torsional elastic frame that is subject to torsional and bending deformations, and it has been shown that 75-85% of the relative displacement of the clamped parts of the torsion bar is performed due to the torsion of the torsion bar, and only 7-10% - due to the bending of the torsion bar and the lever, and the rest is due to the non-linear opening of the clamped part of the torsion bar.

Depending on the effect of the values of the torsional and bending moments, the opening of the clamped part of the torsion bar is investigated, which leads to a decrease in the rigidity of the elastic systems and contributes to the appearance of dissipative forces in the form of structural damping. The shapes of the hysteresis loops formed in the clamped parts due to torsional and bending vibrations have been obtained.

A mathematical model of the electromagnetic vibratory exciters has been created, and a broad mathematical experiment has been carried out to study the dynamics of the electromagnetic vibrators.

The results obtained using the created mathematical model based on the mathematical experiments are in good agreement with experimental studies, and it can be concluded that the created program for mathematical modeling of the electromagnetic vibratory exciters can be successfully used at the design stage of new electromagnetic vibratory exciters.

References

1. S. Graham Kelly. Mechanical Vibrations. Theory and Applications, S I. The University of Akron. 2012, 878 p.
2. Khvingia M.V. Dynamics and strength of the vibrating machines with electromagnetic excitation. M., Mashinostroenie, 1980, 144 p. (in Russian).
3. Isodor Bykhovsky. Fundamentals of vibration engineering. 382 pages; Publisher: Krieger Pub Co; Revised edition (June 1, 1980); Language: English; ISBN-10: 0882755501; ISBN-13: 978-0882755502 .
4. Initial data for calculating torsion shafts. Mechanics of materials, Chapter 3 torsion. 1993. 75-105 p.
5. The Vibratory diagnostics of the machines and equipment. Analysis to vibrations. Publisher GMTY Saint Petersburg. 2004. 156 p.
6. Chelidze M.A., Khvingia M.V. Studying the rigidity of the torsional elements of the vibrating machine. Bull. Georg, Academy of Science, Vol.88, No. 2, Tbilisi, 1977. pp.397-400 (in Russian).
7. Chelidze M.A. About non-linear relationship between the stiffness property of the torsional elastic frame and value of the vibration amplitude. In the book "Machine mechanics", Tbilisi, Metsniereba publishers, 1998, pp.112-118 (in Russian).
8. Makarov A.M. Method for calculating of the torsional elastic elements. Journal "Ore Concentration", No. 5. Leningrad, 1962, pp.45-49 (in Russian).
9. Feodosiev V.I. Strength of materials. M. "nauka" 1999, 554p. (in Russian)
10. Yurii Zalutskyi, OleksandrZhytenko, IhorKuzio. Analysis of modern investigations of vibratory processes of wheeled vehicles. 2016. 350 p.
11. Ya. G. Panovko, Internal Friction in Vibrations of Elastic Systems. Fizmatgiz, Moscow (1962), -184 c. (in Russian),
12. Chelidze M.A., Khvingia M.V. Studying the damping coefficient of the torsional vibrating machine. In the book "Energy dissipation at vibrations of the mechanical systems". Kiev, Naukova Dumka, 1980, pp. 192-201 (in Russian).
13. Khvingia M.V., Tsulaia G.G., Gogilashvili V.N., Tatishvili T.G. Constructive damping in the nodes of vibration machines. Tbilisi, GPI publishers, 1973, 138 p. (in Russian).
14. K. Rainer Massarsch. Effects of Vibratory Compaction. Geo Engineering AB, Stockholm, Sweden. 2002. 10 p.
15. PaoloL. Gatty. Applied structural and mechanical vibrations. (teory and methods. Second edition). 2014. 316 p.

16. H. Irreter, D. Balaschov. Transient Resonance Oscillations of a Turbine Blade with regard to Non-Linear Damping Effects. 2011. 179-186 p. https://doi.org/10.1002/zamm.20000801415.
17. Filippov A.P. Oscillations of deformable systems. M.: Mashinostroenie, 1970, 736 p (in Russian)..
18. Indeitsev, D.A., Krivtsov, A.M. Advanced Problems in Mechanics. 2019, St. Petersburg, Russia. 420 p.
19. Chegodayev D.E., Ponomaryov Yu.K.. Damping. Publishing house of Samara State Aerospace University. Samara, 1997. 334 p . (in Russian).
20. Henrik Sonnerlind. Damping in Structural Dynamics: Theory and Sources. 2019.294 p.
21. Parametric oscillation and mixing. R. L. Byer, R. L. Herbst. 2005. Pages 81-137.
22. I. F. Goncharevich and E. G. Gudushauri. Some Aspects of Modern Development of Vibratory technology. Journal of Machinery Manufacture and Reliability. 2008, Volume 37, Issue 5, pp 513–516.
23. Excitation of poliharmonic vibrations in single-body vibration.(Dynamics of Mining Machines with Elastic Connections) by SL Bukin - Jul 5, 2014. 144 156 p.
24. B.I.Krukov. Dynamics of vibratory machines, Kiev, "Naukova-dumka" 1967, 210p. (Russian).
25. N.S.Piskunov. Differential and integral calculus, 2d v, Moscow, "Nauka" 2011, - 576 c (in Russian).
26. V.A.Bauman, I.I Bikhovski. Vibration machines and processes in building. Moscow, 1977. 250p. (in Russian)
27. I. I. Blekhman. Vibration Mechanics and Vibration Rheology. Theory and applications. M., Fizmatlit, 2018 (in Russian).
28. Chelidze M., Zviadauri V., Tedoshvili M., Volkdvas V., Khvadagiani A. Determination of the useful work of the vibration exciter with the help of oscillograms of free damping. Proceedings of the V Georgian-polish international scentific-technical conference. Transport bridge Europe-Asia. Kutaisi, Georgia, 15-18.10.2019. pp153-161.
29. M.Chelidze. On the solution of differential equations of oscillations of electro-magnetic exciter. Bull. Georg, Academy of Science, 156, 2 1997, 266-267 pp.
30. M.Chelidze. Influence of Electromagnetic Disturbing Force on Dynamic Stability of Vibration. Bulletin of the Academy of Sciences of Georgia 160 N 2 Tbilisi, 1999. 4p.

31. G.A.Zasman, O.M.Todes. Course of general physics, 2d v. Moscow, 1974 350p. (Russian)
32. M. Chelidze, V.Zviadauri. "Generating of sub harmonic resonant oscillations and problems of their stability" JVE Journal of vibroengeening. V. 10 Issue 4. December Riga, 2008 4p.
33. Merab A. Chelidze, Victor S. Zviadauri, George I. Tumanishvili. Process of Compaction of Plastic Materials under Influence of Vibrations. Proceedings of the World Congress on Engineering and Computer Science 2010 Vol II WCECS 2010, October 20-22, 2010, San Francisco, USA
34. A. Chatterjee. A Brief Introduction to Nonlinear Vibrations, Mechanical Engineering, Indian Institute of Science, 2009.
35. Željko V. Despotović, Milan Jović. Mathematical model of electromagnetic vibratory exciter with incremental motion. INFOTEH-JAHORINA Vol. 13, March 2014. 91÷96 pp.

PART III
THE LOW-FREQUENCY ELECTROMAGNETIC EXCITERS OF RESONANT VIBRATIONS

Introduction

At the present stage of the revolution in science and technology, special importance is attached to the development and broad application of means of integrated mechanization and automation. In automated systems that regulate technological processes occurring in mechanical and electric drives and other devices, the vibrating reciprocating machines are used to a great extent.

The principle of operation of the vibrating machines is based on generating vibrations that are excited and supported by inertial, piston-type, electromagnetic or other types of the exciters.

Areview of the literature [5, 6, 8, 10, 12, 16] indicates that in terms of the amplitude of the driving force per unit mass, the electromagnetic exciters are far belowthe inertial and hornet-typevibratory exciters. Nonetheless, the vibrating machines with an electromagnetic drive have earnedsustained and growing applications.The design and operational features of these machines allow them to be widely used in mining, metallurgical, construction, machine-building, instrument-making, chemical, food and other industries [1, 7, 11, 15]. Its good points include: simplicity of design, increased reliability and durability, the possibility of fluent regulation of the performance (without stopping the machine) at a strictly specified vibration frequency and practical noiselessness in operation. As a result of the absence of rotating and rubbing pairs, there is no need for periodic lubrication and replacement of worn parts, which significantly reduces the cost of machine operation.

A significant reduction in the dimensions and masses of the electromagnetic vibratoryexciters was achieved by using the resonant tuning of the elastic system. The latter leads to an increase in the sensitivity of the vibration amplitude in relation to changes in the supply current, which makes the electromagnetic vibratory exciter a very convenient object of automatic control.

1. The electromagnetic exciters of resonant vibrations

Practically all the modern electromagnetic vibrating machines operate in a near-resonant tuning of the main mode [3, 4, 9], and the amplitude of the force developed by

the elastic suspension is 5-20 times higher than the amplitude of a driving electromagnetic force (the ratio of these forces is sometimes called the gainratio).

The electromagnetic vibrating machine consists of two, active and reactive masses, interconnected by means of the elastic system. The most commonly used elastic systems are in the form of sets of flat bow springs and helical springs; there are also the elastic elements in the form of the torsional frames, rubber washers and flexible shafts. The masses are fastened to the elastic elements by means of the binding bolts, or installed directly on the end coils of springs. The working member is attached to the active part of the exciter.

By method of power supply, the electromagnetic vibratory exciters are subdivided into the vibratory exciters with power supplywith: alternating current; rectified current; simultaneously alternating and direct current.

The low rigidity of the elastic elements provides great opportunities for fluent variation of resonance characteristics, such as an amplitude, natural frequency and damping coefficient in the nodes of the clamped ends of the elastic elements. In this case, the non-linear effects appear both in the elastic system and in the exciting forces.

The nonlinear properties of the elastic system and the exciting force can be used to generate sub- and superharmonic resonant vibrations without the use of special frequency converters. The exciting force in the electromagnetic vibratory exciters essentially depends on the size of the gap in the electromagnet, and besides is non-linear. The power-supply circuit of the electromagnets and tacticity of the exciter affects significantly this non-linearity.

Therefore, the oscillatory processes in the exciter with the given mass characteristics are, first of all, the processes of interaction of two non-linear factors: the elastic-frictional force and the force of electromagnetic excitation.

In a dynamical analysis of the vibrating machines, the rigidity of the elastic system is picked out from the condition of generating the resonance (near-resonance) vibrations at a given frequency of the exciting force.

The experimental and theoretical studies have shown that along with the main resonances of the system under certain conditions, due to non-linearity of the electromagnet, it is possible to generate the sub- and superharmonic resonance vibrations [4, 16, 17].

The use of these vibrations (especially subharmonic ones) in the vibratory exciters increases noticeably the capabilities of these machines in terms of both reducing the metal consumption of the elastic elements and reducing the inertial loads and the level of radiated noise.

A review of the literature shows that the issue of regulating the amplitude of mechanical vibrations of the electromagnetic vibrating machines operating at low frequencies, for example, in a subharmonic resonance mode, has not been sufficiently studied. The dependence of the damping coefficient and the amplitude of mechanical vibrations on the constant component of the exciting force is also among the issues that have not sufficiently addressed.

2. Methods for the vibration frequency reduction

The basic requirement needed for the operation of the resonant vibrating machines is the correspondence of the natural frequency of the mechanical system with the disturbing frequency, the ratio of which at precise resonance tuning is $\omega_0/\omega_1 = 1$. Proceeding from this, when considering the methods for reducing the vibration frequency of the working member, we shall assume that the natural frequency of the elastic system is pre-set to the excitation frequency.

In order to further reduce the frequency, various phase-shifting and pulse devices are often used to generate the frequency of mechanical vibrations equal to $\omega_1/2$ [13]. The exciters are also applied, in which the effect of the ferroresonance phenomenon is used. In this case, under certain conditions [13], for example, if the capacitance of condenser and the size of the air-gap clearance meet the conditions for the occurrence of voltage resonance, the so-called parametric resonance occurs and mechanical vibrations are generated with a frequency different from the excitation frequency. However, such a system is difficult to tune to resonance, it is sensitive to changes in parameters, and it works unstably, which limits its application.

A downside to these schemes is the need to use the additional frequency conversion devices, which ultimately reduces the overall reliability of the vibrating machine.

Reducing the vibration frequency of the working member, under certain conditions, can be carried out by using a new type of a non-linear subharmonic transducer [16]. Such a regime is realized under conditions when the excitation frequency is equal to ω_1 and the natural vibration frequency of the elastic system is $\omega_0 = \omega_1/2$, and the vibrations of the order of $\omega_0/\omega_1 = 1/2$ are excited. The main advantage of the subharmonic mode is the reduction in the frequency of mechanical vibrations of the vibrating machine without the use of the additional frequency converters, ease of maintenance and design reliability.

The increased interest in the problem of the frequency reduction is primarily due to the fact that the intensification of some technological processes is associated with the use of low-frequency mechanical vibrations, for example, for compacting the concrete

mixtures [1, 6], in the automated lines for oriented supply of parts [12, 15], etc. A decrease in the frequency of vibrations of the working member, naturally, reduces the speed of transporting material as many times as the frequency has decreased. Therefore, to maintain a constant speed of transportation of material, it is necessary to increase the amplitude of mechanical vibrations. For example, for the subharmonic mode (ω_0/ω_1 = 1/2), it is necessary to have the speed $V = 2A_{\text{mech}}*\omega_1/2$. The overall benefit in terms of vibration isolation lies primarily in halving the force of inertia $2A_{mech}*(\omega_1/2)^2 = A_{mech}*\omega_1^2/2$. Consequently, the load on the supporting structures is reduced by the same factor. In addition, the rigidity of the expensive elastic system decreases by $1/(\omega_0/\omega_1)^2 = 4$ times, and the noise of the machine also decreases.

3. Special aspects of generating subharmonic vibrations

The mechanism for generating subharmonic vibrations in the electromagnetic vibratory exciters is well described in [16].

The main source of non-linearity in the electromagnetic exciter of vibrations is the electromagnetic force created in a variable gap clearance [4, 16, 17].

Based on the Maxwell's formula, the force developed by the electromagnet is equal to [2],

$$F(x,t) = \frac{B^2 S}{2\mu_0} \qquad \text{(III.1)}$$

Magnetic induction B is proportional to the magnetic flux Φ, that is $B = \Phi/S$, therefore

assuming that magnetic induction in the gap clearance is uniform, we obtain the following relationships for the flux and voltage balance:

$$\begin{cases} \Phi = \frac{\mu_0 SW}{\delta(1-x/\delta)} i \\ ir = U(t) - W\frac{d\Phi}{dt} \end{cases}, \qquad \text{(III.2)}$$

usually, $U(t) = U_0 \sin(\omega,t)$.

These ratios allow to make qualitative predictions about the nature of the exciting force.

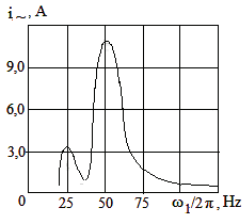

Fig. III.1. The diagram of the excitation current components in a subharmonic mode

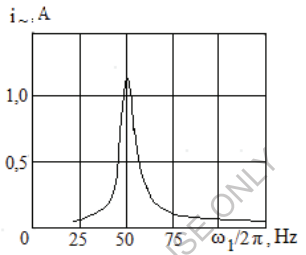

Fig. III.2. The electric current diagram

To a first approximation, based on physical considerations confirmed by experimental data, the oscillation spectrum of the supply current $i(x,t)$ contains the main components – the constant A_o and variables with the frequencies ω_1 ,ω_2 and the amplitudes A_1, A_2. The frequencies of the exciting current ω_1 and the working member ω_2 are not equal, $\omega_1 \neq \omega_2$. The constants Ao, A_1, A_2 are unknown and depend on the parameters of the oscillatory mode of the machine. Fig. III.1 and III.2 illustrate the dependences $i(\omega_1)$, obtained for a machine with capacity of 0.5 kW; the elastic system consists of slitting springs.

In the first case (Fig. III.1), there is no regulation current (direct current $I = 0$); for the subharmonic mode, i contains all three components, however $A_o << A_1 << A_2$.

In the second case (Fig. III.2), there is the bias current (I = 4,5 A); Figure shows only the alternating part of the current and the accompanying constant part; $A_o << A_1$.

Let's write the expression for the electric current in following form as follows:

$$I = A_0 + A_1 sin(\omega_1 t - \varphi_1) + A_2 sin(\omega_2 t - \varphi_2), \qquad \text{(III.3)}$$

where φ_1 ,φ_2 – the unknown phase shifts, which, like A_o, A_1, A_2, can be determined

approximately.

We expand the right side of the expression Φ in a series in powers of x/δ, and w represent the force F in the following form:

$$F(x,t) = \left(\frac{\mu_0 W^2}{2S\delta}\right)^2 [A_0 + A_1 \sin(\omega_1 t - \varphi_1) + A_1 \sin(\omega_2 t - \varphi_2)]^2 \times \sum_{n=0}^{\infty} (n+1)\left(\frac{x}{\delta}\right)^n =$$

$$= \left(\frac{\mu_0 W^2}{2S\delta}\right)^2 \left[a_0 - \frac{A_1^2}{2} cos2(\omega_1 t - \varphi_1) + E(t)\right] \times \left[1 + 2\frac{x}{\delta} + E(t) \times \left[1 + 2\frac{x}{\delta} + E(x)\right]\right]$$

where

$$a_0 = A_0^2 + (A_1^2 + A_2^2)/2$$

$$E(t) = -(A_2^2/2)cos2(\omega_2 t - \varphi_2) + 2A_0[A_2 sin(\omega_2 t - \varphi_2) + A_1 sin(\omega_1 t - \varphi_1)] +$$

$$+A_1 A_2[cos(\omega_2 t - \varphi_2 - \omega_1 t - \varphi_1) - cos(\omega_2 t - \varphi_2 + \omega_1 t - \varphi_1)];\ E(x) = \sum_{n=2}^{\infty}(n+1)(x/\delta)^n. \qquad \text{(III.4)}$$

Taking into account the structure of $F(x,t)$, in which the influence of x and t on the exciting force is expressed in the form of separate functions - factors, we represent it in the form as follows:

$$F(x,t) = \left(\frac{\mu_0 W^2}{2S\delta}\right)^2 \left[a_0 - \frac{A_1^2}{2} cos2(\omega_1 t - \varphi_1)\right]\left(1 + 2\frac{x}{\delta}\right) + F_1(x,t), \qquad \text{(III.5)}$$

where

$$F_1(x,t) = E(t)\sum_{n=0}^{\infty}(n+1)(x/\delta)^n + E(x) \times \left[a_0 - \frac{A_1^2}{2} cos2(\omega_1 t - \varphi_1) + E(t)\right].$$

The active mass vibration differential equation will be written as follows

$$m\ddot{x} + c\dot{x} + kx = \left(\frac{\mu_0 W^2}{2S\delta}\right)^2 \left[a_0 - \frac{A_1^2}{2} cos2(\omega_1 t - \varphi_1)\right]\left(1 + 2\frac{x}{\delta}\right) + F_1(x,t). \qquad \text{(III.6)}$$

This equation consists of linear and parametric terms, as well as a non-linear function that in the summed movement does not contain a small parameter. Therefore, it is inappropriate to ascribe to its solution only parametric properties, and it would be more correct to say that it has the parametric properties with the limitations attributed to the non-linear equations.

The presence of linear terms in the right-hand side of the equation (6) after their

formal combination with similar terms in the left-hand side of the equation ultimately leads to the following form of the equation:

$$m\ddot{x} + c\dot{x} + [k_1 - k_2 cos2(\omega_1 t - \varphi_1)]x = a_0 - k_2 cos2(\omega_1 t - \varphi_1) + b_1 F_1(x,t), \quad \text{(III.7)}$$

where k_1 - is the system's reduced rigidity, which depends on the physical rigidity of the linear elastic element and the additional electromagnetic component, which also has the properties of linear spring; k_2, δ_1 - parameters of the equation:

$$k_1 = k - \left(\frac{\mu_0 W^2}{2S\delta}\right)^2 \left(\frac{2a_0}{\delta}\right); \quad k_2 = \left(\frac{\mu_0 W^2}{2S\delta}\right)^2 \frac{A_1^2}{2}; \quad b_1 = \left(\frac{\mu_0 W^2}{2S\delta}\right)^2.$$

The presence of the coefficients $a_0 \neq 0$, $k_2 = O$ in the right-hand side of the equation points out that the summed movement will contain a purely forced component with a frequency of $2\omega_1$ that is equal to the modulation frequency of the reduced rigidity, which, as is known, for the parametric systems is the cause of the emergence of additional resonances in each of the instability zones, the effect of which rapidly decreases as the zone number and damping coefficient increase [17].

The main properties of the nonlinear parametric equation (III.7) include: the existence of zones of unstable vibrations near the critical excitation frequencies

$$\omega_{cr} \approx 2\omega_0/n, \quad n = 1, 2, 3, \ldots.$$

where $\omega_0^2 = k_1/m$; the main zone here is $\omega_{cr} \approx 2\omega_0$; the multiplicity of vibrations, among which some are stable and the rest are unstable; the existence of an upper limit for the increase in the amplitude, which is limited mainly by the non-linear properties of the equation; the effect of damping on the lower vibration threshold.

These features have a significant impact on the development and stabilization of parametric vibrations in the main zone.

4. The exciters with frequency separation of operating vibrations

With a view to ensuring stability of the amplitude of low-frequency vibrations, there was developed the scheme of the vibratory exciter, the operation of which is based on the principle of the magnetic flux partition along two oppositely located identical branches.

Figure III.3a shows the vibrator'sscheme, while Figure III.3b illustrates the scheme of the coil connections (depending on the design, it is possible to use both the *U*-shaped and *H*-shaped magnets). The vibrator contains the active I and reactive 2 masses, connected by the elastic system 3 (for example, in the form of packages of flat bow springs). Two *U*-shaped magnetic cores 4 and 5 are fixed on the active mass I, while the middle magnetic core with the exciting coil 7 is fixed on the reactive mass 2 (Fig.III.3a). The exciting coil 7 for the *H*-shaped magnet is installed on the central part of the middle magnetic core 6 (Fig.III.3b). The natural frequency of the relative oscillations of the masses I and 2 is equal to half the frequency of the action of the excitation pulses ω_1.

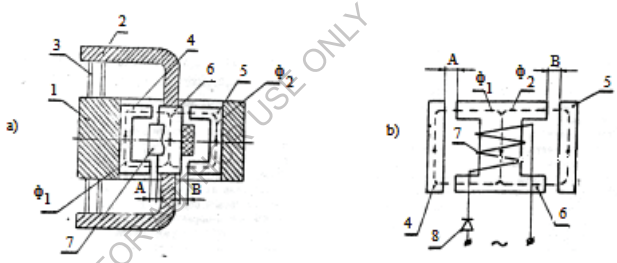

Fig.III.3. The diagram of the exciter with frequency separation of operating vibrations: a) with the U-shaped magnet and the elastic system; b) the diagram of the coil (winding) connections of the H-shaped magnet suitable also for the U-shaped magnet

The vibrator works as follows. The passage of current through the coil 7 causes the emergence of split variable magnetic fluxes Φ_1 and Φ_2, which, after overcoming the resistance of the air-gap clearances *A* and *B*, are closed through the magnetic cores 4 and 5. As a result of a certain initial structural difference (for example, $\Phi_1 > \Phi_2$, in the first half-periodic supply current, the middle magnetic core*b* will be attracted to the marginal magnetic core 4. Due to a decrease in the air-gap clearance *A* and an increase in the gap clearance *B*, the magnetic fluxes will mainly complete through a lower air resistance *A*, that is, there will be a significant increase in Φ_1 and a decrease in Φ_2. This will lead to an increase in the traction force from the side of the gap clearance *A* and its decrease from the side of *B*, and thereby the deflection of the elastic system.

Due to the presence of diode 8 in the second half-period of the supply current, there is no traction force of the electromagnet, the elastic system returns the mechanical system back to its original position,

since ω_0/ω_1 = 1/2, and by inertia, the neutral position will pass and the air-gap clearance *B* will decrease. The magnetic fluxes caused by the second impulse of the traction force will basically be locked through the air-gap clearance *B*, that is, the traction force from the side of *B* increases with a decrease in *A*.

Thus, the elastic system bends in the opposite direction.

Further, it's happening again, in consequence of which the low-frequency vibrations are excited with a frequency equal to half the frequency of the traction force of electromagnetic excitation (this regime will be considered to be the main regime of operation of this vibratory exciter).

The operation of the exciter of vibrations according to the scheme shown in Figure III.3 is described by the following differential equations [18, 19]:

$$m\ddot{x} + c\dot{x} + kx = \pm F(x,t)sign\Phi; \quad \text{(III.8)}$$

$$W\Phi + a(\delta - \dot{x})\Phi = U(t); \quad \text{(III.9)}$$

$$\text{sign } \Phi = \begin{cases} 0 & when \quad \Phi < 0; \\ 1 & when \quad \Phi > 0; \end{cases}$$

$$F(x,t) = \Phi^2 / 2\mu_0 S\,;\; a = r/\mu_0 SW\,;\; U(t) = U_0 \sin(\omega)\,;$$

where the "+" sign in the right-hand side of the equation (III.8) is taken when the magnet attracts from the side of the air gap clearance *A*, and the "-" sign is taken when the magnet attracts from the side of the gap *B*.

Direct substitution of the numerical values yields the one-kilowatt serial vibratory exciter, and the equations take on the following form:

$$x = -6{,}5\dot{x} - 24649\ddot{x} \pm 340804\Phi^2 sign\Phi;$$
$$\Phi = 1{,}5\sin(\omega t) - 300(\delta - x)\Phi.$$

Based on the results of the solutions, an amplitude-frequency characteristic was constructed, which is shown in Figure 3.4a. The system is non-linear. At a natural frequency of ω_0 = 25Hz there is an abruptfailure of oscillations at the excitation frequency of ω_1 > 46Hz. In order to get oscillations at a frequency of ω_1 =50Hz (i.e. to adjust the vibratory exciter to the industrial frequency), the natural frequency of the system should be increased by 2-3 Hz, we take ω_0 = 27,5 Hz. In this case, the frequency

response (AFC) moves to the right, in the direction of increasing ω_1. A decrease in the vibration amplitude for a system with ω_0 = 27,5 Hz is associated with an increase in the rigidity of the elastic system when other parameters are unchanged. The vibration amplitude is controlled by changing U_o.

When the excitation winding is powered from the mains supply of an industrial frequency 50 Hz without diode 8, due to the squaring effect, the frequency of the propulsive burns of the electromagnet is doubled. Therefore, when tuning the elastic system to a frequency of 25Hz, it seems that a subharmonic mode of the order ω_0/ω_1 = 25/100 = 1/4 should be excited, but really, there is excited the subharmonics 1/2, since the main regime of operation of this machine when it is powered via a diode 8, is the regime with dividing the excitation frequency by two.

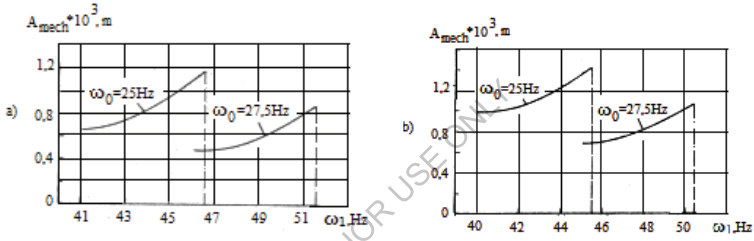

Fig.III.4. The amplitude-frequency characteristic of the vibratory exciter:
a) powered via a semiconductor diode; b) powered without a diode

The equations describing. the work of the exciter of vibrations when it is powered without a diode have the form of (III.8), (III.9) with the difference that the symbol sign is absent in the equation (*I*). The (AFC) frequency response for this regime is shown in Figure 3.4*b*, which actually repeats the nature of the machine's operation when it is powered via a diode, but is shifted by 1Hz downward.

Figure III.5 shows oscillograms of steady-state vibrations of the regime with a diode at ω_0 = 25 Hz. with the following parameters: ω_1 = 41Hz; б) ω_1 = 46Hz.; в) ω_1 = 47Hz - failure of oscillations.

The symmetrical arrangement of the tractive force impulses relative to the abscissa indicates the alternate action of this force from the sides of the air-gap clearances *A* and *B*. For the case with ω_1 = 47 Hz, these impulses become of the same sign, this indicates that the vibrator from the resonance mode of frequency division of operating vibrations goes into the forced mode and the attraction occurs only from one side of the magnet, for

example, from the side of the gap *B*.

Studies have shown that the considered scheme of the exciter allows to generate stable low-frequency vibrations of essential resonance (when the frequency of operating vibrations is two times less than the excitation frequency) and subharmonic resonance of the order of 1/2 (when the frequency of operating vibrations is four times less than the excitation frequency). In addition, the effect of certain additional non-linearity is manifested, which relocates the region of existence of operating vibrations and gives the system a softer characteristic.

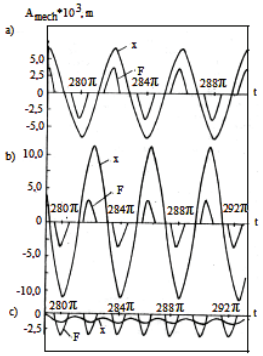

Fig. III.5. Oscillogram of the displacement of ***x*** and excitations ***F*** of steady-state vibrations with parameters: a) frequency supply $\omega_1 = 41$ Hz; $\omega_1 = 46$ Hz; в) $\omega_1 = 47$ Hz.

5. Methods for controlling the vibration amplitude

Subharmonic vibrations with a parametric action of vibration excitation are accompanied by an increase in the amplitude up until the collision of the lifter with a magnet stator.

The growth of the amplitudes can be limited by adjusting the damping in the exciter, directly affecting the parameters of the electromagnet (the magnitude of the saturation of the magnetic circuit, the constant component of the disturbing force), or by adjusting the bias current. Let us consider the methods of damping regulation in the vibratory exciter.

6. Saturation control of the magnetic core

In the electromagnetic mechanisms, the magnetic field strength H or current i is a function of the magnetic flux Φ. The relationship between these quantities is characterized by a hysteresis loop, which can be represented as the sum of two functions - the average curve $H_{cp} = f_{md}(\Phi)$ and the function $H_n = f_n(\Phi)$ symmetrical relative to an

axis Φ (Fig. III.6), [14].

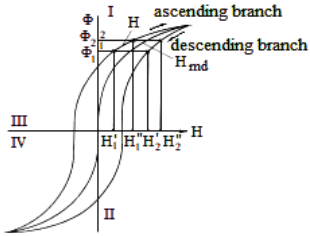

Fig. III.6. Components of the magnetic hysteresis loop

Usually these functions for the unsaturated state of the magnetic circuit are described by the following expressions:

$$H_{md} = a\frac{\Phi}{c-\Phi}; \qquad H_n = \frac{H_{max}}{\Phi_{max}}\sqrt{(\Phi^2_{max} - \Phi^2)}. \qquad \text{(III.10)}$$

The function H_{md} describes the skeleton curve of the loop; the second function that fits the equation of the ellipse, describes the contour of the conditional loop.

The total field value for the ascending (+) and descending (-) branches is

$$H = H_{md} \pm H_n \qquad \text{(III.11)}$$

Formulas (III.10) - (III.11) are valid for the upper part of the loop; the lower, negative part, is described by the same formula (III.10), but it is necessary to change the sign before the H, that is, $-H = H_{md} + H_n$.

According to the experimental hysteresis loop for a typical power-supply circuit of the electromagnet, the constants a and $c$are determined, there are derived the values H_1', H_1'', H_2', H_2'' - two pairs of values of intensity of a magnetic fields for sections ϕ_1, ϕ_2 (Fig. III.6), chosen arbitrarily in the first quarter on the ascending and descending sides of the loop.

Average values of intensities:

$$H_1 = (H_1' + H_1'')/2$$
$$H_2 = (H_2' + H_2'')/2.$$

Inserting by pairs the values (H_1, Φ_1), (H_2, Φ_2) into the equation of skeleton curve, we get:

$$a = \frac{\phi_2/\phi_1 - 1}{H_2/H_1 - \phi_2/\phi_1} H_2;\ c = \frac{H_2/H_1 - 1}{H_2/H_1 - \phi_2/\phi_1} \phi_2 . \qquad \text{(III.12)}$$

In the symmetrical loops, the upper and lower parts (*I, IV, II, III* - quadrants) have the constants *a, c* of the same magnitude; in the asymmetric loops, the values of *a, c* from the upper and lower parts are different, that is, they are determined separately for two arbitrary sections of the upper and lower parts. Points H_2, Φ_2 are replaced by points H_{max}, Φ_{max} for the loops with a small deviation from the ellipse. An experimental hysteresis loop for a two-stroke, half-kilowatt vibration machine, is shown in Figure III.7; certaininsignificant shift of the loop relative to the axis H is due to the presence of a bias current in the half cycle of the load.

The structural diagram of the device for removing the experimental hysteresis loop is shown in Figure III.8. The alternating current is fed to the horizontal input of a two-coordinate oscilloscope, using a calibrated shunt III_1, transformer $T1$ (transformation ratio - 1), a signal amplifier and a phase shifter (the bridge circuit consisted of two fixed resistors, a capacitor and one variable resistor). For the purpose of summing the alternating current i and the direct current I_2, the secondary winding of the transformer $T1$ is connected in series with the calibrated shunt III_2. The measurement and registration of the magnetic flux in the air-gap clearance was carried out using a Hall sensor - D_x), which was glued on the stator pole of the electromagnet. The signal taken from D_x, through two identical amplifiers and phase shifters, is transmitted to the input of the vertical scan of the oscilloscope. The phase shift error is eliminated using the phase shifters.

In the experimental hysteresis loop shown in Figure III.7, the constants *a, c,* of the upper and lower parts of curve are different; however, in the simulation model, with a view to simplifying the calculation, the hysteresis loop will be regarded as symmetrical, and the asymmetry will be further taken into account by the constant term *I2W2*.

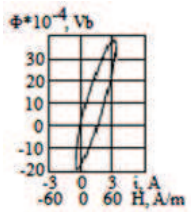

Fig. III.7. A real hysteresis loop

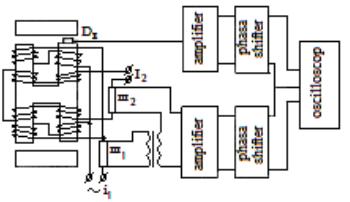

Fig. III.8. The diagram of the device for the hysteresis loop removal

On the experimental loop, an arbitrary point is taken, for example, a point with a magnetic flux $\Phi_1 = 35*10^{-4}$ Wb, which corresponds with the intensity $H_1 = 55$ *A/m*; $\Phi_{max} = 38\text{-}10^{-4}$ *Wb*, $H_{так} = 60$ *A/m*, $a \approx 480$ *A/m*; $c = 340\text{-}10^{-4}$ *Wb*.

The Ampere's circuital law [2], which describes the operation of the two-stroke vibrating machine, takes account of the hysteresis phenomena in the magnetic core, as well as the constant component $I_2 W_2$. Then

$$i_1 W_1 + I_2 W_2 = (l - 2x)H(\Phi) + \frac{1}{\mu_0 S}(\delta - x)\Phi. \qquad \text{(III.13)}$$

The value (l — $2x$) takes account of change in the average length of the magnetic field lines.

The function $H(\Phi)$ describes the hysteresis in the magnetic core. Thus, to solve the problem, we have the following equations:

$$m\ddot{x} + c\dot{x} + kx = \frac{k_m}{\mu_0 s}\Phi^2 sign\Phi; \qquad \text{(III.14)}$$

$$i_1 r_1 + W_1 \frac{d\Phi}{dt} = U_1 \sin \omega t; \qquad \text{(III.15)}$$

$$i_2 r_2 = U_2; \qquad \text{(III.16)}$$

$$i_1 W_1 + I_2 W_2 = (l - 2x)H(\phi) + \frac{1}{\mu_0 S}(\delta - x)\phi; \qquad \text{(III.17)}$$

$$H_{md} = a\frac{\phi}{c - \phi}; \qquad \text{(III.18)}$$

$$H_n = \frac{H_{max}}{\phi_{max}}\sqrt{\phi_{max}^2 - \phi}; \qquad \text{(III.19)}$$

$$H = H_{md} \pm H_n. \qquad \text{(III.20)}$$

The initial parameters of a half-kilowatt vibratory feeder are as follows: $W_1 = 1300$; $W_2 = 650$; $r_1 = 22\ \Omega$; $r_2 = 6\ \Omega$; $S = 120*10^{-4}\ m^2$; $U_1 = 380$ *V*; $U_2 = 0\ 4 \div 24$ *V*; $m_1 = 230$ *kg*; $m_2 = 420$ *kg*; $m = 147$ *kg*; $\psi = 0{,}03$ - a value of the total damping coefficient; $k = 3{,}6*10^6$ *N/m* - the rigidity of the elastic system; $l = 1{,}0$ *m*.

For all considered cases of the magnetic state of the electromagnet [see the equations (III.13) - (III.20)], the upper half of the loop is described by the expression (III.20), the lower half - by the expression (III.20) with the opposite sign.

The results of solving demonstrate that the introduction of an unsaturated hysteresis loop does not limit the growth of the amplitude and the system operates in the impact mode, as in the case without regard for the loop.

Introduction of a hysteresis loop with varying degrees of saturation limits the amplitude of mechanical vibrations to $2A_{mech} = (1{,}84 \div 0{,}9)*10^{-3}\ m$.

Thus, by changing the degree of saturation of the magnetic core, it is possible to generatethe amplitude-controlled subharmonic resonant vibrations of the order of 25/50 = 1/2.

It is known that the area of the hysteresis loop characterizes the energy that passes into a unit volume of the steel of the magnetic coreduring one cycle of magnetic reversal, and is calculated according to the formula [2]

$$Q = \int_0^B HdB = \int_0^{\phi} \frac{H}{S}\, d\phi \ . \qquad \text{(III.21)}$$

For the case with symmetrical curve (the ellipse area), we have

$$Q = \pi\phi H/S \, . \qquad \text{(III.22)}$$

Below are the values of the loss density obtained by formula (III.22) for different saturation modes of the magnetic core, when $\omega_o/\omega_1 = 25/50$.

Table III.1

H, A/m	--	60	340	650	1300	2400
$2A_{mech}*10^3$, m	4,0	4,0	2,0	1,8	1,3	0,9
$Q*10^{-2}$	--	0,6	1,8	4,2	10,5	20,4
ψ	0,04	0,04	0,06	0,08	0,09	0,19

The values of damping coefficients of the system were obtained from the oscillograms of free damped oscillations.

Figure III.9 shows oscillograms of the electromechanical characteristics of the machine in the mode of subharmonic resonant vibrations, when $2A_{mech} = 0{,}5*10^{-3}m$; $\psi = 0{,}25$.

This method can be applied in practice as follows. The electromagnet designed for operation in a subharmonic mode is calculated so that its magnetic core is saturated. Then, by the excitation current drop by means of the adjusting device (rheostat, thyristor unit, etc.), the degree of saturation of the magnetic core changes and the vibration amplitude is adjusted.

In the powerful vibrating machines, to get the maximum amplitudes, the traction force of the electromagnet is required, the characteristics of which (cross-sectional area of the winding wire and magnetic core, turning number) correspond with the characteristics of the unsaturated subharmonic vibratory exciter; at the same time, at a minimum vibration amplitude, the electromagnet must be saturated, for which it is necessary to increase the cross-sectional area of

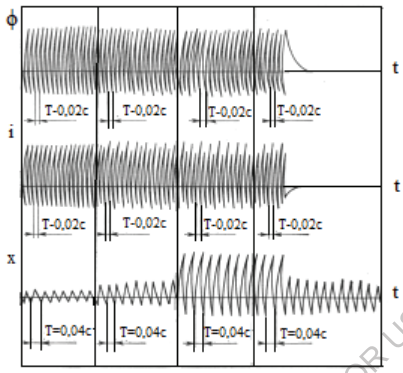

Fig. III.9. Transient processes of a subharmonic mode

the winding wire, while maintaining its turning number (the cross-sectional area of the magnetic core is constant). In this case, the traction force becomes highly non-linear, the consumed current, magnetic losses and the mass of the exciter increase, which noticeably worsens its operational and energy indicators.

7. Control using the constant component of the exciting force

Regulation and limitation in magnitude of the amplitude in the low-hysteresis subharmonic

machines is achieved by introducing a constant component of the exciting force. The schematic diagram of the vibratory exciter is shown in Figure III.10.

Vibrations between the active m_1 and reactive m_2 masses are excited by the rectified current i_1, passing through a semiconductor diode VD_1 and the excitation winding W_1 , which creates a pulsating traction force F_1. With the help of the half-wave rectified voltage obtained by the diode bridge VD_2—VD_5, the direct current passes through the winding W_2, which, in turn, excites a constant traction force F_2, directed opposite to the force F_1.

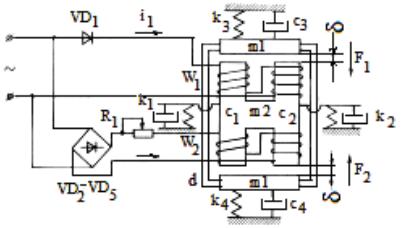

Fig. III.10. The diagram of the one-stroke vibratory exciter with the adjustable amplitude of subharmonic vibrations

The lifters of the electromagnet are rigidly connected by means of the frame *d*; the total force acting on the vibratory exciter during the period of action of the force F_1 will be equal to the difference between these forces: $F = F_1 — F_2$, while when $F_1 = 0$, the total force $F = F_2$. By changing the force F_2 using the rheostat, it is possible to continuously adjust the vibration amplitude of the working member of the machine and the subharmonic mode.

Operation of the exciter of vibrations of thevibrating machine according to the indicated scheme is described by the following differential equations [16]:

a) in the conducting part of the period

$$m\ddot{x} + c\dot{x} + kx = F_1 - F_2 ; \quad \text{(III.23)}$$

$$\frac{d}{dt}(L_1 i_{1dr}) + r_1 i_{1dr} + r_{dr} i_{1dr} = U_1 \sin \omega t ; \quad \text{(III.24)}$$

$$\frac{d}{dt}(L_2 i_2) + r_2 i_2 + R_1 i_2 = U_1 |\sin \omega t| ; \quad \text{(III.25)}$$

b) in the non-conductive part of the period

$$m\ddot{x} + c\dot{x} + kx = F_2 ; \quad \text{(III.26)}$$

$$\frac{d}{dt}(L_1 i_{1rv}) + r_1 i_{1rv} + r_{rv} i_{1rv} = U_1 \sin \omega t ; \quad \text{(III.27)}$$

$$\frac{d}{dt}(L_2 i_2) + r_2 i_2 + R_1 i_2 = U_2 |\sin \omega t| , \quad \text{(III.28)}$$

where

$$F_1 = \frac{1}{2} L_{01} \delta \frac{i_1^2}{(\delta - x)^2} ; \qquad L_1 = \frac{L_{01}}{1 - x/\delta} ;$$

$$F_2 = \frac{1}{2} L_{02} \delta \frac{i_2^2}{(\delta + x)^2} ; \qquad L_2 = \frac{L_{02}}{1 + x/\delta} ;$$

c - coefficient of total damping of vibrations of the mechanical system; *k* — the

aggregate coefficient of rigidity of the elastic system; L_1, L_2 - inductances of windings W_1, W_2, depending on changes in the air-gap clearances; L_{01}, L_{02} - inductances with a fixed lifter; r_{dr}, r_{rv} - resistances of an open and closed diode VD_1; i_{1dr} - instantaneous value of the excitation current with an open diode; i_{1rv} - reverse current of a closed diode; i_2 - the electric current in the vibration amplitude control circuit; other designations were adopted earlier. Further, taking into account the smallness of i_{1rv} (i_{1rv} / $i_{1dr} \approx 1/1000$, we take $i_{1rv} = 0$.

With a view to obtaining a computer solution of a givensystem of differential equations, below are the parameters of the vibratory feeder, for which the computer experiment was carried out: $U_1 = 380V$; $U_2 = 24V$; $r_1 = r_2 = 0{,}45\Omega$; $r_{dr} = 0{,}1\Omega$; $\delta = 4*10^{-3}$m; $L_{O1} = L_{02} = 0{,}09$ Hn; $R_1 = 6\Omega$; $m = 180$kg; $t = 180$kg; damping coefficient $\psi = 0{,}08$; rigidity of the elastic system $k = 4{,}6*10^6$ N/m.

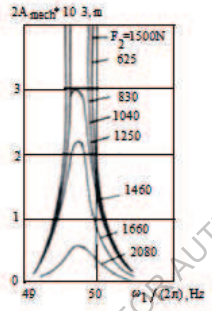

Fig. III.11. The dependence of AFC on variation in F_2

Figure III.11 shows the AFC (frequency response) of the vibrating machine in a subharmonic mode of vibration for various values of the constant component of atractive force F_2. The natural frequency of the elastic system $\omega_0/(2л)$ = 24,8 Hz; damping coefficient ψ = 0,08; the maximum tractive forceof disturbance F_1 = 2290 N. The resonance peak occurs at $\omega_1(2л)$ = 49,6 -- 49,8 Hz. As the force F_2 decreases, the vibration amplitude increases and reaches the value $2A_{mech} = 3.2*10^{-3}$m. With a force $F_2 \leq 1000$ N, the entire air-gap clearance $\delta = 4*10^{-3}m$ is selected, and a collision occurs between a stator and a lifter of the electromagnet; from this moment the machine is not in serviceable condition.

The growth of the amplitude at AFC (frequency response) as F_2 decreases, can be formally identified with the role of damping in a mechanical system. Therefore, the constant component is attributed to the external damping factors.

Figure III.12 shows the change in the amplitudes of subharmonic vibrations

depending on change in the traction force F_2 for a machine with the same parameters as in Figure III.11, at different excitation frequencies.

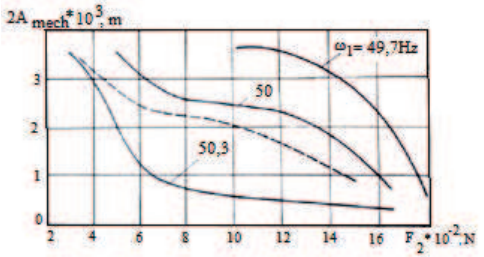

Fig.III.12. The dependences of the amplitude of subharmonic vibrations and F_2 with different ω_1

The results given in Figure III.12 show that more effective regulation of the vibration amplitude is obtained at the exciting frequency of $\omega_1/(2л) = 49,7 \div 50,3$ Hz. The vibration amplitude under these conditions changes in the range of $F_2 = 400 \div 1700$ *N*. When operating in the resonance peak mode ($\omega_1/(2л) = 49,7$Hz), in order to regulate the vibration amplitude, more energy is consumed than in the modes $\omega_1/(2л) = 50$; 50,3 Hz; in the first case $F_2 \geq 1000$ *N*, in the second case - $F_2 \geq 400$ *N*. However, the existence of a relationship between ψ and F_2 allowsfor changing the sensitivity of the machine control.

Figure III.13 shows oscillograms of changes in the currents, exciting forces and forces of regulation, as well as their displacements. With a decrease in the current i_2 and the tractive force F_2 at a constant amplitude of the force F_1, the vibration amplitude increases, and vice versa. Oscillograms indicate the asymmetry of vibrations caused by the interaction of forces F_1 and F_2, and the existence of an additional component (50 Hz) in oscillogram of the displacements at small amplitudes. With an increase in the amplitude, these components disappear, and the system enters the mode of subharmonic resonant vibrations.

Figure III.13 shows the solution of the equations (III.23) - (III.28), written with respect to the currents i_1, i_2. The oscillogram of the traction force F_1 is similar to the oscillogram of the current i_1. The force F_2, corresponding with the direct current of regulation i_2, is also constant in both half-periods, although it is shown on the oscillogram in the form of alternating positive and negative segments; this is due to the feature of the simulation of the equations (III.23) and (III.26), in which F_2 is negative in one case and positive in the other case.

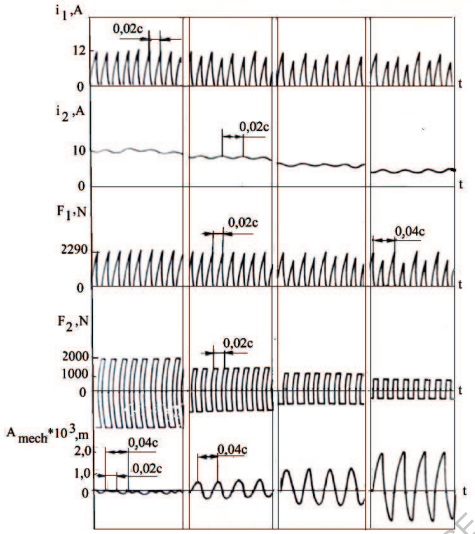

Fig. III.13. Forms of mechanical and electric characteristics when controlling the amplitude using a constant component F_2

Mathematical modeling made it possible to study the magnitudes of the amplitudes of the exciting force and displacements with other parameters of the vibratory exciter of subharmonic vibrations. The research results at $\omega_1/(2\pi)$ = 50 Hz and $\omega_0/(2\pi)$ = 24,8 Hz are shown in Table. III.2.

In these experiments, a relationship is found between the damping coefficient of the system and the tractive force F_2 required to obtain the operating vibration amplitude. With increasing the damping coefficient, the traction force F_2 decreases, at which the vibration amplitude remains the same, for example, $2A_{mech}$=1,0*10^{-3}*m* (Table III.2). The subsequent increase in the damping coefficient completely damps down the vibration amplitude. The interval ψ = 0,2 ÷ 0,3 is critical for this system. Consequently, we can say that the tractive force F_2 plays the role of certain conditional additional damping, which, in contrast to the forces of mechanical damping in the elastic system, can be easily and stably regulated over a wide range, making it possible to accurately reach the level of the critical damping coefficient in the mode of sub-harmonic vibrations.

While maintaining the above calculated parameters of the serial vibratory feeder, converted according to the scheme shown in Figure III.10 at the standard excitation frequency $\omega_1/(2\pi)$ = 50Hz, the experiments were carried out on a real machine. The result of the experiment is shown by the dashed line in Figure III.12.

As we can see, the relationships $A_{mech} = A_{mech}(F_2)$, obtained theoretically and

experimentally, coincide quite satisfactorily within the limits of the practical spread of the initial parameters of a real machine (the spreads in the ohmic resistance of the winding, turning number, the cross-section of the magnetic coreis about 8-10 %).

Table III.2

ψ	F_1, N	F_2, N	$2A_{mech}*10^3$,m
0,06	2290	2290	0,6
		2080	0,7
		1660	0,9
		1460	1,4
		1350	2,4
		1250	2,8
		1040	3,7
		0	3,7
0,1	2290	2290	0
		2080	0
		1660	0
		1460	0,2
		1250	0,5
		1040	1,0
		830	1,2
		728	1,9
		625	2,5
		416	3,7
		0	3,7
0,2	2290	2290	0
		2080	0
		1660	0
		1460	0
		1250	0
		832	0,3
		625	0,6
		416	0,95
		270	1,25
		166	3,7
		0	3,7
0,3	2290	0-2290	0

Thus, the studies carried out have shown the feasibility of creating the low-frequency vibration exciters, in which the amplitude of subharmonic vibrations is regulated using a

constant component of the exciting force.

Pursuant to the model studies carried out, the exciters of subharmonic vibrationshave been developed, the use of which has been made possible in the low-frequency machines with an adjustable amplitude.

8. Regulation of the free frequency of the elastic system using the bias current

During operation, the characteristics of the vibrating machine may vary. For example, in the vibrating machines, the added mass changes the natural frequency of the system and, in order to ensure maximum performance, there is a need for its adjustment.

To this end, let us consider operation of thevibratory exciter (Fig. III.14), in which a bias winding with turning number W_3 and the rheostat R_2 are added. In this case, the exciting force

is created by simultaneous action of the rectified current i_1, current i_2 and the bias current i_3. By creatinga bias current, it is possible to control the natural frequency of the system, while the creation of a current i_2 allows to control the amplitude of mechanical vibrations.

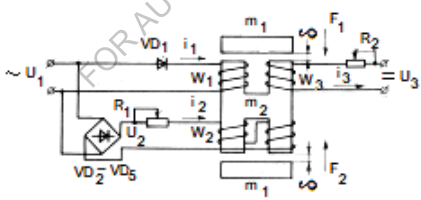

Fig. III.14. The control scheme of the amplitude of a one-stroke vibratory exciter

The operation of thisvibratory exciter is described by differential equations (III.23) - (III.28), but on the right-hand side of the equation (III.24), a voltage e is added, taking into account the effect corresponding with the bias current when the disturbing force F_1 is formed. The voltage balance equation takes the form

$$\frac{d}{dt}(L_1 i_1) + r_1 i_1 + r_{dr} i_1 = U_1 \sin \omega t + e \qquad \text{(III.29)}$$

Based on the results of the solutions, the AFC (frequency responses) of the vibrating machine wereconstructed. Figure III.15 shows the frequency response of the vibratory exciter of the main resonance mode (50/50; ψ = 0,06; i_3 = 0), and Figure III.16 illustrates the frequency
response of the subharmonic mode (25/50; ψ = 0,06; i_3 = 8A). If for the main mode with an increase in the bias current, the change in the natural frequency is very effective and is about 3Hz (6%), then for the subharmonic mode this change is insignificant and does not exceed 0.5Hz, and therefore hadno use in the low frequency machines.

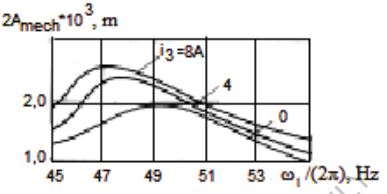

Fig. III.15. The dependence of AFC on the bias current in the main mode

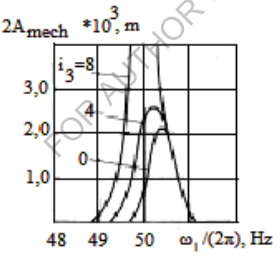

Fig. III.16. The dependence of AFC on the bias current in the subharmonic mode

Of interest is the interconnection of the damping coefficient of the system in the subharmonic mode with two other changing parameters: the vibration amplitude control current i_2 and the bias current i_3. To this end, different modes of operation of the exciter were simulated at a constant excitation frequency $\omega_1/(2\pi)$ = 5OHz. Errors in the manufacture and assembly of the elastic system were simulated by changing the natural frequency $\omega_0/(2\pi)$ = 24,5÷26Hz, damping coefficient ψ = 0,1÷0,03, and the electric currents $i_2 = i_3 = 4 \div 8A$. Experiments suggest that by changing ψ, the number of variants of the varying values i_2, i_3, at which the amplitude of mechanical vibrations reaches its

maximum value (in this case, $2A_{mech} = 3{,}7mm$), also changes depending on the setting the system for resonance ω_0/ω_1. Thus, using the constant component of the exciting force created by the bias current, a constant magneticfield emerges that prevents the movement of the lifter. The magnitude of the preventing force depends on instantaneous gap; the magnetic field strength plays the role of the additional variable rigidity; the constant component of the system's rigidity is created by the mechanical elastic elements. Since in this case there is a non-linear system, the total rigidity of which depends on i_3 (generally on $i_2 + i_3$), by changing parameters of the magnetic field, it is possible to adjust the total rigidity and natural frequency within $\pm \Delta\omega o$ (practically $\Delta\omega_o \approx \pm$ 0.5 Hz). When combined with the method of direct control of the force F_2, it is possible to effectively control the amplitude of subharmonic vibrations; however, this somewhat complicates the regulatory scheme by adding the additional winding W_3.

9. The effect of the bias current constant component on the damping coefficient

The force of attraction depends nonlinearly on the gap clearance in the electromagnet, as well as on the constant and variable components of the total supply current. The DC attractive component has an additional damping property. The latter is due to a decrease in the elastic resistance force of the magnet with a decrease in the amplitude of the mechanical vibrations of the working member, which increases the instantaneous amplitude of the gap, and vice versa. The presence of the hysteresis loop of the variable component of the magnetic field enhances the vibration damping property. When the system is turned off in a field of constant attractive force (AC power supply to the magnet is terminated), the damping coefficient increases by approximately 2-7 times (at the high bias currents).

The power required to move the material, that is, for useful work, does not depend on the constant component of the current; only the power consumed by the machine changes to overcome internal resistances and create periodic vibrations of the working member.

The experimental determination of the damping characteristics was carried out on a machine with a low-hysteresis elastic system.

The constant component of the excitation (current strengthi_2) fluctuated between 0 and 4A. At higher values of i_2, the lifter sticks to the core from the side of the regulating magnet.

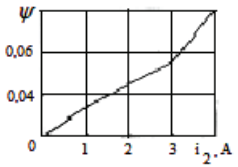

Fig. III.17. The dependence of damping coefficient on variation in the constant component of the excitation current

Thus, in the transient modes when the machine is turned on or off, when there is an exponential increase (to a maximum) or a decrease (to zero) in the strength of the constant component of the current, this factor has a short-term but significant effect on the intensity of progressing the transient processes.

Conclusions

Studies of the nonlinear electromagnetic exciter of vibrations conducted through the theoretical calculations and mathematical modeling of the main electric and mechanical characteristics, as well as by means of the field tests of a real physical model,allow us to draw the following conclusions:

1. A nonlinear exciting force with a linear nature of the mechanical system plays a central role in the excitation of the main and subharmonic modes in the vibrating machines;

2. The developed new scheme of the exciter allows remotely, in the process of operation, to fluentlycontrol the amplitude of subharmonic vibrations using the negative component of the exciting force;

3. Using the method of mathematical modeling of operation of the exciter of vibrations with a nonlinear exciting force, it has been shown that:

a) the constant component of the magnetic flux affects the generation of the total damping coefficient of the system for both the main and subharmonic resonance modes;

b) fluent control of the amplitude of subharmonic vibrations using the constant component of the exciting force is more effective compared with saturation of the electromagnet;

4. A comparison of the results of studies of a real vibrating machine with a mathematical model indicates a good agreement between the mathematical statement of problem and the experiment;

5. The results obtained in this work (in particular, obtaining an amplitude-controllable subharmonic resonance mode) can significantly reduce the mass and dimensions of the vibration exciter, lower the level of radiated noise and transfer of dynamic loads to the support structures.

acknowledgements

This work was supported by Shota Rustaveli National Science Foundation of Georgia (SRNSFG) [N FR17_292], "Mathematical modeling of the vibratory technologic processes and design of the new, highly effective machines"

References

1. Bauman V.A., Bykhovskiy I.I. Vibrating machines in building industry. M., Vyshaya Shkola, 1977, 265 p. (in Russian).
2. Bessonov L.A. Theoretical foundations of electrical engineering, M., Vyshaya Shkola, 1973, 750 p. (in Russian).
3. Biderman V.L. Theory of mechanical vibrations. M., Vyshaya Shkola, 1980, 408 p.
4. Blekhman I. Vibratory mechanics. Nonlinear dynamic effects, common approach, application. World Science. p.509. 2000.
5. Boldea I., Nasar S. A. Linear Motion Electromagnetic Devices. New York: Taylor&Francis, 2001. 270 p.
6. Bozhko A.E., Belykh V.I., Ivanov E.M., Myagkokhleb K.B. Applied theory of controlling the electromagnetic vibratory exciters: monograph, Kharkov, KhPI, 2010, 320 p. (in Russian).
7. Brodskiy Yu.A., Kolosov S.L., Shalunov B.S. Vibrating conveyors – technolgically pure type of industrial transport."Heavy Engineering Industry", No. 1, 2004 г. pp. 35-37 (in Russian).
8. Bykhovskiy I.I., Dorokhova A.D. The issues of the design of the electromagnetic vibrators. Collected papers of Russian Research Institute Stroidormash "Exploring the construction and road-making machines", M., 1972, pp.88-89. (in Russian).
9. Despotović Željko V., Lečić Milan, Jović Milan R., DjuricAna. Vibration control of resonant vibratory feeders with electromagnetic excitation, FME Transactions (2014) 42, 281-289 pp.
10. Edward S.Electromechanical systems, electric machines, and applied mechatronics, Boca Raton, Fl.: CRC Press, 2000. 782 p.
11. Doi,T.,Yoshida, K., Tamai, Y., Kono, K., Naito, K. and Ono, T.: Feedback control for electromagnetic vibration feeder, JSME International Journal, Series C, Vol. 44, No. 1, pp. 44-52, 2001
12. Goncharevich, I.F., Frolov, K.V., Rivin, E.I.:Theory of vibratory technology, Hemisphere Publishing Corporation, New York, 1990.
13. Ormotsadze D.E. A phase-shifting device for controlling the vibratory bunkers. Proceedings of VNIIGSHE, "Special technological equipment for production of light-duty electric machines", Tbilisi, 1980, pp.35-37. (in Russian).
14. Panasenkov M.A. The equations of the dynamic hysteresis loops. Elektrichestvo, No. 3, 1972, p.91. (in Russian).
15. Povidaylo V.A. Calculation and design of the vibratory feeders. M., Mashgiz, 1962,

149 p. (in Russian).
16. Poturayev V.N., Franchuk V.P., Chervonenko A.G. Vibrating transport machines. M., Mashinostroenie, 1964, 328 p. (in Russian).
17. Khvingia M.V., Tedoshvili M.M., Svanidze V.S., Chelidze M.A. The low-frequency electric vibrating machines. L., Mashinostroenie, 1989, 96 p. (in Russian).
18. Khvingia M.V., Dynamics and strength of the vibrating machines with electromagnetic excitation. M., Mashinostroenie, 1980, 145 p. (in Russian).
19. Despotović Željko V., Jović Milan. Mathematical model of electromagnetic vibratory exciter with incremental motion. Infoteh-Jahorina Vol. 13, March 2014. 91÷96 pp.